

*Digital Comprehensive Summaries of Uppsala Dissertations
from the Faculty of Medicine 2141*

Breaking to Understand: DNA Repair in Response to Cancer Therapy

MEHRAN HARIRI



ACTA UNIVERSITATIS
UPSALIENSIS
2025

ISSN 1651-6206
ISBN 978-91-513-2446-3
urn:nbn:se:uu:diva-553099



UPPSALA
UNIVERSITET

Dissertation presented at Uppsala University to be publicly examined in Rudbecksalen, Rudbeck laboratory, Dag Hammarskjölds Väg 20, Uppsala, Thursday, 15 May 2025 at 09:00 for the degree of Doctor of Philosophy (Faculty of Medicine). The examination will be conducted in English. Faculty examiner: Professor Kai Rothkamm (Department of Radiotherapy, University Medical Center Hamburg-Eppendorf).

Abstract

Hariri, M. 2025. Breaking to Understand: DNA Repair in Response to Cancer Therapy. *Digital Comprehensive Summaries of Uppsala Dissertations from the Faculty of Medicine* 2141. 88 pp. Uppsala: Acta Universitatis Upsaliensis. ISBN 978-91-513-2446-3.

Human DNA constantly faces endogenous and exogenous damage, with DNA double-strand breaks (DSBs) posing the greatest threat to genome integrity. However, DSBs can be leveraged to kill cancer cells, as many treatments act as DSB inducers. The dominant repair pathway, non-homologous end-joining (NHEJ), resolves the majority of DSBs. This thesis explores strategies to sensitize resistant cancer cells through combination therapy and investigates NHEJ's response to varying DSB complexities.

Paper I addresses cisplatin resistance in ovarian cancer. We found that combining cisplatin with the HSP90 inhibitor onalespib enhances sensitivity by increasing DSB levels, inducing apoptosis, and causing G2/M arrest, making it a promising strategy. **Paper II** focuses on glioblastoma (GBM), an aggressive brain tumor with limited treatment options. We demonstrated that onalespib enhances radiosensitivity in 2D and 3D GBM models by increasing DSB levels, promoting apoptosis, and altering protein expression, suggesting that HSP90 inhibition could improve radiotherapy outcomes. **Paper III** investigates the alpha emitter Ra-223, used in bone-metastatic prostate cancer. Our findings revealed that Ra-223 generates clustered DSBs, triggering NHEJ activation, growth inhibition, and apoptosis in prostate cancer cells, with no detectable cellular uptake. **Paper IV** explores pharmacological ascorbate (Asc) effect on NHEJ pathway. We found that Asc induces delayed DSBs, extensive pan-nuclear γ H2AX formation, necrosis, and G2/M arrest in colorectal cancer cells, with stronger effects in XRCC4 KO cells. We concluded that Asc does not generate prompt DSBs, and the delayed DSBs are linked to necrotic nuclear degradation, with sensitivity influenced by cell cycle regulation rather than NHEJ deficiency. **Paper V** examines NHEJ's role in repairing DSBs of varying complexity in colorectal cancer cells. Wild-type cells exhibited both fast and slow repair kinetics, while NHEJ-deficient cells showed only a fast repair phase, followed by repair failure. Non-DSB clusters increased as the DSB:SSB ratio decreased (from calicheamicin to X-rays, bleomycin, etoposide, and temozolomide). These clusters were rapidly removed, independent of NHEJ, highlighting the impact of DSB type/complexity on repair efficiency.

In conclusion, this thesis presents strategies to overcome cisplatin resistance, enhance radiosensitivity in GBM, and elucidate Ra-223 toxicity mechanisms in prostate cancer. It also examines Asc's effects on DSB induction and repair and reveals NHEJ's role in processing complex DSBs. Our findings provide new insights into optimizing DSB repair and therapeutic strategies in cancer treatment.

Keywords: DSB, NHEJ, HSP90 inhibition, X-ray, alpha-particle, clustered DSB, ascorbate, XRCC4, DNA-PKcs, DSB complexity

Mehran Hariri, Department of Immunology, Genetics and Pathology, Cancer precision medicine, Dag Hammarskjölds väg 20, Uppsala University, SE-751 85 Uppsala, Sweden.

© Mehran Hariri 2025

ISSN 1651-6206

ISBN 978-91-513-2446-3

URN urn:nbn:se:uu:diva-553099 (<http://urn.kb.se/resolve?urn=urn:nbn:se:uu:diva-553099>)

*I dedicate this thesis to my parents, **Ashraf Firoozeh** and **Jalal Hariri**; to my motherland, **Iran**, which nurtured me; and to my second home, **Sweden**, which gave me the opportunity to grow.*

A person is defined by the problems they solve and how well they solve them.

List of Papers

This thesis is based on the following papers, which are referred to in the text by their Roman numerals.

- I. Mortensen, A., Mohajershojai, T., **Hariri, M.**, Pettersson, M., Spiegelberg, D. (2020) Overcoming limitations of cisplatin therapy by additional treatment with the HSP90 inhibitor onalespib. *Frontiers in Oncology*, vol 10.
- II. Uffenorde^{*}, J., **Hariri, M^{*}**, Papalannis, E., Staffas, A., Berg, J., Stenerlöv, B., Berglund, H., Malmberg, C., Spiegelberg, D. (2025) Enhancing glioblastoma therapy: Unveiling synergistic anticancer effects of onalespib - radiotherapy combination therapy. *Frontiers in Oncology*, vol 15. (*Equal contribution)
- III. Abramenkovs^{*}, A., **Hariri, M^{*}**, Spiegelberg, D., Nilsson, S., Stenerlöv, B. (2020) Ra-223 induces clustered DNA damage and inhibits cell survival in several prostate cancer cell lines. *Translational Oncology*, 26, 10154. (*Equal contribution).
- IV. **Hariri, M.**, Papalannis, E., Spiegelberg, D., Plotnikov, E., Viktorsson, K., Stenerlöv, B. (2025) Ascorbate induces G2/M arrest and necrosis without generation of direct DNA double-strand breaks. Accepted in *Heliyon*.
- V. **Hariri, M.**, Stenerlöv, B. The role of non-homologous end joining in the repair of different types of DNA double-strand breaks. *Manuscript*.

Reprints were made with permission from the respective publishers.

List of publications not included in the thesis

- VI. Mortensen, A., Berglung, B., **Hariri, M.**, Pettersson, M., Papalannis, E., Malmberg, C., Spiegelberg, D. (2023) Combination therapy of tyrosine kinase inhibitor sorafenib with the HSP90 inhibitor onalespib as a novel treatment regimen for thyroid cancer. *Scientific Reports*, 6;13(1):16844
- VII. Lundsten, S., Berglung, B., Jha, P., Krona, C., **Hariri, M.**, Nelanders, S., Lane, D. P., Nestor, M. (2021) p53-mediated radiosensitization of ¹⁷⁷Lu-DOTATATE in neuroblastoma tumor spheroids. *Biomolecules*, 11, 1965

Contents

| | |
|---|----|
| Introduction..... | 11 |
| 1.1. DNA macromolecule..... | 11 |
| 1.2. DNA damage induction..... | 12 |
| 1.2.1. DNA Base lesions..... | 12 |
| 1.2.2. SSB..... | 13 |
| 1.2.3. DSB..... | 13 |
| 1.2.4. Clustered DNA damage..... | 14 |
| 1.2.5. DSB complexity..... | 14 |
| 1.2.6. Ionizing radiation..... | 15 |
| 1.2.7. Chromatin structure and DNA damage..... | 16 |
| 1.3. DNA repair..... | 16 |
| 1.3.1. BER..... | 17 |
| 1.3.2. NER..... | 17 |
| 1.3.3. MMR..... | 18 |
| 1.3.4. SSB repair..... | 18 |
| 1.3.5. DSB Repair..... | 18 |
| 1.3.6. DSB Repair Phases (kinetics)..... | 25 |
| 1.3.7. Cell Cycle and DSB..... | 26 |
| 1.4. DNA damage and apoptosis..... | 28 |
| 1.5. DNA damage and necrosis/necroptosis..... | 29 |
| 1.6. DNA damage repair and cancer..... | 30 |
| 1.6.1. Genomic Instability and Mutation Accumulation..... | 30 |
| 1.6.2. Defects in DNA Repair Pathways..... | 30 |
| 1.6.3. DNA Damage in Tumor Progression..... | 31 |
| 1.6.4. Targeting DNA Repair Pathways..... | 31 |
| 1.6.5. Combination therapy..... | 31 |
| 1.6.6. Synthetic lethality..... | 32 |
| 2. Aim..... | 33 |
| 3. Results..... | 34 |
| 3.1. Paper I..... | 34 |
| 3.1.1. Introduction and Aim..... | 34 |
| 3.1.2. Methods..... | 35 |
| 3.1.3. Results..... | 35 |
| 3.1.4. Discussion and conclusion..... | 39 |

| | |
|---------------------------------------|----|
| 3.2 Paper II | 40 |
| 3.2.1. Introduction and Aim..... | 40 |
| 3.2.2. Methods | 41 |
| 3.2.3. Results | 41 |
| 3.2.4. Discussion and conclusion..... | 46 |
| 3.3 Paper III..... | 47 |
| 3.3.1. Introduction and Aim..... | 47 |
| 3.3.2. Methods | 48 |
| 3.3.3. Results | 48 |
| 3.3.4. Discussion and conclusion..... | 49 |
| 3.4 Paper IV..... | 51 |
| 3.4.1. Introduction and Aim..... | 51 |
| 3.4.2. Methods | 52 |
| 3.4.3. Results | 52 |
| 3.4.4. Discussion and conclusion..... | 56 |
| 3.5 Paper V | 57 |
| 3.5.1. Introduction and Aim..... | 57 |
| 3.5.2. Methods | 58 |
| 3.5.3. Results | 58 |
| 3.5.4. Discussion and conclusion..... | 62 |
| 4. Concluding remarks | 65 |
| 5. Future perspectives | 67 |
| 6. Acknowledgments..... | 69 |
| 7. References..... | 75 |

Abbreviations

| | |
|------------------|---|
| AKT | Protein kinase B |
| Alt-NHEJ | Alternative non-homologous end Joining |
| ATM | Ataxia telangiectasia mutated |
| ATP | Adenosine triphosphate |
| ATR | Ataxia telangiectasia and Rad3-related protein |
| BER | Base excision repair |
| BRCA1 | Breast cancer-associated gene 1 protein |
| BRCA2 | Breast cancer-associated gene 1 protein |
| CDKs | Cyclin-Dependent Kinases |
| CETN2 | Centrin 2 |
| CHK2 | Checkpoint Kinase 2 |
| DDR | DNA damage response |
| DNA-PKcs | DNA-dependent protein kinase, catalytic subunit |
| DSB | Double-strand breaks |
| EGFR | Epidermal growth factor receptor |
| HATs | Histone AcetylTransferases |
| HLS | Heat-Labile Sites |
| HMTs | Histone MethylTransferases |
| HP1 | Heterochromatin Protein 1 |
| HR | Homologous recombination |
| HRK | Activator of apoptosis harakiri protein |
| H2AX | H2A histone family member X |
| γ -H2AX | Phosphorylated H2AX |
| KAP1 | KRAB-associated protein 1 |
| LET | Linear energy transfer |
| MCL | Mantle cell lymphoma |
| MDC1 | Mediator of DNA damage checkpoint protein 1 |
| CHK2 | Checkpoint Kinase 2 |
| MMEJ | microhomology-mediated end joining |
| MMR | Mismatch Repair |
| MN | Micronucleus |
| MRE11 | Meiotic recombination 11 |
| MTIC | Methyl triazeno imidazole carboxamide |
| NAD ⁺ | Nicotinamide Adenine Dinucleotide |
| NBS1 | Nijmegen breakage syndrome 1 |

| | |
|--------------|--|
| NER | Nucleotide excision repair |
| NHEJ | Non-homologous end-joining |
| PARP 1 | Poly (ADP-Ribose) Polymerase 1 |
| PFGE | Pulsed-field gel electrophoresis |
| PI3K | Phosphoinositide 3-kinase |
| PIKKs | Phosphoinositide 3kinase-like kinases |
| Pol θ | DNA polymerase θ |
| PTIP | Pax transactivation domain-interacting protein |
| RAD23B | UV excision repair protein RAD23 homologue B |
| RAD50 | Radiation repair 50 protein |
| RIF1 | RAP1-interacting factor 1 |
| RIPK1 | Receptor-Interacting Protein Kinase 1 |
| PARP 1 | Poly (ADP-Ribose) Polymerase 1 |
| RNF8 protein | Ubiquitin-protein ligase ring finger 8 |
| ROS | Reactive oxygen species |
| RPA | Replication protein A |
| SSA | Single-Strand Annealing |
| SSB | Single strand breaks |
| TFIIH | Transcription initiation factor IIH |
| TRP53BP1 | Tumor suppressor p53 Binding Protein 1 |
| TOP1 | Topoisomerase 1 |
| UV-DDB | Ultraviolet radiation DNA damage-binding protein |
| XRCC4 | X-ray repair cross-complementing protein 4 |

Introduction

Almost all cancer therapy, except surgery, kills tumor cells by inducing DNA damage. DNA double-strand breaks (DSB) is the most lethal form of DNA damage, due to difficulty of correct repair. Almost all DSBs rejoin by non-homologous end joining (NHEJ).

However, the following problems related to NHEJ remain partially or completely unresolved:

- Increasing the efficiency of this pathway for tumor radio-chemosensitization
- The ratio of NHEJ involvement in the overall structure of DNA damage
- Exact nature of DSB structure which activates NHEJ
- NHEJ response to the DSB complexity levels and effect of these complexities on DSB repair pathway choice

This thesis addresses these problems, which are explained in the five included papers.

1.1. DNA macromolecule

The double-stranded helix DNA is considered the origin of life and cell data bank for protein synthesis. DNA consists of almost similar building blocks that repeat along a chain shaped double helix. The DNA helix backbone is a pentose sugar molecule of deoxyribose attached to a phosphate group and coupled by hydrogen bonds to four types of nitrogen-containing bases (adenine (A), guanine (G), cytosine (C), and thymine (T)). The A base specifically pairs with T and the G base always pairs with C. One strand of DNA duplex locates anti-parallel to another strand, this means the 5' end of a single strand always faces to 3' of another strand. Further, phosphate groups link each nucleotide to another vertically and the outer edges of DNA bases are capable of making a hydrogen bond with proteins e.g. during DNA replication (1).

As the cell's largest macromolecule DNA is packed and organized by wrapping around histones, making nucleosomes inside the nucleus. Histones regulate cells' epigenetic traits by chromatin remodeling modification and gene post-translation variations. Histone variants provide a platform for the

recruitment of chromatin-interacting kinases to modify a gene's post-translational variation.

Around 147 DNA base pairs wrap around the nucleosome core structure or histone octamer consisting of eight core particles, two each of H2A, H2B, H3, and H4. The nucleosomes are attached to the H1 linker histone which sits on the nucleosome. H1 histone connects each nucleosome to the other with linker DNA. The length of linker DNA is around 20-90 bp at the entry and exit parts of the nucleosome, forming the shape of beads and string (2–5).

1.2. DNA damage induction

DNA stability is the key player in cell survival and proliferation. This stability is under constant attack by endogenous and exogenous elements. Depending on the source and severity of DNA damage, cells face different fates such as genomic abnormal rearrangement, autophagy, apoptosis, DNA repair, cell cycle arrest, epigenomic alterations, and tumorigenesis. The internal sources can be transcription errors, replication stress, and reactive oxygen species (ROS) from metabolism (metabolic oxidation). Exogenous sources are considered strong elements of assault such as ionizing radiation (inducer of DSB, single-strand breaks (SSB), and base lesions), ultraviolet light (base damage and dimer generator), platinum-based chemotherapeutics (DNA cross-links and DNA adducts inducer), and oxidative agents (abasic sites and SSB generation) (6,7).

1.2.1. DNA Base lesions

Hydrolytic force, oxidative stress, alkylating agents, and ultraviolet light can generate base lesions. The higher molarity of water molecules inside the cell, causes the hydrolytic force to remove the amino group from DNA bases or deamination. The common form of this lesion is the deamination of cytosine and later conversion to uracil. Also, water-induced deamination of adenine produces hypoxanthine (8). It is noteworthy that deamination can happen during DNA replication by DNA polymerase as the most common form of base modification in human normal and cancer cells which happens by substitution of A with G or C to T (9). Oxidative stress from ROS family members (hydroxyl radicals, superoxide radicals, and hydrogen peroxide) is a common cause of oxidation of guanine and forming 8-oxoG, which promotes the substitution of G with T. Hydroxyl free radicals can damage DNA sugar moiety and form 8,5'-cyclopurine-2'-deoxynucleosides (10). Covalent binding of alkylating elements to DNA bases can increase the rate of DNA depurination and generation of 3-methyladenine and 7-methylguanine. Pyrimidine dimer generation from ultraviolet light is another source of base lesions (11).

1.2.2. SSB

The SSB occurs frequently, with up to tens of thousands of them happening in a single cell daily, because of both intracellular metabolites attack and DNA decay. Also, the SSB can occur at the site of ROS damage and DNA repair excision steps or faulty function of topoisomerase (TOP1) enzymes.

TOP1 relaxes supercoiled DNA by producing DNA nick cleavage during transcription. The collision of cleaved DNA with DNA polymerase, RNA, or DNA lesions at proximity can convert cleavage complexes into TOP1-linked SSBs and TOP1-linked DSBs (Fig. 1) (12,13).

Oxidative stress (ROS) from the internal metabolic reaction is the most common cause of SSB. ROS can directly generate SSB via attack and oxidize the sugar molecule of DNA. The indirect action of ROS is through affecting DNA abasic sites, damaged bases, or by interfering in base excision repair.



Figure 1. Different types of DNA damage.

1.2.3. DSB

The DSB is the most toxic type of DNA lesion. The source of DSB can be ionizing radiation, chemotherapeutic agents, ROS, and mechanical forces that break the chromatin structure. Also, replication fork collision with SSB, sugar lesion and base damage can generate DSB. The defective metabolism of telomeres also can lead to DSB formation. DSB is an important part of some vital biological processes inside the human cells such as the initial step at recombination of homologous chromosomes in meiosis, V(D)J recombination, and recombination in immunoglobulin class switching. The repair of DSB lesions is more challenging to the cell than other types of DNA damage and there is a possibility of the transition of non-repaired DSBs to the new generation of cells. G1/S checkpoint activation is slow and can pass unrepaired DSB to the S phase in 4-6 hours after irradiation. In contrast, the G2/M checkpoint is quickly activated by DSBs, but the activation threshold is 10-20 DSB. If the DSB number is below this threshold, then the G2/M checkpoint will not be activated and a cell can be divided carrying an unrepaired DSB (14). The cell's adoption to the low rate of non-repaired DSB can increase the possibility of mutation in tumor suppressor genes or activation of oncogenes. Also, errors in DSB rejoining can generate chromosomal translocation and tumorigenesis. This faulty chromosomal rearrangement in T cell receptor genes happens in

lymphoid cancers (15). Besides direct clustered damage by irradiation, processing of non-DSB clustered lesions can generate complex DSBs (7).

1.2.4. Clustered DNA damage

Clustered DNA damage happens when several DNA lesions are located in close proximity, within approximately 20 base pairs. Inside the damaged cluster there are different kinds of DNA damage such as SSB, DSB, oxidative base, and sugar damage. These lesions can locate on one strand or both strands of DNA close together. DNA clustered damage is associated with genomic instability, elevated mutation, and cancer (16). The basic form of clustered damage is a DSB consisting of two SSB in opposite DNA strands in close vicinity.

1.2.5. DSB complexity

Cancer treatment with X-rays and various cytotoxic drugs primarily kills cells by inducing DSBs, as the most harmful type of DNA damage (17). However, DSBs are highly heterogeneous, varying from simple enzymatically induced breaks to complex DSBs, such as those associated with additional DSBs, single-strand breaks (SSBs), or base lesions within 20-30 base pairs and clustered DSBs within chromatin, induced by X-rays or especially with high-linear energy transfer (LET) radiation (18).

The complexity of DSB can be classified into various levels predicated on the nature of the lesions, their quantity, and their spatial distribution relative to each other. Each DNA-damaging agent has its own DNA lesion signature. For instance, calicheamicin, an exceptionally potent inducer of DSBs, is classified as an enediyne antitumor antibiotic that cleaves DNA at sites rich in pyrimidines (19). Phleomycin, a glycopeptide antibiotic containing copper and derived from *Streptomyces verticillus*, is part of the bleomycin family and induces DNA adduct formation, by disrupting DNA polymerase activity and resulting in the generation of numerous SSBs as well as a limited number of DSBs (20). X-rays are distinguished by their ability to induce clustered DNA damage, encompassing interstrand crosslinks, oxidative base modifications, SSBs, and DSBs, through mechanisms involving both direct ionization and indirect pathways mediated by reactive oxygen species (ROS) (20,21).

Etoposide (ETP) is a topoisomerase II (topo II) inhibitor that transforms temporary DNA breaks into stable DSBs (21). At clinically relevant concentrations, the majority of DNA damage caused by ETP is SSBs. At higher concentrations, with saturation of topo II ligase pockets, etoposide can generate DSBs (22,23). Temozolomide (TMZ) is an alkylating agent that forms DNA cross-links, inhibiting DNA replication. The DNA damage induced by TMZ primarily consists of base pair mismatches and SSBs, with little to no generation of DSBs (24,25).

1.2.6. Ionizing radiation

Ionizing radiation is a high-frequency energy with a short wavelength from natural or synthetic sources which can produce ions when interacting with matter. It strips off the atom's electrons, producing a nucleus with a positive charge. Natural types of ionizing radiation are cosmic radiation and radon. The exposure from synthetic sources can be from medical imaging, treatment devices, and nuclear energy production wastes. There are different types of ionizing radiation such as photons and charged particles with different biological effects. A radiation's biological effect depends on the amount of energy absorbed by interacted biological matter or delivered dose per unit of biological target define by gray (Gy) or joules per kilogram (26). Further, the biological effect is also dependent on the amount of energy that the ionizing particle, or photon, delivers to the encountered material along its track, in each distance unit ($\text{keV}/\mu\text{m}$), defined as the ionizing radiation linear energy transfer (LET). High-LET particles like alpha-particles and heavy ions have typical LET of 70-200 $\text{keV}/\mu\text{m}$. In contrast the deposition from low-LET radiations like γ -rays and X-rays are in the range 0.1-2 $\text{keV}/\mu\text{m}$. (27).

1.2.6.1. Biological effects

Both high and low-LET radiation can induce biological damage directly and indirectly by energy transfer, especially to the nucleus which makes it a unique tool for DNA damage induction. The direct effect comes from the radiation-delivered dose to the phosphodiester backbone. The indirect effect is through interaction with the surrounding environment of DNA such as water, oxygen, salts, and proteins (5). This indirect damage is mainly related to the production of hydroxyl radicals and oxygen atoms from water radiolysis. It is estimated that for low-LET radiation one-third of radiation damage on DNA is direct and the rest is indirect (28), whereas for high-LET 50-70% is direct.

1.2.6.2. Radiation-induced clustered DNA damage

Clustered DNA damage is a signature of ionizing radiation. Both high-LET and low-LET radiation can induce highly complex DNA damage or clustered DNA damage. The complexity of damage increases with elevated LET and the cluster formation is related to the activation of several electrons after the initial hit from the first activated electron (29). For high-LET, damage are clustered along and around the track of travel through the nucleus. In contrast, the low-LET radiation damage is more randomly distributed (30). For example, 1 Gy of low-LET γ -rays produces about 1000 ionization tracks in one mammalian cell nucleus compared to only 4-5 tracks produced by 1 Gy of α -particles.

All types of ionizing radiation initial insult can be followed with the help of induced radiation track structure simulation. The Monte Carlo simulation of the low-LET ionization track shows 30% complex DSBs in at least one

lesion together with base damages. This number is 90% for high-LET. The number of non-DSB clusters is around 4 times more than DSB at low-LET and 8 times more for high-LET (7). The clustered DNA lesions have the highest correlation with the final biological cell fate (31).

Metabolic oxidative stress cannot generate this type of damage. Also, reactive radicals from the indirect effect of ionizing radiation are not likely to produce clustered damage. Therefore, if the indirect oxidation rate of ionizing radiation and oxidative chemical become the same, irradiation is much more toxic because of extra direct damage induction in the form of clustered damage.

1.2.7. Chromatin structure and DNA damage

DNA is more protected from radiation when wrapped around histones than transcriptionally active open parts and linker DNA. The inner part of DNA that faces the histone is more protected than the outer DNA surface. This histone protection provides physical cover and less exposure face to irradiation and radiomimetic agents. However, ROS due to their very small size still can interact with a large part of nucleosome DNA (32). Nevertheless, histones removal from DNA using high salt increases the DSB induction 20-40 fold after removing H2A and H2B, and it elevates to around 70 fold by removing all core histones (5).

Chromatin packaging heterogeneity influences the binding sites of DNA-damaging cytotoxic drugs and the accessibility of ROS to DNA. This packaging will also influence both the distribution of DNA damage and the DNA repair proteins accessibility to initiate the repair (33). If DNA damage is complex, alternative repair pathways may process some DSBs before the activation of major pathways like NHEJ and HR (discussed below), leading to slower repair. Complex DSBs in compact chromatin may require chromatin-related kinases for modification and repair access (34,35).

1.3. DNA repair

DNA damage can transfer to the daughter cells after mitosis or meiosis to increase the probability of genetic defects. To protect DNA integrity through cell division and metabolism all eukaryote cells develop profound DNA repair machinery. This system includes three main parts. First, the sensing section identifies and recognizes the type of DNA lesion. After understanding the DNA damage occurrence, the second part of the DNA repair machinery becomes active by the initiation of a cascade of alarm messages via cell signaling. In the third part, the cell reacts to the DNA repair signals by programmed cell death or apoptosis, senescence, necrosis, cell cycle arrest, or repair of the damaged DNA lesions (36). This dynamic process is concomitant with

chromatin modulation and rearrangement to adjust the chromatin structure for accessibility and transcription by DNA repair modulators at the damage site and whole chromatin. These DNA repair strategies help multicellular organisms to hamper defective cells with heavily damaged DNA from propagation and reduce the possibility of cancer (37). In general view, the DNA repair system in its different forms is designed to cut the lesion out of the DNA and insert the correct sequence of nucleotides (38). Here the important DNA repair pathways of BER (Base Excision Repair), NER (Nucleotide excision repair), MMR (Mismatch repair), SSB repair, and DSB repair will be briefly discussed in the following section.

1.3.1. BER

Most abnormal bases and DNA lesions from oxidative and alkylating elements, do not distort the DNA and can be repaired fast (few minutes) via BER in the G1 phase. BER function is inside the bigger context of cell repair machinery and not just as an isolated pathway (39). The repair initiation starts with the recognition of the damaged base by DNA glycosylase which cleaves the N-glycosylic bond of a base to the DNA sugar backbone, leaving a baseless AP site. APE1 endonuclease processes the AP site and cleaves the phosphodiester bond producing a SSB. At this point, BER continues with the short (single nucleotide replacement) or long-patch repair (2-10 nucleotide resynthesis). In the classic BER or short-patch BER the Pol β recognizes the one nucleotide gap (3'OH and 5' P ends) and removes the 5' P end and activates XRCC1 and Lig3 to complete the repair by ligating the DNA ends. If the 5' P end of SSB is blocked and not possible to process by SSB end-processing kinases (Pol β , APE1, PNKP, Aprataxin, TPD1) long-patch repair takes over. In this way, resynthesizing of 2-10 AP nucleotides starts with Pol δ which displaces the strand. Then flap endonuclease 1 cuts the flapped strand and DNA ligase I, ligates the DNA (40).

1.3.2. NER

NER has a more complicated process than BER with the detection of DNA distortion. It is in charge of fixing the DNA cross-link and DNA adducts. NER consists of two sub-pathways of transcription-coupled NER (TC-NER) and global genome NER (GG-NER).

GG-NER: protects DNA from duplex distorting damages. DNA distortion recognizes by the XPC-RAD23B-CETN2 complex with the help of UV-DDB. Then XPC binding to the damage site dissociates RAD23B.

TC-NER: During the stalling of RNA transcription, UVSSA, USP7, and CSB start interaction with RNA polymerase II and accumulate at the transcription site. Then after increasing the affinity of CSB to RNA pol II, CSA forms

a complex with CSB which leads to backtracking or reverse translocation of RNA Pol II to make the lesion accessible for repair.

From this point, the repair process is common for TC-NER and GG-NER. After lesion detection, the TFIIH complex binds to the damaged site, and CAK dissociates from the TFIIH complex. XPG endonuclease binds to the NER complex or TFIIH. Then TFIIH opens the DNA duplex around the damage site from 5' to 3'. XPD verifies the lesion with the help of TFIIH XPB and XPA. Meanwhile, RPA protects the undamaged nucleotides. The XPA recruits the XPF-ERCC1 complex for lesion incision (No return point) and XPG cuts the damaged strand around 22-30 nucleotides long. Then PCNA recruits DNA Pol δ , DNA Pol ϵ , or DNA Pol κ to fill the gap. Finally, ligation happens by DNA ligase 1 or DNA ligase 3 (41).

1.3.3. MMR

MMR is responsible for fixing replication errors and single nucleotide mismatches from DNA polymerase action. First MSH2-MSH6 complex detects the mismatch and forms the sliding clamp. Then EXO 1 cut out the nucleotide. RPA protects the strand from degradation and EXO 1 action. DNA polymerase δ synthesizes the nucleotide and finally, DNA ligase seals the DNA (42).

1.3.4. SSB repair

SSB can be generated directly from ROS, abortive TOP1 function, or during the processing of closely located lesions. It can be induced indirectly during BER, NER, and MMR and has an extensive overlapping repair process with them. In the direct SSB repair process, PARP 1 (Poly (ADP-Ribose) Polymerase 1) activates by SSB and binds to the lesion site. It starts recruiting downstream DNA end-processing elements APE1, APTX, and PNKP. Then Pol β , Pol δ , or Pol ϵ fill the nucleotide gap. In the end, DNA ligates by DNA ligase 3 or DNA ligase 1 (12).

1.3.5. DSB Repair

DSB initiate by lesion sensing, followed by a cascade of intra-cellular interwoven signaling to stimulate DSB repair and cell cycle checkpoints activation. Two important chromosomal DSB mediators, 53BP1 and γ H2AX (43), besides three members of the phosphoinositide 3-kinases (PI3Ks) family including ATM (Ataxia telangiectasia mutated), ATR (Ataxia telangiectasia and Rad3-related protein), and DNA-PKcs (DNA-dependent protein kinase catalytic subunit), as transducer DSB repair signaling, launch the cascade of protein phosphorylation to activates DSB repair pathways (6,44). Here characteristics of these mediators, transducers, and non-homologous end joining

(NHEJ) and homologous recombination (HR) pathways with emphasis on NHEJ are discussed.

1.3.5.1. 53BP1

The phosphorylation of the 53BP1 protein is important for DSB repair activation. The p53-binding protein 1 known as p202, TDRD30, p53BP1 or TRP53BP1 protein with over 200 kDa and 1972 amino acid encodes by *TP53BP1* gene located on the human's chromosome number 15 (15q15.3). The expression of this gene in the brain is higher than in other organs (45,46). It is a multifunctional protein belonging to the Tudor domain protein family. The Tudor domain enables the protein to read histones by detecting and binding to methylated arginine and lysine residues to modify histone and accelerate DNA damage repair response (47). Besides the well-known role of 53BP1 in DNA damage response, it plays different roles in cellular processes, like apoptosis, autophagy, and aging (45).

In the DNA damage response chain, 53BP1 plays downstream of PIKKs, ATM, ATR, and MRN complex (MRE11-RAD50-NBS1). 53BP1 protein doesn't act as an enzyme per se, but it functions as a substrate to mediate other proteins' functions possible in a cell cycle-dependent manner. In the time of DNA damage, the histone recognition starts with the dimethylation of histone H4 at Lysine 20. 53BP1 through its Tandem Tudor domain has selective specificity to bind to this dimethylated site to make 53BP1/H4-K20me2 Complex (48). Also, 53BP1 assembly to the site of DSB facilitates by ubiquitylation of it through RNF8 and RNF 168 catalyzation and recruitment of p97 protein to the damage site. This reaction leads to the removal of L3MBTL1 protein from the methylated site of histone H3K4 lysin20 and accelerates more 53BP1 binding to the damage site (49). Moreover, the 53BP1 Tudor domain acts as a mediator of DNA damage response sensors to effectors of checkpoint kinase 1 (CHEK1), checkpoint kinase 2 (CHEK2), ATM, breast cancer-associated gene 1 (BRCA1), and topoisomerase II-binding protein 1 (TOPBP1) (45).

53BP1 has a crucial role in DSB repair pathway choice by providing a recruitment scaffold for sensors and effectors of DDR (DNA Damage Response). 53BP1 is involved in HR and NHEJ by activation of p53 and also can function independently of p53. It stimulates the DSB repair pathway in favor of NHEJ versus HR by competing against ubiquitination via BRCA1. ATM phosphorylates 53BP1 to recruit RIF1 and PTIP to the damaged site. This complex of proteins promotes NHEJ by protecting DSB ends from resection in the cell cycle G1 phase. But in S/G2 cell cycle phases, BRCA1 C Terminus (BRCT) domain inhibits and antagonizes phosphorylation of 53BP1 by ATM. As a consequence, HR becomes the dominant repair pathway in the S/G2 phases (Fig. 2).

The mechanistic resolution of 53BP1 during the S phase is not clear yet. The consequence of defective 53BP1 function is hypersensitivity to ionized irradiation with error in DNA damage checkpoint, abnormal cell cycle

regulation, and defective DNA damage repair (50,51). Imaging of 53BP1 accumulation into so called foci after e.g. radiation-exposure, serve as a common biomarker for DSB.

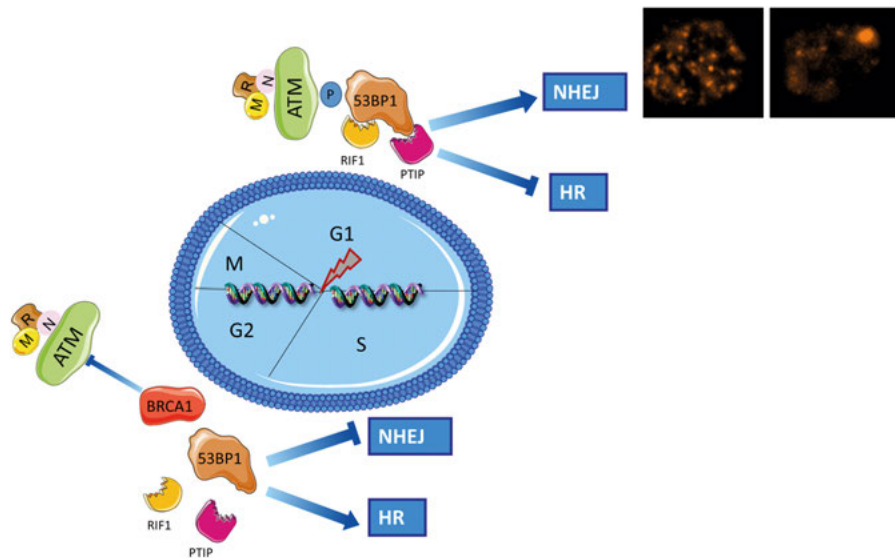


Figure 2. 53BP1 cell cycle-dependent function under the effect of BRCA1 at DSB repair. The immunofluorescence image of HCT116 cells shows 53BP1 biomarker in orange in S and G phases.

1.3.5.2. γ H2AX

Out of all H2A histones in vertebrate cell, 2-25% are H2AX conserved variant encoded by the *H2AFX* gene on chromosome 11 (52,53). One of the initial DSB responses is the quick phosphorylation of histone H2AX at Ser-139 to form γ H2AX(54). The role of γ H2AX in DDR is to make DNA accessible for the recruitment of repair factors. It holds broken ends close together during repair to avoid losing chromosomal sites (55). Moreover, γ H2AX reduces chromatin density at the site of damage and repositions the nucleosome for anchoring DNA broken ends. Also, γ H2AX plays a role in checkpoint activation response for DNA repair (56). After DSB happens three main kinases of ATM, ATR, and DNA-PKcs are contributing to H2AX phosphorylation with overlapping parallel functions. However, ATM is the main direct activator of H2AX phosphorylation (6). The other activation way is indirectly from the MRN complex which directly interacts with the DSB site and then recruits ATM. Then ATM phosphorylates H2AX through auto-phosphorylation and monomerization. Also, phosphorylation of MDC1 can lead to H2AX phosphorylation (57).

γ H2AX foci fluorescent imaging after irradiation revealed that up to 30 Mbp can be modified as the result of H2AX phosphorylation leading to huge chromatin relaxation. These foci are detectable after minutes of irradiation by reaching the peak in 30 minutes. After 1 h the number of foci starts to decline (58). After finishing the DSB repair, γ H2AX foci disappear. However, the complete DSB repair stage that leads to foci clearance is not well understood. It is still elusive if this DSB repair completion happens after DSB rejoining or chromatin remodeling (53). Defective H2AX in mice model, make them extremely radiosensitive with genomic instability, defective G2/M cell cycle checkpoint, and retardant DNA repair (59).

Visualization of chromatin modification by immunofluorescence staining is a sensitive biomarker of DNA damage and repair. The γ H2AX immunostaining is 100 times more sensitive than other DSB detection methods such as PFGE for detecting 1 focus in every 30 cells after receiving of 1mGy ionizing radiation dose without the need for lysing cells. The PFGE DSB detection threshold for ionizing radiation is 5 to 10 Gy which is much higher than γ H2AX immunostaining. This high sensitivity makes γ H2AX imaging a versatile marker for DNA damage and repair detection not only for various types of ionizing radiation but also for a wide variety of DNA-interacting chemical agents (59).

1.3.5.3. ATR

ATR is one of the DSB repair main kinases with many substrates in response to DNA replication stress, the vast range of genotoxic insults, and cell proliferation. Activated ATR, phosphorylates CHK1 for the regulation of the cell cycle, DNA repair, deoxynucleotide synthesis promotion, DNA replication fork restart, and prevention of DSBs formation. Single-stranded DNA coated by replication protein complex A (RPA) recruits ATR via ATRIP. This binding follows by adding a TopBP1 activator to ATRIP and C-terminal PRD in ATR to trigger ATR kinase action. A main function of ATR is the phosphorylation of protein kinase CHK1. Activated CHK1 promotes the degradation of CDC25A to end the inhibitory phosphorylation in CDKs for sake of cell cycle progression. Genotoxic stress leads to the inactivation of CHK1 followed by cell cycle arrest. This delay gives more time for the cell to fix the damage before entering mitosis. In case of extensive and not repairable damage, cells will enter senescence or apoptosis pathways. The second vital function of ATR is protecting replication forks by inhibiting CDKs to restrain replication origin firing. This inhibition safeguards the repair factor's pool and prevents replication exhaustion (6,60). Many cancer cells' survival is dependent on the ATR signaling pathway which makes it a good candidate for tumor radio and chemo-sensitization (61).

1.3.5.4. ATM

ATM is one of the main DSB repair signal transducers which is activated by DSB, oxidative stress, and chromatin change. After DSB, ATM autophosphorylates at Ser198 which changes the close dimer of ATM to the active monomer state for the recruitment of downstream partners (62). However, the majority (80%) of DSB outside of the S phase, are repaired via NHEJ and independent of ATM, and the rest minority is repaired by ATM, DNA-PK, and MRN complex. It is suggested that ATM participate in NHEJ for bridging the DSB gap. In the deficiency of DNA-PKcs, ATM becomes hyperactive. The biological relevance of this interaction in normal cells is preventing the cell from entering the unwanted apoptosis phase. ATM is not necessary for HR initiation but it promotes DNA end resection process in favor of HR by phosphorylation of CtIP. In response to DSB, MRN recruits ATM to the DSB site and activates it. The mechanism of this activation is not fully understood. One of the interesting roles of ATM is in the positive feedback loop of γ H2AX activation by MDC1 and MRN complex phosphorylation. Also, histone H2AX and MDC1 activation by ATM promotes RNF8 and RNF168 activation in favor of 53BP1 recruitment (6).

1.3.5.5. NHEJ

The human cell repairs DSBs by recruiting two staddle pathways of NHEJ as a less accurate quick way and HR as a slow precise way (63). The cell chooses between HR and NHEJ to repair DSBs based on the cell phase (37). NHEJ is active in all cell phases, especially in G0/G1 and early S phase by directly using the ends of DSBs for ligation (64). But HR is recruited more during the S/G2 phase to perform the error-free repair by using sister chromatid to restore genuine DNA integrity (65,66). Recent findings show that when DSBs occur in DNA transcriptional-associated regions, HR fixes it and NHEJ repairs more chromosome abnormalities in G2 (67).

The NHEJ initiation starts by loading Ku 70/80 heterodimer with strong binding affinity to DNA broken ends. The binding of Ku, protects two DNA ends from nucleases (68). Ku recruits DNA-PKcs to bridge the gap. Another critical function of DNA-PKcs is recruiting Artemis to initiate DNA-end processing (69). KU and DNA-PKcs complex is responsible for DNA-end tethering followed by recruitment of other repair factors for NHEJ like XRCC4, XLF, DNA ligase IV, PAXX, and Artemis in an orchestrated fashion. Each of these recruitment processes facilitates part of NHEJ. XRCC4 is necessary to stabilize LIG4 to make a complex with XLF. This complex establishes the final step of DNA ends ligation. The main elements for DNA end-ligation are Ku heterodimer, XRCC4, LIG4, and XLF (68) (Fig. 3).

1.3.5.5.1. KU

KU is a heterodimer protein with Ku70 and Ku 80 subunits. Ku subunits have a vonWillbrand antigen domain (vWA), C-terminal domain, and core or central domain. The last domain is used for direct binding to DNA and making dimers by forming a ring shape to encompass two ends of DSB. Ku has a strong affinity ($K_d=10^{-9}$ M) for DSB and binds to it in a sequence-independent manner by loading Ku70 close to the DSB end and Ku 80 away from the DNA end. Ku provides a scaffold for loading all DSB repair elements onto the lesion site. Besides DSB end bridging, Ku stabilizes DNA end ligation at the end of DSB repair. Ku has an indirect role in DSB repair by involvement in cell cycle checkpoint activation and apoptosis signaling. It protects the telomere's end from DSB repair trimming and excision (70). A deficiency of Ku70/80 in humans is fatal and disrupts telomere protection and maintenance (71).

1.3.5.5.2. DNA-PKcs

DNA-PKcs is a large (460 KDa) versatile serine-threonine protein kinase with playing different roles from, NHEJ and apoptosis to nonnuclear pathways (72). After DSB, the C terminus of Ku activates DNA-PKcs for DSB bridging to provide a scaffold for recruiting other partners of NHEJ (73). However, the interesting regulatory function of DNA-PKcs laid into its possibility of autophosphorylation. It can be autophosphorylated at S2056 and T2609 HEAT-repeat sites for DNA repair. This autophosphorylation changes the assembly formation of it to the DSB site for disassociation and DSB end ligation. The T3950 autophosphorylation at the kinase domain shuts down the DNA-PKcs kinase activity.

Besides the pivotal role in DSB repair, DNA-PKcs involves in several cancer-related processes. DNA-PKcs interaction with Snail1 (E-box binding transcription factor) drives genomic instability and tumor malignancy. DNA-PKcs phosphorylates Snail1 followed by DNA damage which reciprocally blocks DNA-PKcs activity. Additionally, DNA-PKcs activation is associated with spindle apparatus stability during mitosis by regulation of microtubule dynamics and chromosomal integrity. Recent studies revealed the possibility of functional change in DNA-PKcs performance in cancer by losing its protective activity by tumor progression. Another out of DSBs repair role of DNA-PKcs is its activation by hypoxia through the HIF family in cancer which affects the cell's survival. Also, DNA-PKcs plays a significant role in energy regulation of tumor environment metabolism by phosphorylation of AMPK in glucose deprivation. The other role of DNA-PKcs is its ability to activate tumor-associated immunity response by binding to foreign DNA. This pleiotropic characteristic of DNA-PKcs makes it an attractive target to approach human malignancies through multiple pathways using inhibitors (74,75).

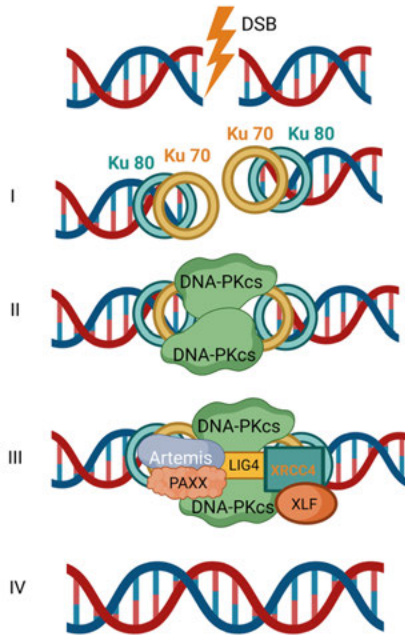


Figure 3. NHEJ pathway steps in repair of a DSB (Created with BioRender.com)

1.3.5.6. HR

HR as a dominant DSB repair pathway at S and G2 phases starts by recruiting MRN complex to flank the DSB for DNA end resection (from 5' end). If DSB ends are not clean (hairpins and proteins), DSB end resection accomplishes with the help of CtIP endonuclease leading to the generation of single strand 3' tail. RPA binds quickly to this single-stranded DNA for protection. Then it replaces by RAD51 and RAD54 which activates the complementary DNA search of sister chromatid and D-loop formation. In the next step, D-loop dissociates and repair continues by non-crossover repair or double Holliday junction structure repair through non-crossover or crossover recombination. The DNA polymerase synthesizes the new DNA on invading strand and finally DNA ligase 1 seals the DNA (5,76).

1.3.5.7. Alternative Pathways for DSB repair

If the main DSB repair pathways are compromised or inhibited, alternative repair pathways can be activated. NHEJ mutations are rare in human cells. For this reason, it is still unclear if components of alternative DSB repair pathways have other functions in DSB processing beyond being distinct NHEJ backup pathways (77,78). However, it is known that DSB repair pathway choice between NHEJ, HR, Alt-NHEJ (Alternative Non-Homologous End Joining) or

SSA (Single-Strand Annealing) is based on difference in DNA end resection activity. Protecting DSB ends with KU70-KU80 allows NHEJ to avoid extensive resection. While Artemis and the DNA-PKcs complex can perform resection, it is minimal, involving fewer than 20 bp. In contrast CtIP and MRN complex carry out extensive 5' to 3' resection to generate 3' overhang for HR, Alt-NHEJ, and SSA. SSA typically needs more homology (>20 pb) base pairs than Alt-NHEJ (4-6 bp). HR requires a homologous template with homology typically greater than 50 bp for efficient repair following DNA end resection (79).

1.3.5.7. 1. Alt-NHEJ

Alt-NHEJ also known as MMEJ (microhomology-mediated end joining) is a backup repair pathway that can be activated when NHEJ is defective. This pathway uses short microhomologies at the break site to rejoin the broken DNA ends. Alt-NHEJ typically operates on less than 20 bp microhomology, most often 4–6 bp. Alt-NHEJ promotes by CtIP and MRN complex resection, followed by PARP 1 and Pol θ (DNA polymerase θ) recruitment as central kinases for Alt-NHEJ. Alt-NHEJ is error-prone and can lead to deletions or insertions at the break site (79,80)

1.3.5.7. 2. SSA

Similar to HR, SSA pathway is mostly active in S and G2 cell cycle phase due to availability of sister chromatid. Some studies suggest that HR and SSA compete for DSB repair in S phase (81,82). SSA uses more than 20 bp of homology (83). BLM and EXO 1 perform extensive resection. Then RPA binds to ssDNA to activate SSA or HR. In this point RAD52, mediate annealing of large homologies in favor of promoting SSA, leading to F (XPF)–ERCC1 complex cutting the residual 3' overhangs before ligation. Finally, XRCC1/Ligase III ligates the DNA ends. In contrast, after BLM and EXO 1 resection and RPA binding, RAD51 mediate strand exchange associated with BRCA1, BRCA2 and RAD54 to promote HR pathway (79–81).

1.3.6. DSB Repair Phases (kinetics)

DSB repair occurs in two distinct phases: a fast phase and a slow phase. The fast repair phase, occurring within the first two hours, primarily involves DSBs located in euchromatin, where the open and accessible chromatin structure allows for the rapid recruitment of NHEJ and HR components. During this phase, NHEJ repairs approximately 80% of DSBs. The slow repair phase, lasting 2 to 24 hours, is associated with DSBs in heterochromatin, where tightly packed chromatin must first undergo modifications and relaxation to permit access for repair components. In this phase, HR plays a more significant role, as it requires extensive DNA end resection and the presence of a

sister chromatid, making it more active in G2 and S phases of the cell cycle (Fig. 4).

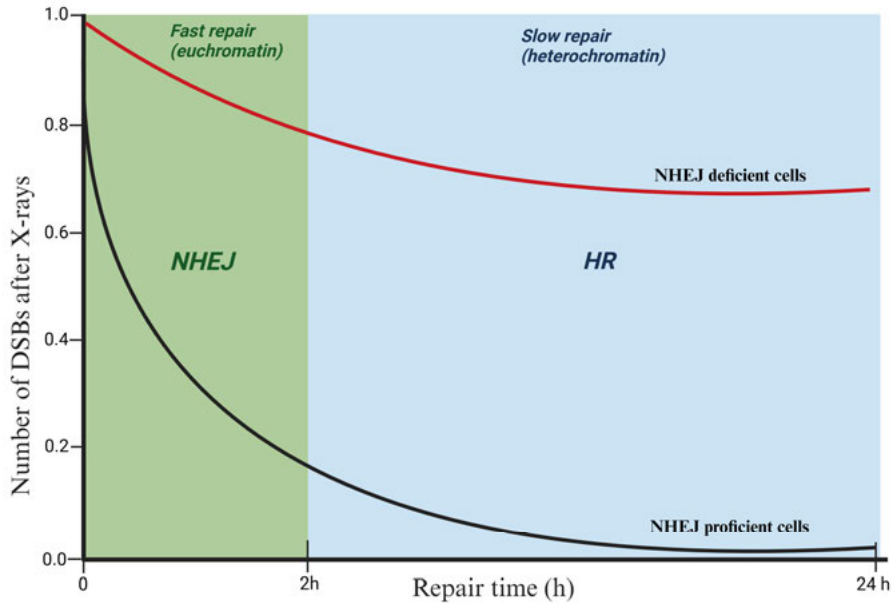


Figure 4. Schematic model of DSB repair kinetics in asynchronous cells. In NHEJ-proficient cells exposed to 40 Gy X-rays, most DSBs are rapidly repaired by NHEJ in the fast phase. The remaining DSBs were repaired by resection-dependent HR in the slow phase of DSB repair. NHEJ-deficient cells fail to efficiently resolve DSBs due to the absence of the primary DSB repair pathway. Illustration adapted from Shibata & Jeggo, 2020 (Created with BioRender.com).

Chromatin remodeling is crucial for facilitating the repair of DSBs, particularly in heterochromatin. Various chromatin-modifying enzymes, such as HATs (histone acetyltransferases) and HMTs (histone methyltransferases), modify histones to relax chromatin, making a more accessible space for repair factors. Proteins like KAP1 (KRAB-associated protein 1) and HP1 (Heterochromatin Protein 1) are phosphorylated to relax chromatin, allowing HR repair. Additionally, ATM, phosphorylates histone H2AX (γ H2AX), to recruit MDC1, 53BP1, and BRCA1, which coordinate the DNA repair. These chromatin modifications is necessary for repair kinases effective operation and prevention of DNA lesion accumulation (84,85).

1.3.7. Cell Cycle and DSB

Mitotic cell cycle in human cells has two phases: interphase (duplication of cellular content) and M phase (mitosis) (segregation of cellular content) for ensuring the timely and correctly duplication of cells and its genomic material.

During S phase (synthesis phase), cells initiate DNA replication. There are two gap phases or G phases before (G1) and after S phase (G2). During G1 phase, cell undergoes growth and preparation for DNA replication. In the G2 phase, DNA replication, which is initiated in the S phase is completed, and the cell prepares for mitosis by checking for DNA damage, repairing errors, and producing proteins necessary for chromosome segregation. M phase has four parts: prophase (chromosome condensation, spindle formation, and nuclear envelope breakdown), metaphase (chromosome alignment), anaphase (chromatid separation), and cytokinesis (cytoplasmic separation).

In interphase, cell cycle progression is controlled before and after S phase. The main regulator of cell cycle progress is activity of CDK (Cyclin-Dependent Kinase) (86,87). CDK1, regulated M phase, CDK2 regulates G1 to S phase progression, and CDK4/6 regulates early G1 phase and G1 to S phase progression. CDK needs cyclin protein to become active. Cyclins (A, B, C, D, and E) are proteins that bind to CDKs to control the transition between different cell cycle phases. For example, in G1, Cyclin D binds to CDK4/6 to help cell to pass through G1 checkpoint. Cyclin E binds to CDK2 to prepare cell for DNA replication in late G1 phase (passing G1 checkpoint) and in the beginning of S phase. Cyclin A, regulates the DNA replication and transition to M phase. Cyclin B drives the cell into M phase for proper cell division. Blocking CDK activity can push the cell from the G1 phase into the G0 phase, a resting state (88).

Cell cycle mainly control DNA replication and subsequent segregation of DNA between daughter cells. In cancer cells, cell cycle checkpoints are not defective and only specific parts of cell cycle control is disruptive. The recent studies showed that cancer cells are mainly disable to exit from cell cycle and as a result they don't stop dividing. Therefore, most of cell cycle machinery must be functional for cancer cells to survive. This point, suggests the importance of difference between DNA damage checkpoint (preventing DNA damage accumulation) and DNA replication stress checkpoints (prevent replication stress-induced DNA damage). Cancer cells often have impaired DNA damage checkpoint, allowing continuous proliferation of cells with accumulation of DNA lesions. But, replication stress checkpoint are rarely defected in cancer cells due to dependency of cancer cells on them to tolerate intense replication stress. Also, cancer cells are dependent to mitotic checkpoint for prevention of chromosome mis-segregation (89).

Cell cycle checkpoints are activated in response to DNA damage during interphase, replication stress in S phase, and spindle assembly failure in M phase. CHK2 (Checkpoint Kinase 2) is crucial for halting cell progression from G1 to S and from G2 to M phase. DSBs can activate CHK2 in interphase via ATM. Then, ATM phosphorylates and activates p53, a tumor suppressor protein that regulates apoptosis and cell cycle arrest. Phosphorylated p53 blocks CDK2 activity and halts the cell cycle. DNA damage in the form of

SSBs activates ATR. ATR then recruits CHK1 to block the activation of CDK1/2, which leads to the inhibition of mitotic entry (90,91)

Cell cycle checkpoints play a crucial role in performing accurate DSB repair and preventing genomic instability. These checkpoints act as surveillance mechanisms that stop cell cycle progression in response to DSB, giving time for repair processes to correct the lesions before the cell proceeds to mitosis. The G2/M checkpoint is particularly important for preventing the segregation of damaged chromosomes to enter mitosis with unresolved DSBs. The checkpoints also coordinate to the replication forks stabilization and regulate the mitotic DNA damage response, to ensure lesion processing after escape from checkpoint surveillance (92). This coordination is done by preventing of excessive origin firing and inhibiting replication fork collapse to avoid accumulation of SSB (91)

During mitosis, main DNA repair pathways are inactivated, but checkpoints stop transition of DNA lesion into mitosis (93). NHEJ is active in G1/S/G2 phase, while HR perform only in S/G2 phase after DNA replication. (94,95) (Fig. 5).

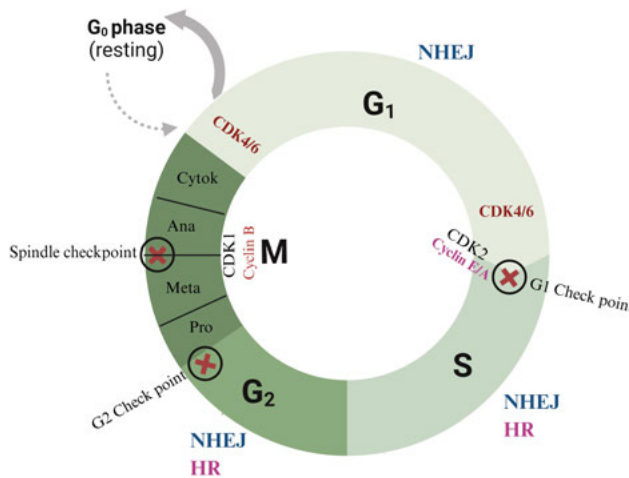


Figure 5. Cell cycle regulation phases and main DSB repair pathways (Created with BioRender.com).

1.4. DNA damage and apoptosis

The apoptotic response is the most sophisticated form of programmed cell death that associates with chromatin condensation, nucleus fragmentation, DNA cleavage, and cell volume reduction (96).

Apoptosis can be activated in both ways of DNA damage dependent and independent. Here DNA damage-dependent apoptosis is briefly introduced.

DSB is one of the main activators of DNA damage-dependent apoptosis. Damaged DNA can trigger apoptosis directly through death receptor FASR (through JNK), mitochondria (JNK), and caspase3/7 (CAD) activation. It can also promote apoptosis indirectly through ATM, ATR, and MYC. Direct activation of FASR, leads to caspase 8/10 phosphorylation which activates caspase 3/7 apoptotic kinase or initiates mitochondrial apoptosis through BID. After phosphorylation of ATR by DNA damage, it activates caspase 2 or p53. Here caspase 2 can initiate mitochondrial apoptosis or activates caspase 3/7 via the mediation of ICAD. Activated p53 elevates the activation of the death receptor FASR and promotes mitochondrial apoptosis through BAX, BCL-2, BCL-XL, and BAK. Phosphorylated ATM, activates the CHK2 checkpoint, then p53 becomes activated and promotes mitochondrial apoptosis or the FASR pathway. The involvement of MYC in DNA damage-dependent apoptosis is still not fully revealed. It is shown that activating MYC after DNA damage, phosphorylates NOXA, which leads to mitochondrial apoptosis (97).

1.5. DNA damage and necrosis/necroptosis

While apoptosis is well defined after DNA damage, emerging evidence suggests that DDR can also trigger necrosis/necroptosis under certain conditions (98). Necrosis considered an unregulated, accidental form of cell death caused by severe stress like overwhelming DNA damage. However, recent data show that specific DDR failures can lead to necrotic cell death. Complex DSBs from radiation or genotoxic agents can overwhelm NHEJ and HR repair machinery leading to ATP (Adenosine Triphosphate) depletion, mitochondrial dysfunction, and plasma membrane rupture leading to necrosis (99). Necroptosis is a programmed form of necrosis, mediated by receptor-interacting protein kinases RIPK1 (Receptor-Interacting Protein Kinase 1) and RIPK3, along with the pseudokinase MLKL. DDR pathways related to activation of PARP and ATM, have been associated to necroptosis (100). When PARP is overactivated under extensive DNA damage, NAD⁺ (Nicotinamide Adenine Dinucleotide) and ATP will be depleted leading to necroptosis activation. Some studies showed that PARP1 inhibition downregulates necroptosis in favor of necrosis after DNA damage due to preventing loss of energy through NAD⁺ and ATP depletion. Other studies showed opposite effect due to shifting cell death from caspase-dependent apoptosis to caspase-independent necroptosis (101). DNA damage typically induces apoptosis via p53-dependent pathways. However, when apoptosis is inhibited (e.g., by caspase inhibitors), DDR can activate necroptosis through RIPK3 and MLKL, especially in apoptosis-resistant cancer cells (102,103). DDR can exploit to manipulate necroptosis for cancer

treatment. For example, treating apoptosis-resistance cancer cells with PARP or ATM inhibitors could enhance treatment effect by inducing necroptosis (104).

1.6. DNA damage repair and cancer

1.6.1. Genomic Instability and Mutation Accumulation

DNA damage is critical in the development and progression of cancer. The mechanisms of DNA damage involve interactions between genetic and environmental factors, resulting to genomic instability, mutations, and uncontrolled cell proliferation. Genomic instability, is one of hallmarks of cancer, originates from defective DNA repair mechanisms. If this instability leads to mutations in critical genes, such as tumor suppressors and oncogenes, over time, these mutations could drive tumor formation, cancer progression, and metastasis (105,106). There are three main contributors to genomic instability: replication stress which drives from oncogene activation and rapid cell proliferation leading to replication errors (107). Chromosomal instability from defects in DNA repair pathways which leads to chromosomal abnormalities and rearrangements (108). Epigenetic alterations such as DNA methylation and histone modifications can impair DNA repair machinery gene expression (109).

1.6.2. Defects in DNA Repair Pathways

DNA repair pathways are vital for genomic integrity maintenance. However, defects in these pathways can lead to DNA damage accumulation and cancer development. Defects in these pathways, mainly HR and MMR, are significantly associated with cancer development (110). Many cancer types are associated with different types of genetic instability related to DNA damage repair genes such as deficiency in mitotic spindle checkpoint with chromosomal instability in breast cancer, BRCA1 and BRCA2 mutations in hereditary ovarian and breast cancer (impairing HR), and mismatch repair deficiency in hereditary non-polyposis colorectal cancer (38,111). DNA-PK has lower expression associated with genomic instability in the head and neck, and breast cancer (112) whereas overexpression of DNA-PKcs in several cancer types has been linked to poor prognosis. Defective ATM protein leads to ATR upregulation in oral squamous cell carcinomas and higher stages of breast cancer tumors are associated with elevated ATR and pCHEK1n (113).

1.6.3. DNA Damage in Tumor Progression

Once cancer is initiated, DNA repair impairment fuels tumor progression in three ways. Mutation in cell cycle checkpoint regulatory genes such as *TP53*, allow cancer cells to escape from proliferation arrest and apoptosis (114). Genomic instability, can accelerate acquisition of mutations that gives cancer cells the ability of invasion and metastasis (115). DNA repair pathway defects can render resistance trait to cancer cells against chemotherapy and radiation (116).

1.6.4. Targeting DNA Repair Pathways

Defects in DNA repair pathways provide a window of opportunities for targeted therapies. For example, PARP inhibitors can yield synthetic lethality (explained later) in cancer cells with HR deficiency (BRCA-mutated tumors) (117). ATR and CHK1 Inhibitors target replication stress in cancer with HR impairment or high replication stress. DDR inhibitors such as DNA-PK and ATM inhibitors have the potential of tumor radiosensitization (118).

1.6.5. Combination therapy

Combining DDR inhibitors with other cancer therapy modalities has shown promising results. The data showed that DDR inhibitors can enhance DNA-damaging agent's effect by hindering cancer cells from DSB repair, when combined with irradiation. For example, in ovarian cancer, the DDR is frequently defective, which is linked to the cancer's development and resistance to chemotherapy. These alterations are significant in high-grade serous carcinoma (HGSC), where about half of the cases show defects in HR pathway which can be targeted by inducing DSB via radiation and then inhibiting the DSB repair by HR inhibitors (119). Several studies suggests that DDR defects can elevates cancer cell's immunogenicity, making combination with immune checkpoint inhibitors an effective strategy. DDR inhibitors like PARP induce DSBs and genomic instability, leading to micronucleus (MN) formation and cytosolic DNA (DNA presence in cytoplasm instead on nucleus) accumulation in cancer cells. The innate immune system detects MN and cytosolic DNA as pathogenic, similar to viral nucleic acids, triggering interferon (IFN) signaling (cGAS-STING-IFN pathway) and subsequent immune activation (120). For example pamiparib (PARP inhibitor) treatment elevates the PD-L1 expression in pancreatic cancer cells, which in combination with PD-L1 mAb, enhances therapy effectiveness over PARP monotherapy (121).

1.6.6. Synthetic lethality

Although these kinds of mutations make cancer cells hard to eradicate but might open a therapeutic opportunity, based on DSB repair biology called synthetic lethality. To overcome the treatment resistance problem, we need to aim at the common characteristics of a wide range of tumors. Induction of DSB by oncogenes is a common condition of all cancer cells. Oncogenes induce aberrant proliferation of cancer cells which elevates DNA replication stress and DSB rate with the possibility of telomere erosion and caretaker genes mutations. Induced DSB in cancer cells trigger the DDR and put the cell in the repetitive cycle of DSB and DDR. Cancer cells' DDR pathways (partially defective but working and active) normally rely on the S/G2 checkpoint for continuous proliferation which makes it an interesting target to stop the cell from dividing. It means we can use the cancer cell's survival strategy against itself based on the synthetic lethality concept (122). Synthetic lethality refers to a condition that one defective cellular pathway enforces the cell to shift to another pathway as a backup to survive which is not to be used under the cell's normal status (6). Simultaneous perturbation of both pathways will end in cell death. But this strategy is applicable just for the portion of cancer types or subtypes that has defective DNA repair pathways. For capturing the therapeutic window in all cancer types we need to induce conditional synthetic lethality by manipulating of cell's metabolic condition and environmental stress (123).

For example, it was shown that genotoxic stress induction by radiation and HSP90 inhibitor onalespib led to overcoming cisplatin resistance in ovarian and head and neck cancer (124). Many DNA repair proteins like ATM and DNA-PKcs are HSP90 protein clients. Another example of targeting the DNA repair system is the use of PARP inhibitors. HR pathway deficiency has been detected in pancreatic, ovarian, breast, and prostate cancers which increases tumor cells' genomic instability. HR becomes defective when BRCA 1 and BRCA 2 genes are not functional, then the 5' DSB end can't be resected and as a result 3' end overhang can't be loaded by RAD51. The BRCA-defective cells can normally repair this lesion by using BER instead, but the use of PARP-inhibitors will block BER and lead to synthetic lethal therapy of BRCA-deficient tumor cells. PARP inhibitors can kill cancer cells from multiple pathways. One way is by blocking BER which leads to the conversion of SSB to DSB and death of the cell for being not able to repair these DSBs during the S phase by HR. The other mechanism is the trapping of the PARP1 enzyme inside chromatin (125–128).

2. Aim

The overall aim of this thesis is, first, to understand how to exploit DSB formation and NHEJ repair pathways in the context of combination therapy to sensitize cancer cells to chemotherapy and irradiation. Second, to reveal the nature and involvement of DSB and NHEJ repair pathways in different types of DNA damage with varying complexities in cancer cells.

The specific aims of the thesis are presented below in the form of the studies performed:

- The aim of **paper I** was to investigate the DSB-inducing potential of the new generation of HSP90 inhibitors, onalespib, to overcome cisplatin resistance in ovarian cancer
- In **paper II** the goal was to explore the DSB-inducing potential of HSP90 inhibitors, onalespib, to overcome radiotherapy resistance in patient-derived glioblastoma
- The aim of **paper III** was to explore the nature and involvement of DSBs induced by Ra-223 in different prostate cancer cells
- The goal of **Paper IV** was to explore the effect of ascorbate-induced oxidative stress on DSB generation and NHEJ pathway in colorectal cancer cells
- The aim of **paper V** was to investigate the effect of different levels of DSB complexity on NHEJ pathway

3. Results

3.1. Paper I

Overcoming Limitations of Cisplatin Therapy by Additional Treatment with the HSP90 Inhibitor Onalespib

3.1.1. Introduction and Aim

Cisplatin has been in use for over 40 years and is a cost-effective first-line treatment for several solid cancers, including ovarian, head and neck, and testicular (129). It works by forming DNA inter- or intra-strand crosslinks through binding to reactive metal-binding sites of N7 atoms of guanine and adenine bases in the DNA major group. The drug also interacts with many nucleophilic non-DNA targets in the cytoplasm due to its highly electrophilic properties leading to additional cytotoxic effects against cancer cells (130). The effectiveness of this compound varies with different cancers, with ovarian and head and neck cancers providing the greatest challenge due, in part, to the development of resistance (131,132). Acquisition or innate resistance of cisplatin has been linked to multiple mechanisms, primarily involving reduced uptake and accumulation of the drug in cancer cells due to the downregulation of copper 1 and 2 transporters (CTR1 and CTR2) as cisplatin intracellular active transporters and increasing cisplatin efflux from through activity of copper efflux proteins (ATP 7A and ATP7B) (133–136). Additionally, altered nucleotide excision repair (NER) pathways by upregulating ERCC1 which acts in DNA excision, and activation of general stress response pathways via heat shock proteins have been linked to increased cisplatin resistance (133,137).

HSP90 is a highly conserved molecular chaperone that plays an important role in the formation and maturation of proteins involved in a variety of cellular pathways, making it a promising target in cancer therapy (138,139). Over 300 HSP90 client proteins have been discovered such as epidermal growth factor receptor family (EGFR), signal transduction proteins (AKT and ERK), and DNA damage response proteins (ATM and DNA-PK) (140). Many of these proteins are related and overexpressed in cancer which makes malignancy addicted to them. This cancer cell dependency gives the opportunity of cell killing using HSP90 inhibitors by blocking multiple oncogenic pathways simultaneously. HSP90 inhibitors can block the client protein chaperoning

function by targeting N-terminal ATPase. Newer generations of HSP90 inhibitors like onalespib (AT13387) with less hepatotoxicity, and better biological function are in phase II of clinical trials in treatment of solid tumors (141). Due to the similar effect of ionizing radiation and cisplatin we hypothesize that maybe onalespib can potentiate the cisplatin effect via elevated DSB levels. This combined treatment is of great interest as it provides more accessible and cheaper cancer treatment.

In this study, we investigated the ability of the new HSP90 inhibitor onalespib to increase the effectiveness of cisplatin and reverse cisplatin resistance *in vitro* in cancer cell lines. We tested the effects of the drugs on the head and neck squamous cell carcinoma cell line H314 and on ovarian cancer cell lines SKOV3, A2780, and its resistance clone A2780CIS, and also studied the molecular mechanisms of the combination treatment.

3.1.2. Methods

Cell lines: the human ovarian cancer cell line SKOV3, human head and neck squamous cell carcinoma cell line H314, human ovarian cancer cell lines A2780, and the cisplatin resistant clone A2780CIS.

Assays: XTT viability assay, clonogenic survival assay, wound healing assay, *Trans*-well migration assay, western blot, flow cytometry analysis of apoptosis, cell-cycle distribution, γ H2AX and 53BP1 expression analysis via Immunofluorescence Staining (Confocal Microscopy).

3.1.3. Results

The optimal concentration of cisplatin and onalespib were defined by XTT viability assay and clonogenic assay after 24 h and 72 h of incubation with drugs.

XTT assay: The cisplatin monotherapy decreased all cell lines' viability measured by XTT assay in a concentration-dependent manner. The A2780 cell line was the most sensitive cell to 500 nM cisplatin mono treatment (72 h) by losing >50% of viability. The viability of SKOV3 and H314 cells decreased by 57.5 and 53 % when exposed to 10 μ M cisplatin and by 70 and 71 % when exposed to 25 μ M. Similarly, 10 μ M and 25 μ M cisplatin caused a decrease in viability in the A2780CIS cells of 58 and 98 %, respectively. The XTT test showed that as the concentration of onalespib increased, its effect of decreasing cellular viability intensified. At 100 nM there was an 11% and 45% drop in SKOV3 and H314 cells, respectively, while 1 μ M caused a decrease of 60% and 90% in the same cells. The strong effects were seen in A2780 and A2780CIS cells which were much more sensitive to the monotherapy of onalespib. With 100 nM, a decrease of 80% and 70% were recorded, and nearly complete elimination of viability was seen when the concentration was increased to 1 μ M. At 72 h, a significant decrease in viability was seen in all

combination treatments with 10 μ M cisplatin compared to monotherapy, effectively reducing survival to near zero. The effects of the combination were greater at higher concentrations of cisplatin (500 nM) and onalespib (\leq 100 nM).

Clonogenic assay: In the clonogenic assay, combination therapy of cisplatin and onalespib decreased survival fractions (SF) across all cell lines compared to untreated controls and onalespib mono treatment, with A2780 and H314 cells being the most sensitive. The 500 nM cisplatin and 100 nM onalespib combination significantly decreased cell colony-forming ability compared with onalespib monotherapy in all cell lines ($p \leq 0.05$). Clonogenicity of H314 and A2780 cells decreased significantly ($p \leq 0.0001$) in all combinations. Combinational exposure led to smaller, and more irregularly shaped colonies (Fig. 6).

Cell cycle: Cell cycle analysis of SKOV3 cells with PI staining after combinational exposure (500 nM cisplatin and 100 nM onalespib) for 96 h showed an increased signal of G2/M arrest (32.5%) compare to cisplatin (12.1%) and onalespib (26.6%) mono treatment.

Foci assay: Cisplatin and onalespib dual therapy significantly elevate the DSB biomarker's (γ H2AX and 53BP1) response level compared to monotherapy in SKOV3 and A2780CIS cells (Fig. 7).

Apoptosis assay: The dual treatment significantly increases apoptotic response in SKOV3 and A2780CIS cancer cells compared to mono treatment groups. Flow cytometry analysis with Annexin V and caspase 3/7 showed that the combination therapy of 500 nM cisplatin and 100 nM onalespib yielded 45% Annexin V and 72% caspase 3/7 activity in SKOV3 cells and 20% Annexin V and 27% caspase 3/7 activity in A2780CIS cells which significantly more than either mono treatments (Fig. 8).

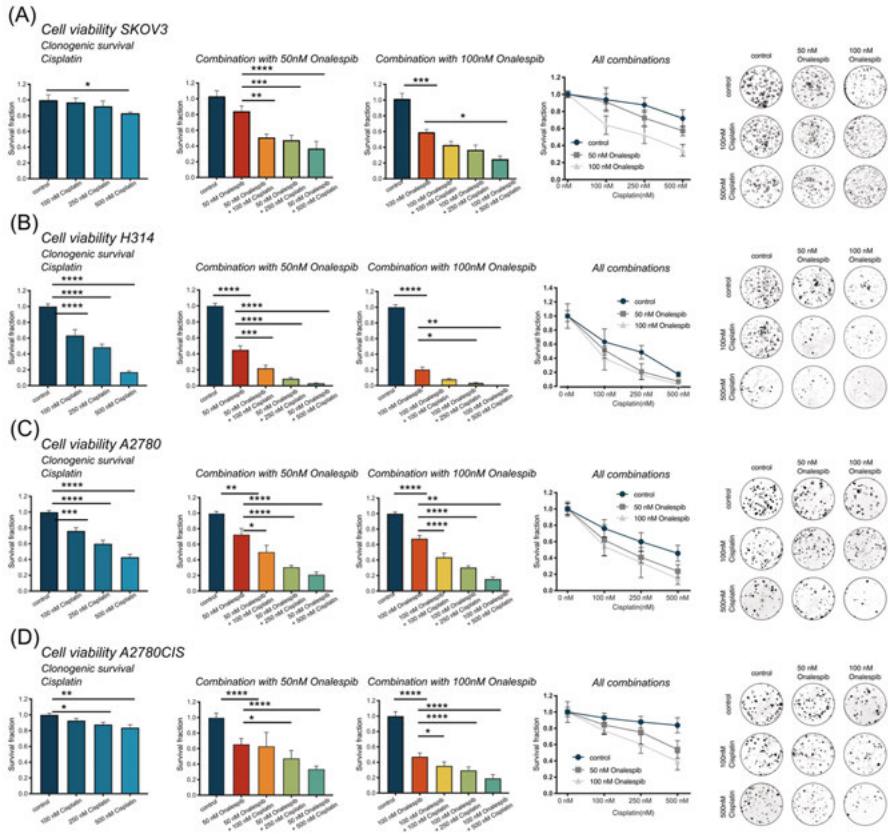


Figure 6. Clonogenic assay results of SKOV3, H314, A2780, and A2780CIS cells after exposure to 0, 100, 250, and 500 nM cisplatin or in combination with 50 or 100 nM onalespib for 24 h. N = 3, error bars = SD. * $p < 0.05$, ** $p < 0.01$, *** $p < 0.001$, **** $p < 0.0001$.

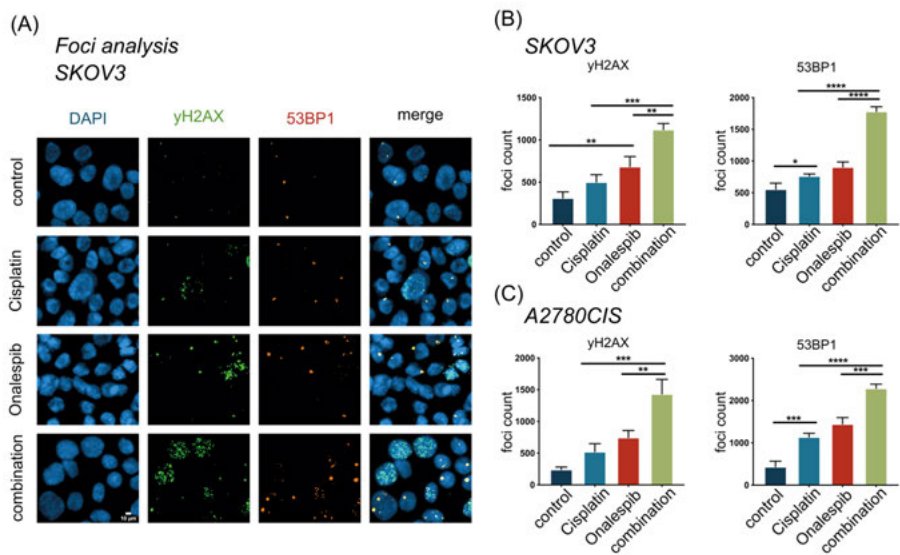


Figure 7. The DSB biomarkers of γ H2AX and 53BP1 in SKOV3 cells were significantly more expressed in combinational treatment group (500nM cisplatin + 100nM onalespib, 96 h exposure) than monotreatment. error bars = SD. $**p < 0.01$, $***p < 0.001$, $****p < 0.0001$.

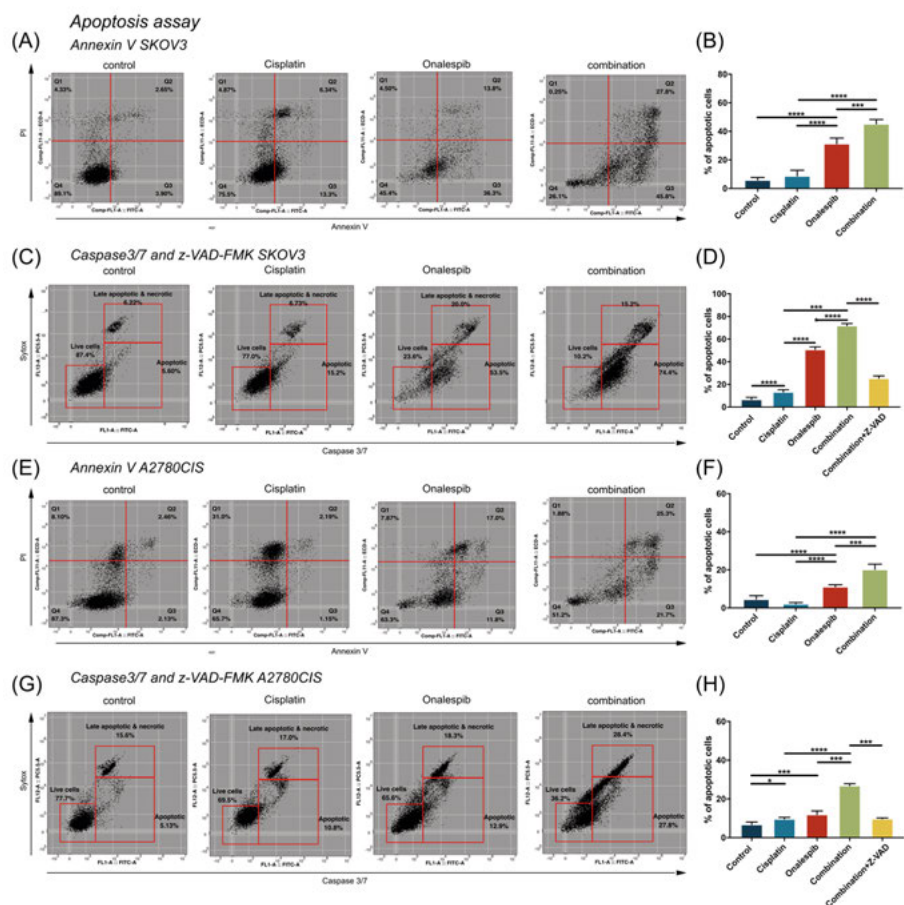


Figure 8. Apoptotic biomarkers (Caspase3/7 and Annexin V) were significantly increased after combinational exposure (500 nM cisplatin and 100 nM onalespib exposure for 96 h) in comparison with mono treatment at SKOV3 and cisplatin-resistant cell line A2780CIS. error bars = SD. $*p < 0.05$, $**p < 0.01$, $***p < 0.001$, $****p < 0.0001$.

3.1.4. Discussion and conclusion

Cisplatin, one of the most widely used cancer drugs, despite of high initial response, has limitations such as rapid resistance development and adverse side effects, leading to the exploration of combination therapies (131). Multiple studies have shown that using HSP90 inhibitors like onalespib in combination therapy, is effective in reversing drug resistance in several cancers, due to blocking a wide range of vital proteins for the survival of cancer cells such as DNA damage repair proteins. However, there is still limited knowledge of the mechanisms behind this. In this study, four cell lines (SKOV3, H314, A2780CIS, and A2780) were selected because of their cisplatin-resistant development. The A2780 is cisplatin sensitive and the parent of the A2780CIS cisplatin-resistant cell line. Results showed that onalespib monotherapy was

effective against all cell lines, with A2780 being particularly more sensitive than others. However combinational exposure was significantly more effective than either mono treatment with consistent results at both XTT survival and clonogenic assay in accordance with previous studies (142). The potent effect of combined treatment is likely due to the DNA repair inhibition by onalespib after DNA damage induction of cisplatin. Even though cisplatin monotherapy did not affect the proliferation and migration of cells in wound healing assays, combination therapy reduced it in a dose-dependent manner. The combination therapy reduced the proliferation of H314 without affecting its migration but it reduced both traits at SKOV3. Dual treatment significantly increased SKOV3 cell apoptotic levels consistent with previous studies (143).

Onalespib monotherapy significantly downregulated EGFR and AKT expression at both 50 and 100 nM but cisplatin treatment did not affect their expression significantly which made it difficult to interpret the combination treatment effect using Western blot.

The main DNA damage effect of cisplatin is through intra-strand crosslinks which activate the NER repair pathway. The ERCC1 is the main player in the NER repair pathway which is upregulated in cisplatin resistance. However, nucleotide excision of cisplatin-generated DNA adducts via NER can produce DSBs. As a result, these DSBs could not repair effectively due to the general inhibition of ATM, ATR, and DNA-PKcs by onalespib. This inhibition can lead to DSB accumulation and shift the dominant repair pathway from NER to the NHEJ pathway. Significantly increased γ H2AX and 53BP1 DSB biomarkers in the combination group supported this fact.

In conclusion, our results showed the effective participation of onalespib in the elevation of cisplatin potency and toxicity in cisplatin-resistant cells leading to higher DSB induction and apoptotic rate.

3.2 Paper II

Enhancing Glioblastoma Therapy: Unveiling Synergistic Anticancer Effects of Onalespib-Radiotherapy Combination Therapy

3.2.1. Introduction and Aim

Glioblastoma (GBM) is the most prevalent brain tumor in adults, with a median survival time of less than 15 months despite treatment (144). Its occurrence in children constituting 3–15% of primary central nervous system (CNS) tumors. Despite the rarity, pediatric GBM is resistant to therapy and has a high mortality rates, with a 5-year survival of less than 20% (145,146). The upregulation of DNA damage response (DDR) have been described as important contributors to GBM drug resistance (147). The mechanisms behind GBM

resistance to treatment are poorly understood, emphasizing the urgent need for new treatment modalities.

Recent data showed the molecular chaperone heat shock protein 90 (HSP90) as a promising target for radiation treatment improvement in GBM (139,148–152). HSP90 inhibitors have higher affinity for the intertumoral HSP90 compared to the HSP90 in normal cells, due to the increased ATPase activity of HSP90 in tumor cells (153). We used Onalespib, a second-generation HSP90 inhibitor with tolerable toxicity profile (154) and the ability of penetrating the blood-brain barrier (155). Onalespib already has undergone phase I clinical trials (156). Furthermore, efficacy of Onalespib against gliomas as a single agent or as a combination therapy with TMZ have been demonstrated *in vitro* and *in vivo* (155). This onalespib effectiveness can be associated to ability of targeting several DDR pathways (151).

We aim here to investigate the effectiveness and molecular mechanisms of combining the HSP90 inhibitor Onalespib with external beam radiotherapy in GBM cell lines *in vitro*, providing a robust model to explore GBM's genetic diversity. The widely used U343 MG and U87 MG cell lines, characterized by wild-type p53, are valuable for studying radiation resistance and tumor invasiveness. However, their long-term culturing may have diminished their molecular complexity. In contrast, the patient-derived lines U3013MG and U3024MG retain genetic heterogeneity (157), exhibit sensitivity to specific therapies, and display distinct DNA repair defects. This combination approach bridges personalized GBM therapy development with the continuity of existing research.

3.2.2. Methods

Cell lines: glioblastoma cell lines U87 MG (HTB-14), U343, the human patient-derived GBM cells U3013MG and U3024MG.

Assays: XTT viability assay, clonogenic assay, Migration/Proliferation assay, Proteomic analysis Proximity Extension Assay, Proximity Extension analysis, cell cycle distribution, Immunofluorescent Biomarker of DSB repair, western blot.

3.2.3. Results

XTT assay: Four cell lines U343 MG, U87 MG, U3013MG, and U3024MG were treated with varying Onalespib doses, followed by radiation after 24 hours, with viability measured 72 hours post-treatment. Results showed dose-dependent reductions in cell viability for established cell lines U343 MG and U87 MG under both monotherapies, with Onalespib (100 nM) reducing viability by 47% and 44.5%, respectively. U87 MG was more radiation-sensitive, with 46.4% survival at 4 Gy compared to 68% for U343 MG. Combined treatment further decreased viability, demonstrating synergistic effects at higher

drug doses (>10 nM) and 6 Gy radiation. Additive effects were seen at lower radiation doses unless Onalespib concentrations exceeded 50 nM for U343 MG. In patient-derived lines, U3013MG and U3024MG were less responsive to low Onalespib concentrations, with significant reductions only at 100 nM. However, both lines were highly radiation-sensitive, with viability reduced by 70.1% and 82% at 2 Gy, respectively. Synergy was observed at specific drug-radiation combinations: U3013MG showed synergy at 10–50 nM with 6 Gy, while U3024MG exhibited synergy at 100 nM combined with 4 or 6 Gy. Overall, combined treatment was most effective across all cell lines, particularly at higher drug and radiation doses.

Clonogenic and spheroid growth assay: Clonogenic and 3D tumor spheroid assays confirmed the potent efficacy of Onalespib combined with radiation in glioblastoma models. Clonogenic assays revealed that both treatments independently reduced survival in a dose-dependent manner, with complete colony loss at 50 nM Onalespib, regardless of radiation. Combination therapy showed enhanced efficacy, significantly reducing clonogenicity even at lower radiation doses. For instance, 2 Gy with 25 nM Onalespib decreased colony formation by 78.2% (U343 MG) and 83.5% (U87 MG). In 3D tumor spheroids, combined treatment also outperformed individual therapies, though spheroids exhibited lower sensitivity than 2D models. Untreated spheroids showed rapid growth, with volumetric increases of 1386% (U343 MG) and 3720% (U87 MG) after 14 days. In contrast, 250 nM Onalespib and 6 Gy slowed growth to 14% and 41%, increasing doubling times to 67.31 and 26.23 days, respectively. Synergistic effects were confirmed with Loewe synergy scores >10 for several drug-radiation combinations. Live-dead cell analysis revealed higher doses increased dead cell populations, despite similar spheroid sizes three days post-treatment. Limiting dilution assays demonstrated a dose-dependent decline in spheroid-forming efficiency for U87 MG, U3013MG, and U3024MG cells. Untreated controls formed spheroids efficiently, while combination therapies substantially inhibited this capacity (Fig. 9).

DSB repair Foci assay: We assessed DDR (53BP1 and γ H2AX foci) in U343 MG and U87 MG cells treated with Onalespib, radiation, or their combination. Onalespib and radiation monotherapies significantly increased foci, with Onalespib causing a stronger effect than radiation. Combining Onalespib with radiation further amplified DSB accumulation. At 6 Gy, the combination led to dramatic increases in 53BP1 and γ H2AX foci, indicating overwhelming DNA damage and impaired repair. U87 MG cells showed a smaller increase in foci compared to U343 MG, but the combination still resulted in poor DSB repair. Foci co-localization of 53BP1 and γ H2AX was observed, with some proteins localized in distinct nuclear regions. Western blot analysis confirmed increased γ H2AX expression in all treatment groups, especially with radiation. Overall, Onalespib combined with radiation effectively decreased DSB

repair capacity by inducing complex DSBs, significantly impairing repair in both cell lines (Fig. 10).

Cell cycle distribution: We used flow cytometry to analyze the cell cycle distribution in U343 MG and U87 MG cells after 48-hour exposure to Onalespib (100 nM), radiation (2 and 4 Gy), and their combinations. Radiation (4 Gy) reduced the G0/G1 phase population and increased G2/M phase cells, with a stronger G2/M arrest observed when combined with Onalespib. In U343 MG, 21% were arrested in G2/M, and in U87 MG, 31% were arrested. Onalespib also reduced S-phase cells, particularly in U87 MG. These changes were statistically significant. Western blotting revealed Onalespib suppressed p21 expression, while radiation alone or with Onalespib increased p21, indicating cell cycle arrest and activation of cell death pathways.

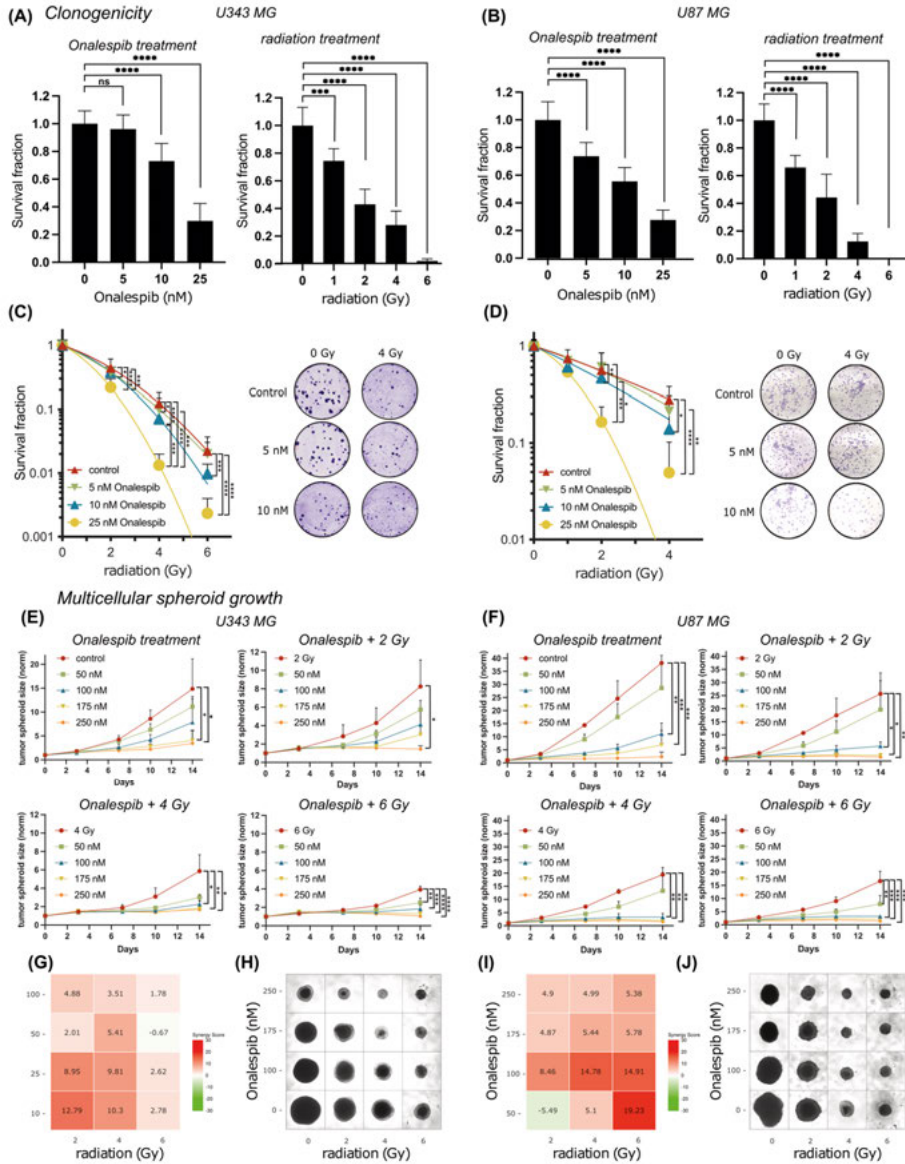


Figure 9. Colonogenic survival and spheroid growth of U343 MG and U87 MG cells. SF of Onalespib and X-ray of U343 MG A) and U87 MG cells B) SF of Onalespib and X-ray combination of U343 MG C) and U87 MG D). Colony images of the mono and combined exposures of Onalespib and X-rays. Onalespib mono and combine therapy with X-ray in spheroid of U343 MG E) and U87 MG F). Normalized spheroid volume (mm³) over time, (means \pm SD, $n \geq 3$). Synergy scores for U34mg G) and U87 MG I). Representative spheroid images of the U343 MG and U87 MG at the endpoint (H) and (J). Data plotted as means \pm SD, $n \geq 3$. * $p < 0.05$, ** $p < 0.01$, *** $p < 0.001$ and **** $p < 0.0001$.

DSB analysis-U343 MG

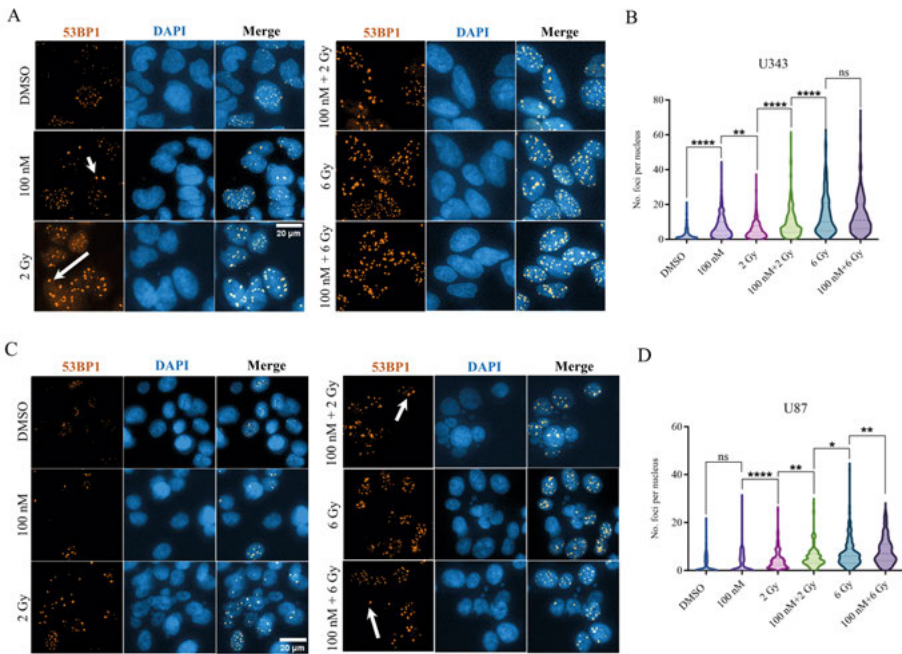


Figure 10. 53BP1 foci quantification of U343 MG and U87 MG cells. A) Confocal images of U343 MG cells exposed to 100 nM Onalespib and 2-6 Gy X-rays. Arrows show counted 53BP1 foci. B) Plots of U343 MG, 53BP1 foci per cell. C) Microscopy images of U87 MG cells exposed to 100 nM Onalespib and 2-6 Gy X-rays. Arrows show 53BP1 foci. D) Plots of U87 MG, 53BP1 foci per cells. Data presented as means \pm SD, n = 2. * $p < 0.05$, ** $p < 0.01$, *** $p < 0.001$ and **** $p < 0.0001$.

Proteomics: Proteomic analysis of U343 MG cells treated with Onalespib, radiation, and their combination showed substantial protein expression changes impacting cancer pathways. Onalespib predominantly downregulated tested proteins, radiation upregulated them, and combination therapy amplified necrosis and apoptosis markers like c-Flip and caspases. Radiation-induced DNA damage increased p21, reversing Onalespib's suppression and promoting cell cycle arrest. Onalespib reduced FOLR3 and FOLR1, counteracting radiation's folate demands and possibly reducing tumor aggressiveness. VEGFA expression dropped significantly with combination therapy, suggesting impaired tumor vascularization. TRAIL, linked to apoptosis and necrosis, surged with combination therapy, intensifying tumor cell death. Functional pathway analysis highlighted reduced growth signaling, enhanced immune modulation, p53-driven DNA damage responses, and increased apoptosis, emphasizing the combination treatment's potential to synergistically disrupt tumor progression (Fig. 11).

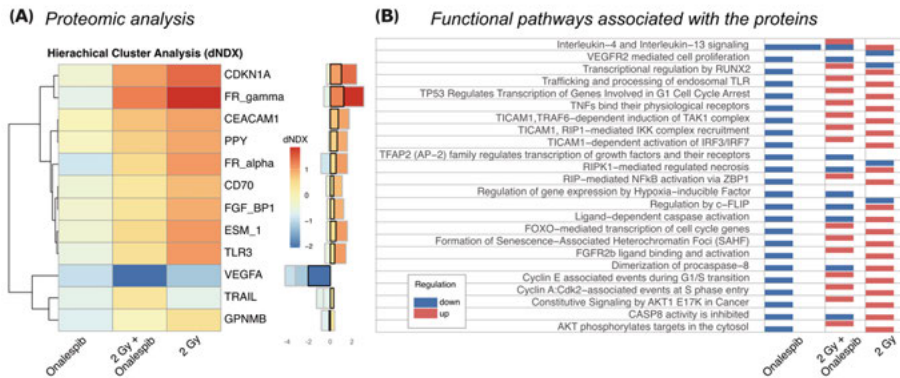


Figure 11. A) Panel of differential proteins expressed between treatments ($SD > 0.5$). Hierarchical clustering analysis shows the most notable changes in protein expression degrees observed in U343 MG cells treated with X-ray, Onalespib, and their combination, relative to control. The value highlighted in red, indicates higher expression compared to control, and negative values are in blue, showing lower expression. B) Functional analysis indicating the biological pathways where the differential protein expression is depicted.

3.2.4. Discussion and conclusion

GBM's poor prognosis stems from HSP90 overexpression and aggressive growth. HSP90 is 2- to 10-fold higher in cancer cells, aiding survival during tumorigenesis (155,158). Targeting HSP90 with agents like Onalespib, which passes the blood-brain barrier, may improve treatment efficacy (159,160). Combination therapy, including Onalespib and radiotherapy, enhances anti-tumor effects by decreasing cell viability and clonogenicity in glioma cell lines.

In tumor spheroid models, mimicking hypoxic conditions, Onalespib reduced proliferation and spheroid formation, with combination therapy showing the strongest effects. This aligns with other studies showing radiosensitizing effects of HSP90 inhibitors in GBM spheroids (161,162). Furthermore, Onalespib reduced wound healing, impacting migration and invasion, though the specific interaction with EPHA2 was not observed in our analysis (163,164).

Onalespib disrupts DNA repair, increasing DSBs, as evidenced by γ H2AX and 53BP1 foci, suggesting inhibition of repair pathways, including homologous recombination and non-homologous end joining. This enhanced radiosensitivity was seen in combination treatment, particularly in U343 MG, though U87 MG showed resistance, likely due to its stronger DNA repair capacity (151). Studies also indicate Onalespib's synergistic effects with TMZ in glioma models (155). Moreover, it increases radiosensitivity in hypoxic regions, often resistant to radiotherapy (147,161).

Proteomic analysis confirmed Onalespib's impact on protein expression in several functional pathways, particularly p21, which was upregulated in the combination treatment, highlighting its role in cell cycle arrest and DNA repair (165–168). VEGFA, linked to angiogenesis, was reduced by both treatments, with the combination showing stronger inhibition. TRAIL, involved in apoptosis and necroptosis, was notably elevated in the combination group, suggesting enhanced cell death pathways (169–171).

Despite promising results, this study has limitations, such as the use of the U87 MG cell line, which may not fully represent the original model (172). Further studies with glioma organoid models and traditional validation methods like Western blotting are needed. While Onalespib showed no adverse effects in other tumor models (149), its potential neurotoxicity in brain tissue requires further investigation. Preclinical studies should assess its impact on brain cell survival and neurogenesis.

Overall, our findings support combining Onalespib with radiotherapy as a promising strategy for GBM treatment, especially for resistant cases. However, more research is needed to optimize dosing and evaluate toxicity in clinical settings.

3.3 Paper III

Ra-223 Induces Clustered DNA Damage and Inhibits Cell Survival in Several Prostate Cancer Cell Lines

3.3.1. Introduction and Aim

Radium-223 dichloride, an analog of calcium that can bind to bone hydroxyapatite in newly formed bone structures, is one of the alternatives for the treatment of bone metastatic prostate cancer. In this type of targeted alpha therapy, the patient's survival increases to 3.6 months with less pain (173). However, the molecular mechanism of Ra-223 action is not fully understood especially in the DSB generation and repair context. In this study, we produce a bone-like structure to mimic the bone metastatic condition to study Ra-223 interaction with bone and prostate cancer cells. First, we explored the bone surface interaction and cell internalization of Ra-223. Then the survival and growth of cells were examined in 2D and 3D spheroid models. The DSB repair and generation were studied using PFGE and immunofluorescent staining of DSB biomarkers. Finally, we examined cell fate using an apoptosis assay. The study results showed extremely stable bonding of Ra-223 with the hydroxyapatite (HAp) without cancer cell internalization. The conditioned Ra-223 on the HAp-coated surface reduced cell clonogenicity and 3D spheroid growth higher than free Ra-223. Also, drug treatment activated NHEJ consistent with high-LET radiation outcomes

leading to high levels of apoptosis. The toxicity of Ra-223 is likely related to α -particles decay and its interaction with the nucleus.

3.3.2. Methods

Cells: Prostate cancer PC3 and brain metastatic prostate cancer DU145 cells, and Prostate cancer 22RV1 cells.

Assays: Clonogenic assay, Spheroid assays, apoptosis, PFGE, DSB repair foci assay, flowcytometry, western blot, real-time affinity measurements with LigandTracer.

3.3.3. Results

LigandTracer: Real-time affinity quantification of Ra-223 with HAp surface and with DU145 cells using LigandTracer showed extremely strong binding of Ra-223 and HAp within 2 h with >99% continuous affinity signal until 24h without disassociation (Fig. 12A). Interestingly cells didn't uptake Ra-223 within 2 h (Fig. 12B).

Clonogenic assay: The clonogenicity of all three cell lines (PC3, DU145, and 22RV1) significantly decreased after exposure to media containing different concentrations of Ra-223 in a similar pattern. Interestingly when PC3 and 22RV1 cells were exposed to HAp-coated surface conditioned with 500 Bq/ml Ra-223, the colony-forming ability was extremely reduced compared to free Ra-223 treatment.

Spheroid assay: After six days of being exposed to 250 Bq/ml and 500 Bq/ml of free Ra-223, the growth of 22RV1 spheroids was significantly suppressed ($p = 0.0248$ and $p = 0.0019$, respectively). Treatment with 100 Bq/ml of Ra-223 caused a noticeable reduction in growth after eight days ($p = 0.0182$). At the end of the experiment (18 days), the 250 Bq/ml and 500 Bq/ml groups showed complete growth inhibition, while the lowest activity (100 Bq/ml) reduced the growth by half compared to the control sample.

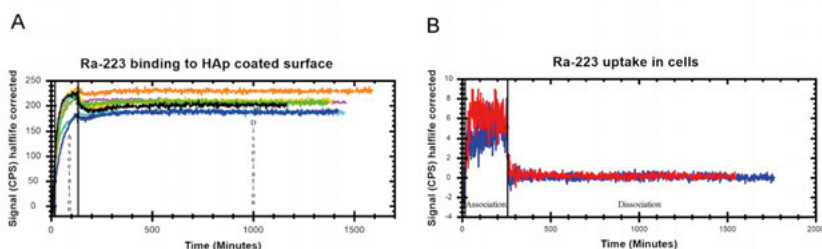


Figure 12. The Ra-223 binds strongly to HAp without any cell uptake. (A) The Ra-223 binding kinetics to the HAp (B) The Ra-223 is not taken up in cells. The solid vertical lines show the border of association and dissociation.

Spheroid outgrowth assay: We tested how spheroid outgrowth was impacted when grown on a HAP surface that was pre-treated with or without Ra223 to simulate *in vivo* conditions. On day 4, 22RV1 spheroid outgrowth was significantly reduced in the 0.5 kBq/ml and 1 kBq/ml groups and this effect persisted until day 10. The treatment did not affect DU145 spheroid outgrowth. However, the treatment did reduce cell density in the central and peripheral regions, making it difficult to score cellular outgrowth at later stages.

PFGE: The Ra-223 DNA fragmentation induction was measured in DU145 cells by PFGE and compared with high-LET X-rays radiation. The result showed random DSB distribution for X-rays and non-random for Ra-223 with the elevated generation of small DNA fragments (<1 Mbp sizes) as a hallmark of high-LET radiation (Fig. 13A).

Foci assay: We evaluated classic immunofluorescence DSB biomarkers of γ H2AX and 53BP1. The confocal imaging results showed a tracklike traverse of the 53BP1 DSB repair signal as a signature of α -particles travel through the nucleus (Fig. 13B)

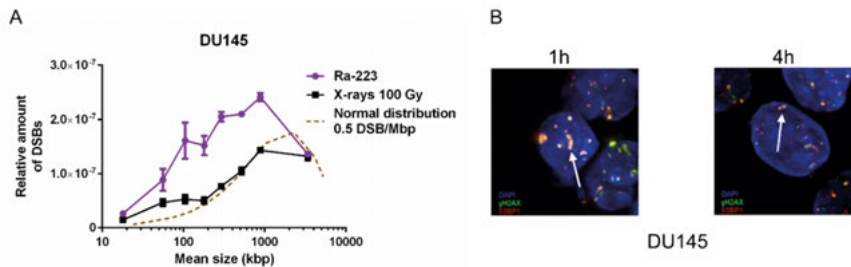


Figure 13. (A) Comparison of DSB fragment distribution from Ra-223 and high-LET X-rays (100 Gy) in DU145 cells using PFGE. (B) Immunostaining of DSB biomarkers (53BP1 and γ H2AX) after Ra-223 (100 kBq/ml) treatment showed track lines (white arrows) of α -particles traveling through DU145 prostate cancer cells nucleus after 1 h and 4 h repair time.

Flow cytometry: Flow cytometric analysis of DSB repair key protein DNA-PKcs (T2609 phosphorylation) of PC3 and DU145 cells showed fast and efficient repair of DSBs 4 h after irradiation with 6-11% residual DSB remaining. 22RV1 cells were slower and less efficient in DSB repair.

Apoptosis assay: The Ra-223 apoptotic effect was evaluated by flow cytometric analysis of caspase 3/7-sytox and Annexin V/PI double staining. All three cell lines' apoptotic response for both biomarkers was significantly higher than the control showing strong apoptosis stimulation of Ra-223.

3.3.4. Discussion and conclusion

Ionizing radiation-generated DSB is the most harmful damage to the cell repair system. If these DSBs are not removed or properly repaired, it can result in genetic instability and tumorigenesis (174). Therefore, quantification of

DSB induction and repair is necessary. For DSB induction measurement, and DNA fragment distribution we used PFGE. DNA fragmentation distribution analysis showed clustered DSBs with <1 Mbp after Ra-223 exposure in prostate cancer cells. This finding is in line with the result of high-LET ion irradiation results (175,176). To measure DSB repair, we tried using immunostaining of DSB biomarkers. However, during this study, we realized that foci counting is not an accurate way of DSB quantification of alpha particles since it may underestimate the DSB number. In this case, one detected focus may have several aggregated DSBs close together (177). At the same time, these foci images gave valuable information about the physical shape of induced clustered damage. The image acquisition of fluorescently stained γ H2AX and 53BP1 foci demonstrated track-like distributions of DNA clustered lesions inside the nucleus. These clusters are associated with a track line of alpha particle travel through the folded chromatin (178).

To overcome the quantification of aggregated DSBs we used the relative fluorescence intensity of phosphorylated (T2609) DNA-PKcs, as a marker of the DSBs repair kinetics and NHEJ activation (179). The results showed that NHEJ repair activation was the result of clustered DSB induction by Ra-223. The activated NHEJ repair pathway and the early repair kinetics measured by flow cytometry were in line with previous PFGE analysis measuring rejoining of DNA after ion irradiations (180) suggesting that the high toxicity of the DNA damage caused by the high-LET irradiation is due to the clustering of highly complex DSBs. As a result of toxic DNA clustered, Ra-223 reduced cell survival regardless of the cell type, indicating the potential use of Ra-223 treatment in ADT resistance bone metastases prostate cancer.

Conditioned HAp, reduced cell survival more than free Ra-223 in 2D. Free Ra-223 in the growth media was able to decrease the cell survival in monolayers and 3D spheroids and induce high levels of apoptosis (181). However, this does not reflect the actual *in vivo* condition, as only a small number of the α -particles will be able to hit the cells when Ra-223 is evenly distributed in the media. To address this issue, we quantified Ra-223 binding to the HAp surface by using LiganTracer. The results demonstrated strong binding of Ra-223 to the HAp surface without cell internalization, showing that all damages are induced by decay events outside of the cell. The results were consistent with previous observations which showed Ra-223 redistributed to the bones within 2 h of being injected into the bloodstream (182).

Cells (22RV1 and PC3) and spheroids (22RV1) seeded on top of the HAp surface, conditioned with Ra-223, showed greater cell growth inhibition compared to free Ra-223 exposure in media. This is likely due to the α -particle source being located at a closer distance to cells in the HAp-conditioned setup. However, DU145 spheroids outgrowth was not affected by placing them on top of the conditioned HAp layer, even though their survival was compromised. This result suggests that Ra-223 cannot inhibit the migration of all

prostate cancer cell types. The possible explanation could be cells entering apoptosis or locating far from the reach of α -particles.

In conclusion, the stable localization of Ra-223 inside the HAp structure without entering the cell shows how this radionuclide acts *in vivo* by migrating to the bone remodeling site and irradiating invading cancer cells to the metastatic node. This finding validates previous biodistribution studies (182,183). The elevated apoptotic response of all three studied cell lines suggested that the severity of DNA clustered damage forced cells toward programmed cell death due to the unrepairable nature of initial DNA damage. These data are in line with previous investigations (184). The role of prostate cancer Arv7 in Ra-223-induced DNA damage needs more investigation in future studies.

3.4 Paper IV

Ascorbate Induces G2/M Arrest and Necrosis Without Generation of Direct DNA double-strand breaks

3.4.1. Introduction and Aim

Intravenous high-dose infusion of pharmacological ascorbate (Asc; vitamin C) is used as an adjuvant agent in cancer treatment (185,186). Ascorbate's (Asc) cytotoxicity in cancer cells is attributed to DNA damage caused by the generation of reactive oxygen species (ROS) and H₂O₂. While many studies have reported Asc-induced single-strand DNA breaks, growing evidence points to its ability to induce DSBs, as indicated by H2AX phosphorylation and other biomarkers (187,188). However, the mechanisms involving chromatin modification, the DSBs origin, and the activation of NHEJ remain unclear.

This study aimed to explore the role of DSBs in Asc-induced cell death. Using two NHEJ-deficient cell lines (XRCC4 KO and DNA-PKcs KO), we demonstrated that Asc does not directly cause DSBs but alters chromatin structure by increasing 53BP1 expression and inducing pan-nuclear γ H2AX patterns 24 hours post-exposure, indicative of nuclear DNA degradation. Additionally, Asc triggered necrosis without activating apoptosis in all tested cell lines. XRCC4 KO cells showed a tendency for greater sensitivity to Asc, potentially linked to their inherently greater accumulation in G2/M phase. These findings provide new insights into DSB formation and their involvement in Asc-induced cytotoxicity.

3.4.2. Methods

Cell lines: Human colorectal cancer cell line HCT116, HCT116 DNA-PKcs KO, HCT116 XRCC4 KO, Prostate cancer PC3, Human skin fibroblast GM5757.

Assays: western blot, clonogenic assay, CellTiter-Glo® 2.0 Luminescent viability assay, spheroid assay, pulsed-field gel electrophoresis (PFGE), γ H2AX and 53BP1 foci assay, flow cytometric analysis of apoptosis and necrosis, cell cycle distribution.

3.4.3. Results

We used parental HCT116 with intact NHEJ and two NHEJ deficient derivatives of it (DNA-PKcs KO and XRCC4 KO) besides human prostate cancer cell PC3 and normal human skin fibroblast GM5757 cell line with functional NHEJ pathway.

Clonogenic assay: Asc reduced clonogenicity in all cell lines in a concentration-dependent manner, with similar sensitivity at lower concentrations. XRCC4 KO cells were the most sensitive, losing clonogenic potential beyond 150 μ M, followed by DNA-PKcs KO and HCT116 cells. Colony sizes decreased more in HCT116 cells compared to KO lines. The DNA-PKcs inhibitor NU7441 confirmed the KO phenotype.

Spheroid size and viability assay: Asc caused significant, concentration-dependent reductions in spheroid size and viability across all lines. XRCC4 KO spheroids showed higher sensitivity at higher concentrations, with the greatest size reductions observed between 1000 and 2500 μ M. At 5000 μ M, spheroids lost structural integrity, becoming irregular and disorganized, leading to their exclusion from analysis (Fig. 14).

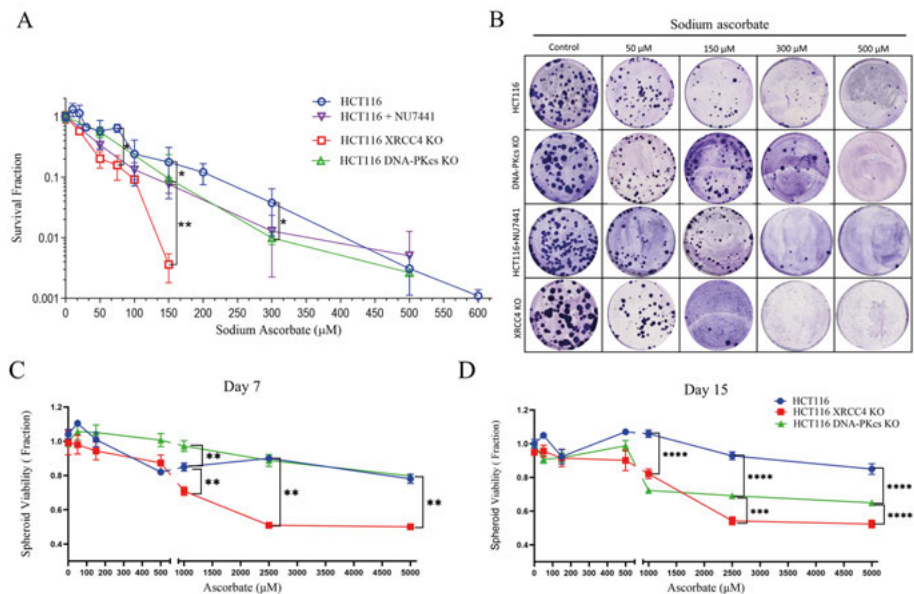


Figure 14. Clonogenic assay and spheroid viability results after treatment with Asc. (A) clonogenicity SF plot of 0-600 μM Asc exposure (2h of HCT116 (\pm NU7441), XRCC4 KO, and DNA-PKcs KO cells. Colonies with >50 cells counted for SF. (B) Colony images (6-well plate). Spheroid viability after 0-5000 μM Asc treatment on HCT116, XRCC4 KO, and DNA-PKcs KO cell's (C) day 7 and (D) day 15. Error are \pm SD, N=3. * $p < 0.05$, ** $p < 0.01$, *** $p < 0.001$, **** $p < 0.0001$.

PFGE: To examine DSB formation following Asc treatment, PFGE analysis was performed. In HCT116 cells, no dsDNA fragments was observed, and the FAR, representing migrated DNA, remained comparable to the control across all Asc concentrations. In contrast, positive controls (40 and 100 Gy X-rays) induced significant DNA fragmentation (Fig. 15A,B). Chromatin alteration during Asc exposure was assessed by quantifying 53BP1 foci in three cell lines after 2 hours of Asc treatment, followed by a 1-hour recovery in fresh medium. The distribution of 53BP1 foci per cell showed no dependency on Asc dose or correlation with the NHEJ status of the cells (Fig. 15C,D,E).

DSB biomarkers assay: We measured 53BP1 and γ H2AX foci per cell 24 hours after Asc exposure to assess chromosomal stress signals. At 500 μM , 53BP1 foci increased in all cell lines, with HCT116 cells showing a sustained elevation at 1000 μM . However, higher Asc concentrations led to a decline in 53BP1 foci, suggesting impaired DNA damage response activation. Validation with 2 Gy X-rays confirmed 53BP1 as a reliable biomarker. For γ H2AX, the response was less pronounced, with no significant differences across cell lines or concentrations. At 500 μM , γ H2AX foci decreased, and nearly disappeared at 5000 μM , indicating potential loss of DSB signaling. Pan-nuclear

γ H2AX signals displayed distinct dose-dependent profiles, especially in XRCC4 KO cells, where the signal increased from 50% at 500 μ M to nearly 90% at 5000 μ M. These findings suggest chromatin change and DNA degradation processes leading to DSB formation over time (Fig. 16A,B,C,D).

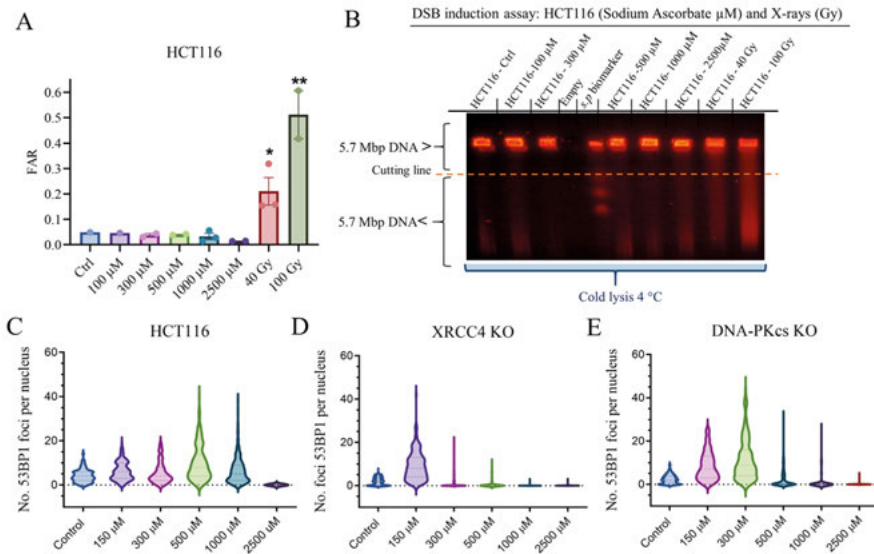


Figure 15. Prompt DSB (>5.7 Mbp) and 53BP1 foci after Asc and X-rays treatment. (A) Prompt DSB measured with PFGE after 2 h Asc exposure (0-2500 μ M of Asc), and with 40 and 100 Gy of X-rays. Error bars are SD, N=3. * $p < 0.05$, ** $p < 0.01$. (B) Sample gel image showing DNA migration in HCT116 cells. 53BP1 foci quantification after 2 h exposure followed by 1 h recovery in (C) HCT116, (D) XRCC4 KO, and (E) DNA-PKcs KO cells (0-2500 μ M Asc treatment).

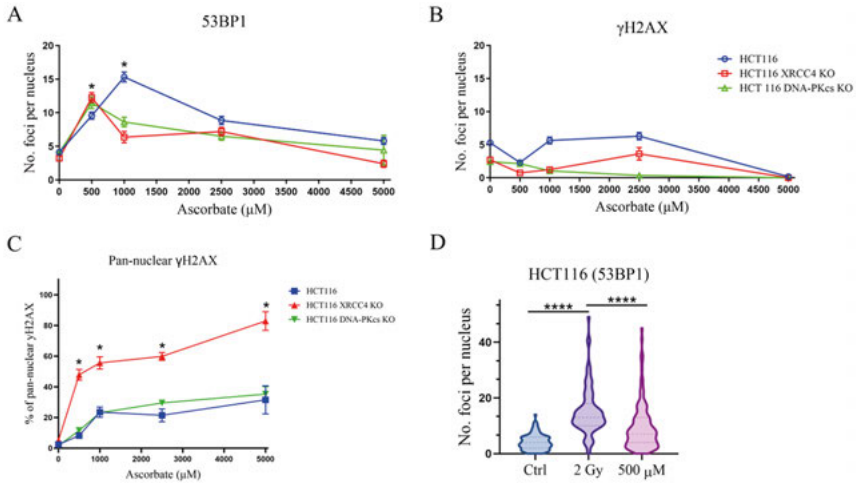


Figure 16. Chromosomal DSB biomarkers expression (γ H2AX, 53BP1), and pan-nuclear γ H2AX formation in cells after Asc treatment. (A) 53BP1, (B) γ H2AX foci, and (C) pan-nuclear γ H2AX after exposure of cells to 0-5000 μ M of Asc for 2 h, followed by 24 h incubation with medium for repair. (D) 53BP1 foci comparison with X-rays and Asc (1 h). Error bars present \pm SEM from around 300 cells per condition. * $p < 0.05$, ** $p < 0.01$, *** $p < 0.001$, **** $p < 0.0001$

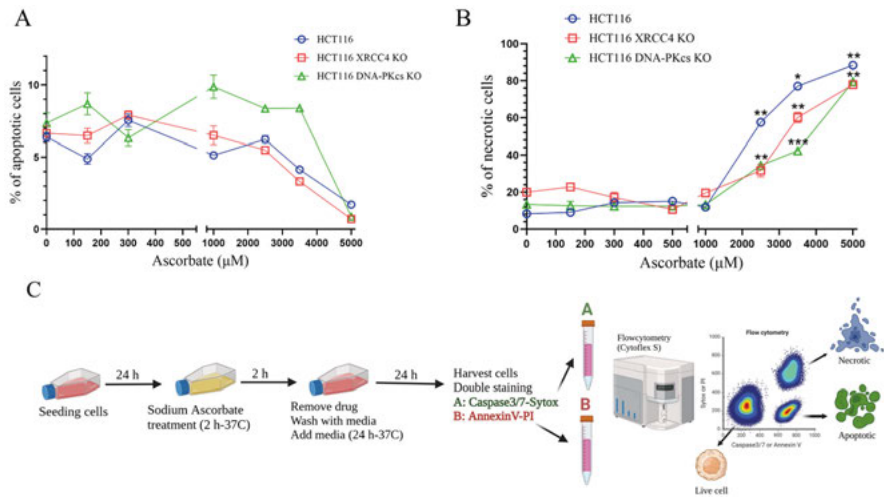


Figure 17. pharmacological Asc generates strong necrotic response in HCT116 cells without apoptosis. (A) Asc treatment (2h) (0-5000 μ M) followed by a 24h incubation in medium before measuring caspase-3/7 signal in HCT116, XRCC4 KO, and DNA-PKcs KO cells by flow cytometry. (B) Necrotic response of 0-5000 μ M Asc (2h), followed by a 24 h incubation in medium using Sytox signal intensity via flow cytometry. (C) Schematic view of cell preparation and assay performance for apoptosis/necrosis measurement. Error bars are \pm SD. * $p < 0.05$, ** $p < 0.01$, *** $p < 0.001$, **** $p < 0.0001$.

Apoptosis and necrosis analysis: To explore the involvement of apoptosis and necrosis pathways, HCT116 and KO cells were treated with various Asc concentrations for 2 hours, followed by 24 hours of incubation with fresh media (48 hours for parental HCT116). Flow cytometry with Caspase 3/7-sytox and annexin V-PI double staining was used to assess apoptotic and necrotic responses. No significant effects on apoptosis or necrosis were observed at 100-1000 μM Asc concentrations after 24 hours. However, concentrations of 2500, 3500, and 5000 μM led to dose-dependent necrosis without activation of apoptosis (Fig. 17).

Cell cycle analysis: The results indicate that the cell cycle distribution of HCT116 cells remained unchanged until 2500 and 5000 μM Asc, which caused G2/M arrest. XRCC4 KO cells exhibited a greater accumulation of cells in G2/M phase under untreated conditions, making them more sensitive to Asc. These cells showed increased sensitivity to moderate Asc concentrations, with a dose-dependent rise in G2/M arrest at 150, 300, and 500 μM . At higher concentrations, XRCC4 KO cells accumulated significantly in the G2/M phase and displayed a dose-dependent increase in sub-G1. DNA-PKcs KO cells also exhibited increased G2/M arrest at 300 and 500 μM , followed by a substantial rise in both G2/M and sub-G1 phases at 1000 and 2500 μM . Interestingly, at the highest concentration, there was no further increase in G2/M arrest, but the sub-G1 phase elevated. Overall, high Asc concentrations caused G2/M arrest in all cell lines, with a stronger effect in XRCC4 KO cells, and increased sub-G1 cells in both KO cell lines (Fig. 18).

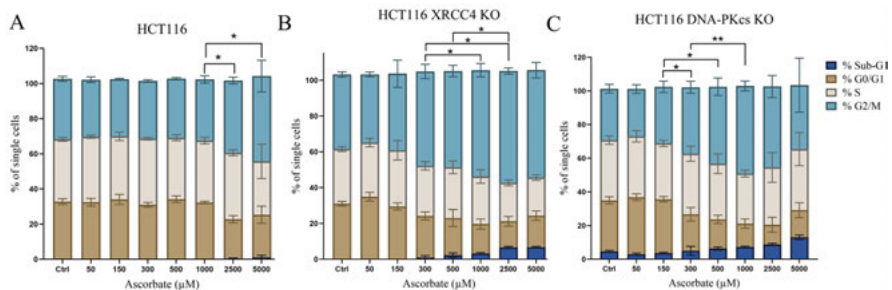


Figure 18. G2/M arrest after Asc treatment. Cell cycle analysis of (A) HCT116, (B) XRCC4 KO, (C) DNA-PKcs KO cells after Asc treatment. Cells were treated with Asc and incubated in medium for 24 h. Error bars represent \pm SD, N=4. * $p < 0.05$, ** $p < 0.01$.

3.4.4. Discussion and conclusion

The study investigated the effects of Asc on DNA damage, focusing on DSB formation and NHEJ using various cell lines, including XRCC4 and DNA-PKcs deficient colorectal cancer cells, and NHEJ-proficient cells (PC3 and GM5757). Results showed that Asc decreased cell survival and viability in

both 2D and 3D models in a dose-dependent manner, with XRCC4 KO cells being the most sensitive, possibly due to having naturally greater number of cells in G2/M phase. Although Asc did not induce direct DSBs (as observed with X-rays), it increased 53BP1-positive cells after 24 hours, suggesting that DSBs may result from SSBs converting into DSBs during replication or due to apoptosis and necrosis (124,188,189). γ H2AX foci expression was weak in response to Asc but showed a strong, dose-dependent pan-nuclear γ H2AX response, particularly in XRCC4 KO cells, indicating oxidative stress-driven overactivation of ATM (190).

Asc did not activate apoptosis but induced necrosis, with ATP depletion playing a key role in promoting necrosis, independent of caspase activation and NHEJ status. GM5757 cells were less sensitive to necrosis than HCT116 cells, consistent with the higher oxidative stress tolerance in normal cells (191). Our study suggested that Asc-induced oxidative stress may shift cell death mechanisms from apoptosis to necrosis, and highlighted that Asc can induce G2/M arrest in all cell lines, with XRCC4 KO cells showing a more pronounced effect (192–194).

Overall, Asc does not directly induce DSBs but contributes to their formation through cellular degradation processes. The XRCC4 KO cells' sensitivity is likely due to having greater number of cells in G2/M phase. These findings may help develop new cancer therapies combining Asc with radiation, cytotoxic drugs, or DNA repair inhibitors (195–197).

3.5 Paper V

The Role of Non-homologous End Joining in the Repair of Different Types of DNA Double-Strand Breaks

3.5.1. Introduction and Aim

Cancer therapies involving irradiation and cytotoxic drugs kill cancer cells by inducing DSBs, the most harmful form of DNA damage (17). DSBs, however, vary in complexity, ranging from relatively clean, enzymatically induced breaks to more complex ones, such as those associated with additional DSBs, SSBs, or base lesions (18).

The complexity of DSBs can be classified based on lesion type, number, and proximity. For example, calicheamicin (CLM), a potent DSBs inducer, cleaves DNA at pyrimidine-rich sites (19). Phleomycin (PHL), generates DNA adducts that disrupt DNA polymerase, yielding numerous SSBs and a few DSBs (20). X-rays induce clustered DNA damage (27,29,198). Etoposide (ETP), causes DNA fragments to become permanent DSBs at ETP high concentrations (21–23). Temozolomide (TMZ), generates base pair mismatches and SSBs with no DSB (24,25). Additionally, the chromatin's heterogeneous

packaging likely affects the localization of cytotoxic drugs, and DNA-binding sites (34).

NHEJ is the main DSB repair pathway, repairing majority of all DSBs throughout the cell cycle by directly ligating DSB ends (199). First, the Ku 70/80 heterodimer recognize the DNA break ends. This high-affinity binding supports the DNA ends from nuclease's reach (68). Ku, bridge the DSB gap by recruiting DNA-PKcs. Next, DNA-end processing starts by DNA-PKcs recruiting Artemis (69). The KU and DNA-PKcs complex are responsible for DNA-end tethering and recruitment of XRCC4, XLF, DNA ligase IV, PAXX, and Artemis. XRCC4-ligase IV form a complex with XLF, for DNA end-ligation. The main factors for this step are the Ku heterodimer, XRCC4, ligase IV, and XLF (68). The complexity of DNA damage influences the efficiency and accuracy of NHEJ.

Despite extensive research, the mechanisms of repairing complex DNA lesions are not fully understood (200), particularly in terms of how lesion complexity affects the efficiency and specificity of NHEJ components in recognizing and processing DNA damage. Moreover, the relationship between DSB complexity and cell fate remains unclear. This study aims to investigate the roles of two core NHEJ kinases, DNA-PKcs and XRCC4, in recognizing and repairing DSBs of varying types or complexity. We used five DNA damaging agents and compared repair kinetics: TMZ, ETP, PHL, X-ray, and CLM.

3.5.2. Methods

Cell lines: Human colorectal cancer cell line HCT116, HCT116 DNA-PKcs KO, HCT116 XRCC4 KO.

Assays: western blot, clonogenic assay, pulsed-field gel electrophoresis (PFGE).

3.5.3. Results

Clonogenic assay: The long-term effects of DNA-damaging agents on HCT116 cells and their XRCC4 and DNA-PKcs knockout (KO) variants were evaluated using clonogenic assay. CLM: HCT116 cells displayed high resistance to CLM, with only minor reductions in survival fraction (SF) at higher concentrations. In contrast, both KO cell lines exhibited a dose-dependent decrease in clonogenicity. XRCC4 KO cells were significantly more sensitive than DNA-PKcs KO cells, particularly at 3, 5, and 8 pM CLM. X-rays: Radiation reduced clonogenicity across all cell lines in a dose-dependent manner. HCT116 cells were the most resistant, followed by XRCC4 KO and DNA-PKcs KO cells. While both KO cell lines were more sensitive than HCT116 cells, DNA-PKcs KO cells demonstrated slightly greater sensitivity than XRCC4 KO cells. ETP: HCT116 cells showed notable resistance compared to KO cells. Both XRCC4 KO and DNA-PKcs KO cells had similar

clonogenic loss, with only minor differences. PHL exposure led to dose-dependent reductions in clonogenicity across all cell lines. HCT116 cells were significantly more resistant than the KO lines, which displayed similar levels of sensitivity. TMZ: All cell lines exhibited a dose-dependent decrease in survival upon TMZ treatment. However, HCT116 and KO cells displayed similar reductions in clonogenicity (Fig. 19).

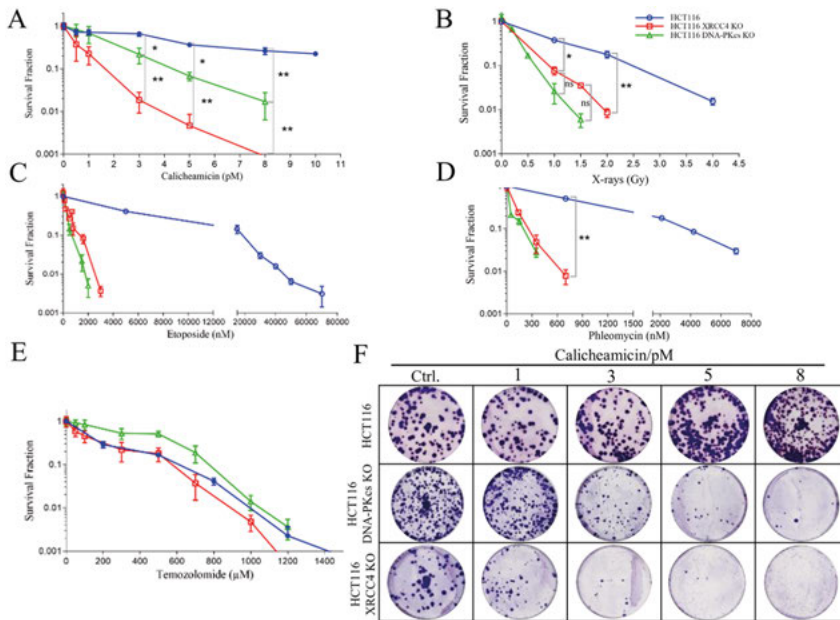


Figure 19. Clonogenic survival of HCT116, HCT116 XRCC4 KO, and HCT116 DNA-PKcs KO cells following treatment with DNA-damaging agents. (A) Clonogenic assay after CLM exposure in HCT116 cells (0-10 pM) and in XRCC4 KO and DNA-PKcs KO cells (0- 8 pM). (B) X-rays (C) ETP (D) PHL (E) TMZ. SF were quantified from colonies with more than 50 cells. Error bars represent \pm SD from three independent experiments. * $p < 0.05$, ** $p < 0.01$, *** $p < 0.001$, **** $p < 0.0001$. (F) Representative colony image after CLM treatment.

Prompt DSB and heat-released non-DSB clusters: To evaluate the ability of DNA-damaging agents to induce prompt DSBs and heat-released non-DSB clusters in HCT116 cells, a DSB induction assay using PFGE was performed. CLM: Treatment with 0, 2, 5, 10, 25, and 50 nM CLM resulted in a dose-dependent increase in both prompt DSBs and heat-released DSBs, with only a small difference between the two (10-15% higher after heat treatment). X-rays: Increasing X-ray doses elevated DSB levels, and heat-release of non-DSB clusters increased DSB with 100%. ETP: DSB yields increased after treatment with 0-300 μ M ETP. No heat-released DSB were observed below 50 μ M but at higher concentrations, heat-treatment increased DSB with approximately 25%. PHL: Exposure to 0-70 μ M PHL showed a dose-dependent

increase in DSBs and heat-treatment increased DSB with approximately 30%. TMZ: No DSBs were detected at concentrations up to 2000 μM . However, a slight increase in FAR was observed at 2500 μM , likely due to its high toxicity. Higher TMZ concentrations led to very high increase of heat-released non-DSB clusters (Fig. 20).

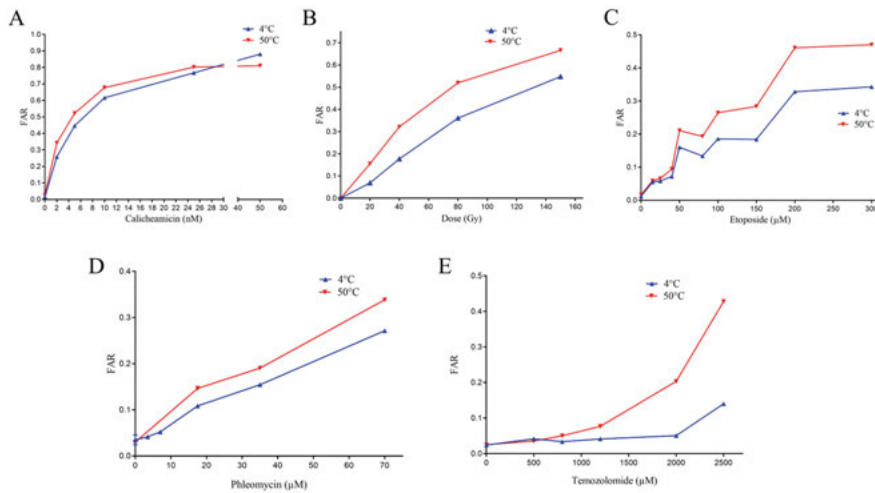


Figure 20. Prompt DSBs and heat-released non-DSB clusters generated by DNA-damaging agents measured by PFGE after treatment with (A) CLM, (B) X-rays, (C) ETP, (D) PHL, and (E) TMZ.

Prompt DSB Repair Kinetics: To evaluate the limitations of DSB repair capacity, DSB repair kinetics assay was performed using PFGE at various time points (0, 15, 30, 60, 120, 240, and 1500 minutes). Repairs occurring within the first 2 hours were classified as fast repair kinetics, while those between 2 and 24 hours were categorized as slow repair kinetics. CLM (2 nM, 30 min): HCT116 cells rejoined DSBs at all time points, achieving complete repair within 24 hours. DNA-PKcs KO cells began removing DSBs during the fast-repair phase but exhibited persistent DSBs later. XRCC4 KO cells showed minimal repair, resolving only ~40% of DSBs by 120 minutes, with an increase in unrepaired DSBs at later times. This highlights the significant sensitivity of both KO cell lines to CLM. X-rays (40 Gy): HCT116 cells rejoined nearly all induced DSBs, while both KO lines repaired only ~20%, underscoring the critical role of NHEJ in resolving radiation-induced complex DSBs. ETP (60 μM , 30 min): All three cell lines repaired ETP-induced DSBs effectively, showing minimal impact of NHEJ deficiency on this process. PHL (52.53 μM , 30 min): HCT116 cells resolved ~80% of DSBs during the fast-repair phase, with residual repair occurring later. KO lines rejoined ~40% of DSBs within 15 minutes, but persistent damage was observed at later time points. DNA-PKcs KO cells displayed greater sensitivity than XRCC4 KO cells. Overall, CLM and X-rays posed the greatest challenge to DNA repair in

the absence of NHEJ, with KO cells repairing only ~20% of DSBs. PHL allowed ~40% repair, while ETP-induced DSBs were effectively repaired (~80%) by both KO and HCT116 cells, suggesting alternative repair pathways, including HR, can partially compensate for NHEJ loss (Fig. 21).

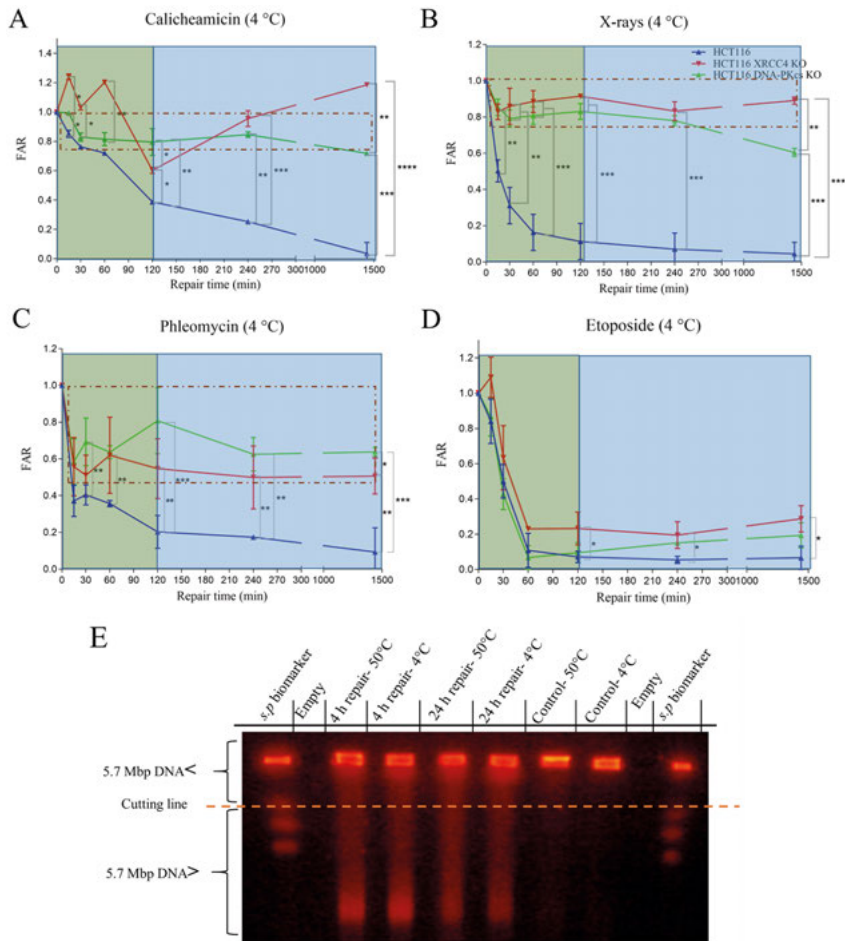


Figure 21. Prompt DSB repair kinetics of HCT116 cells after exposure to DNA damaging agents, measured by PFGE. (A) CLM (30 min), (B) 40 Gy X-rays, (C) 52.53 μ M PHL (30 min), and (D) 60 μ M ETP (30 min). Error bars \pm SD, N=3. * $p < 0.05$, ** $p < 0.01$, *** $p < 0.001$, **** $p < 0.0001$. Green squares, represents the DSB fast repair kinetics (15-120 min) (euchromatin). Blue squares, shows the DSB repair slow kinetics (120-1500 min), (heterochromatin). (E) Sample of PFGE gel image showing DSB repair kinetics in HCT116 XRCC4 KO cells treated with PHL. (F)

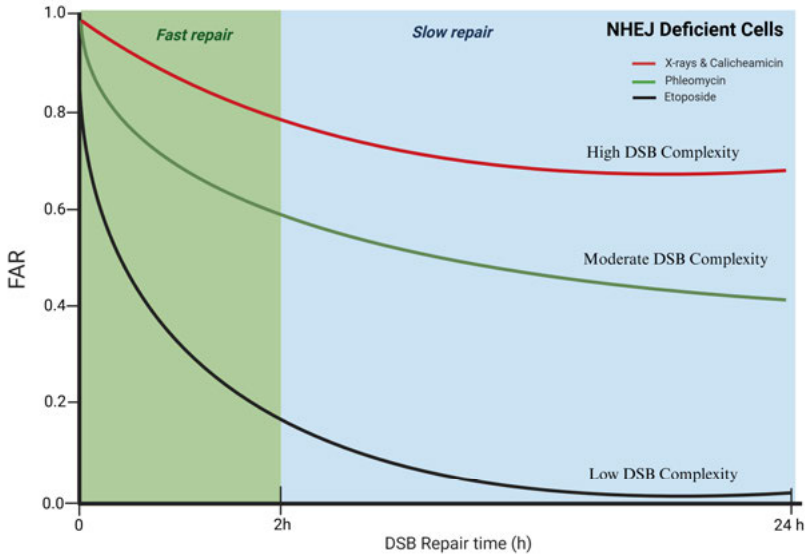


Figure 22. A model of DSB complexity in NHEJ-deficient cells. The illustration is adopted from Shibate and Jeggo, 2020. (Created with BioRender.com)

3.5.4. Discussion and conclusion

Cancer patients receive radio chemotherapeutics during the course of treatment. Cytotoxic agents kill cancer cells by inducing diverse types of DSBs with various levels of DSB complexity. NHEJ is responsible for repairing most of these DSBs. The structure of DNA ends is critical element of DSB complexity and repair. Conventional DSB repair studies typically use DSB ends with 5'-phosphate and 3'-hydroxyl termini, generated either through in vitro constructs or site-specific nucleases. However, this method fails to account for the DNA end structures created by actual DSB inducers in natural or clinical contexts (201).

Our findings revealed that DSB repair kinetics are closely related to the type and/or complexity of the DSBs. In the absence of NHEJ, there was essentially only a fast repair phase (<2h), whereafter there was no repair the following 1-24 hours. Interestingly, KO cells exhibited similar limitations in resolving DSBs induced by X-rays and extremely complex DSBs caused by CLM, suggesting that HR or Alt-NHEJ may be ineffective for repairing these DSBs.

Approximately 50% of DSBs induced by PHL were repaired in the NHEJ KO cells, whereas those caused by ETP (low complexity) were nearly fully resolved (<20% left unrejoined), emphasizing the influence of DSB type and potentially the localization within euchromatin or heterochromatin. In cells

with functional NHEJ, the repair pattern declined with increasing chemically induced DSB complexity, except for X-ray-induced clustered DNA damage. Clonogenic assays showed that NHEJ deficiency sensitized cancer cells to all DSB-inducing agents. However, when DNA damage did not involve DSBs, as seen with TMZ, NHEJ inactivation had no effect on clonogenic survival.

X-rays and CLM, displayed distinct clonogenic responses between XRCC4 and DNA-PKcs knockout cells. Notably, formation non-DSB clusters was observed following exposure to X-rays, PHL, and TMZ but less for CLM and ETP, suggesting that SSBs and heat-labile sites contribute to secondary DSB formation during heat treatment. The rapid resolution of heat-released DSB within 15 minutes was independent of NHEJ, highlighting distinct repair dynamics for this process.

The complexity of DSBs significantly influences the efficiency and accuracy of repair processes. Complex DSBs pose particular challenges due to inhibitory effects on NHEJ caused by end-group structures and lesions like nearby SSBs (202). These breaks often engage multiple repair pathways, potentially leading to competition or interference among them, reducing repair efficiency, slowing repair kinetics, and increasing the likelihood of errors. Despite these challenges, cells have evolved efficient mechanisms for addressing DSBs, often repairing them faster than other types of DNA damage (203). The choice between NHEJ and HR depends on the complexity of the break, with HR being more likely to resolve highly complex DSBs when available (204,205). This observation aligns with Okayasu et al. (2006), who showed that increasing DSB complexity from X-rays to carbon and iron ions, leads to reduced survival rates and repair efficiency in both NHEJ-proficient and deficient human and rodent cells (206). Similarly, our findings corroborate Pastwa et al. (2003), who demonstrated slower repair rates for complex, non-ligatable DSBs induced by bleomycin and γ -rays compared to simpler, ligatable blunt-ended DSBs produced by restriction enzymes (202). We observed nearly complete rejoining of DSBs during the rapid phase after low DSB complexity induction (ETP), both in the presence and absence of NHEJ. This suggests that intact NHEJ repaired almost all ETP-induced DSBs within 2 hours. Our previous findings indicated that, unlike rodent cells, human cells lack alternative NHEJ pathways (207). Therefore, in the absence of NHEJ, HR or Alt-NHEJ likely resolved all DSBs within 2 hours. Since most ETP-induced DSBs are located within euchromatin, our results indicates that the absence of NHEJ likely promotes the activation of HR or Alt-NHEJ in euchromatin regions.

In NHEJ KO cells, PHL-induced 40% of DSBs were resolved during the fast repair phase, most likely in euchromatin, and this may be due to the mixed nature of the damage affecting both euchromatin and heterochromatin (208–211). X-rays damage both chromatin types, but euchromatin, is likely damaged more immediately, making it easier for repair kinases to access. In contrast, heterochromatin is less accessible to repair proteins, requiring chromatin remodeling to make the DNA accessible, leading to slower repair (30). CLM

and X-rays, inducing breaks in both euchromatin and heterochromatin, result in slower and less efficient repair compared to ETP, emphasizing the importance of DSB localization within chromatin (30,212,212).

In conclusion, we explored the relationship between DSB type and complexity, DSB chromatin localization, repair pathway selection, and cell survival (Fig. 22). Our results emphasize the essential roles of DNA-PKcs and XRCC4 in resolving complex DSBs, while highlighting that HR or Alt-NHEJ pathways can partially or substantially compensate for NHEJ deficiencies in cases of moderate or less complex DSBs. Importantly, we show that HR or Alt-NHEJ is not limited to the slow phase of DSB repair but is also active during the fast phase for less complex DSBs, particularly those located in euchromatin. Additionally, the study highlights the significance of chromatin structure, SSB induction, and other cellular factors in interpreting the effects of DNA-damaging agents.

4. Concluding remarks

DSB induction and repair form the foundation of cancer therapy while also being a key factor in cancer resistance to radiation and chemotherapy. Nearly all cancer treatments, except surgery, aim to eliminate cancer cells by inducing DSBs while sparing healthy cells as much as possible. However, the identity, nature, and repair dynamics of DSBs in many cancer treatment modalities remain incompletely understood. A deeper understanding of how different types of DSBs are formed and repaired could lead to more precise and effective therapeutic strategies. Additionally, there is a growing trend in drug repurposing and combination therapy, aiming to enhance treatment efficacy and overcome resistance mechanisms. By integrating novel therapeutic agents with traditional DNA-damaging treatments, it may be possible to exploit DSB repair vulnerabilities and improve patient outcomes. Future research should focus on optimizing combination strategies, refining our knowledge of DSB repair pathways, and translating these insights into clinical applications to advance cancer treatment.

To achieve the goal of optimizing combination therapy and exploiting DSB repair pathway vulnerabilities in cancer cells, it is necessary to understand the DSB repair signatures of commonly used cancer therapeutics and how cancer cells respond to varying levels of DSB complexity arising from combination treatments. A deeper knowledge of these complexities is essential for strategically manipulating DSB repair mechanisms to maximize synthetic lethality in cancer cells while minimizing damage to healthy tissues.

This thesis addresses this challenge through a dual approach. First, we applied combination therapy in a practical setting to assess how DSB induction and repair capacity can be leveraged to sensitize cancer cells. Second, we adopted a fundamental radiochemo biology perspective to uncover the underlying mechanisms governing DSB repair responses to different levels of DSB complexity. By bridging these two approaches, this work contributes to a better understanding of DSB repair dynamics, with potential implications for improving cancer treatment strategies. The major findings of this thesis are summarized as follows:

In **Paper I**, we showed that HSP90 inhibition by onalespib can effectively overcome cisplatin resistance in ovarian cancer cells by increasing DSB lesions while reducing the DSB repair capability of cancer cells. This elevated DSB level was associated with increased apoptosis and G2/M arrest.

In **paper II**, we demonstrated that HSP90 inhibition by onalespib enhances GBM radiosensitivity by increasing DSB accumulation, triggering apoptosis, and promoting cell death in both 2D and 3D models. These findings highlight the potential of combining radiotherapy with HSP90 inhibition as a strategy to overcome GBM resistance.

In **paper III**, we showed that Ra-223 induces track-like clustered DSBs, activating NHEJ and leading to growth inhibition and apoptosis in prostate cancer cells. Notably, Ra-223 imposed its effects without cellular uptake.

In **paper IV**, we found that Asc induces delayed DSBs, marked by pan-nuclear γ H2AX and G2/M arrest, leading to necrosis and reduced cell viability in both 2D and 3D models. This effect was more pronounced in XRCC4 KO cells but was driven by cell cycle regulation rather than NHEJ deficiency.

In **paper V**, we tested how NHEJ responds to different DSB types and complexities in colorectal cancer cells. Wild-type cells exhibited both fast and slow repair kinetics, while NHEJ-deficient cells showed only an initial fast repair phase, with no further repair over 24 hours. As the DSB:SSB ratio decreased across different inducers, non-DSB clusters increased but were rapidly removed in an NHEJ-independent manner.

Overall, our results highlight strategies for manipulating and optimizing DSB repair to overcome cisplatin resistance in ovarian cancer and enhance radiosensitivity in GBM cells. We also revealed the DSB repair response of prostate cancer cells to alpha-therapy with Ra-223. Additionally, we demonstrated the delayed DSB induction effect of Asc and examined the NHEJ response to different DSB complexities in colorectal cancer. These findings provide new insights into NHEJ response biology in cancer.

5. Future perspectives

DNA damage response is central to cancer initiation and progression. Understanding underlying mechanistic interaction of DDR and DSB complexity can improve targeted and combined cancer therapy. Monotherapy in cancer, dating back to the 1940s, revealed that single-agent treatments cannot sustain long-term remission. Since then, the pursuit of combination therapies targeting multiple pathways without overlapping mechanisms has intensified (213). The discovery of oncogenes in the 1980s fueled the rise of targeted therapies aimed at disrupting cancer's key pathways (214). However, the critical question remains: what combination of drugs can achieve a long term/lasting response? The driver of new ideas for combinational therapy can be from the origins of cancer resistant development, such as heterogeneity of tumor cells, mutations, non-genetic transcriptional pathway changes, epigenetic tumor changes, and cell state transition.

In **papers I and II**, we explored DSB optimization through HSP90 inhibition in combination therapy to enhance tumor sensitization. However, these findings require further *in vivo* validation to move closer to clinical application. A future approach building on **papers I and II** is *in vivo* loss-of-function genetic screening (215) to identify key targets for achieving synthetic lethality. This can be complemented by next-generation CRISPR–Cas technology for proof-of-concept validation and drug synergy testing. Data revealed that cancer cells with defects in certain DNA repair pathways showed increased immunogenicity, opening the door for combining DDR inhibitors with immune checkpoint inhibitors, such as PARP or DNA-PKcs inhibitors with PD-L1 mAb for enhanced therapeutic impact (121). Recent advancements in implantable devices for delivering multiple drugs at nanodoses to different tumor regions, combined with multiplex imaging, offer a promising strategy to enhance our study model (216). Moreover, the integration of computational power and AI with large-scale cancer datasets such as Pan-Cancer Analysis of Whole Genomes, The Cancer Genome Atlas, and DepMap (Cancer Dependency Map), alongside lab-generated data, can refine small-scale screening results within the broader cancer landscape, providing more precise combination therapy strategies (214).

The identity, nature, and repair dynamics of DSBs induced by different cancer treatments remain incompletely understood. A deeper insight into how DSBs form and resolve under various therapies is crucial for advancing cancer

treatment. In **papers III, IV, and V**, we tackled these challenges, yet a key unresolved question remains: What drives the fast repair (<30 min) in NHEJ-deficient cells? Is HR or alt-NHEJ compensating within this rapid phase? Addressing these questions requires not only mechanistic studies but also the development of advanced DSB detection techniques capable of capturing rapid repair dynamics, such as flow cytometry (179).

Although we examined chromosomal responses to DSBs through 53BP1 and γ H2AX, key regulators of DNA damage recognition and repair, the structural and functional changes in chromatin architecture following DSB induction remain largely unexplored (35,217). Understanding the spatio-temporal dynamics of chromosome structure in response to different DSB types, particularly in the context of cancer therapy, is crucial. Advanced imaging techniques, chromatin conformation assays, and computational modeling could be instrumental in addressing this gap. Understanding these mechanisms may reveal chromosomal vulnerabilities, identify potential druggable chromatin targets, and pave the way for diagnostic strategies based on chromosomal DSB biomarkers.

6. Acknowledgments

During my PhD journey, I had the privilege of being surrounded by incredible supportive community. This achievement would not have been possible without them.

First and foremost, I sincerely thank to **Prof. Bo Stenerlöv**, my main supervisor, for welcoming me into his group, first as a research assistant and later as a PhD student. Your office door and your heart were always open to me. You have been my guiding light and safe haven through every challenge, whether in research, residence permits, health issues, or even vacations. Your unwavering support, kindness, and patience, even in the most stressful times, have meant the world to me. You have taught me so much and left a profound impact on me, so much so that I now find myself explaining scientific concepts to others just as you do. Thank you for sharing your immense knowledge of DSB repair and for giving me the freedom to navigate this journey, allowing me to make mistakes, fall, stand up, run, stumble again, and ultimately find my footing. I am deeply grateful for how you took me under your wings at the start, guiding me through the early steps, not accepting average data and push me toward to make it perfect, yet gradually letting me fly on my own, find my voice, and carve my own path. This freedom came with great responsibility, and you can be sure that this PhD became deeply personal to me which I poured my whole heart into it.

Prof. Marika Nestor, thanks for accepting to be my co-supervisor. I truly appreciate your positivity, encouragement, vast knowledge, kindness, and generous heart. Your willingness to listen, insightful advice on my post-PhD steps, generosity in providing your lab resources to sharpen my skills, have been invaluable.

Associate. Prof. Diana Spiegelberg, thank you for accepting to be my co-supervisor, receiving me from beginning in the lab, believing in me from our very first project. Your encouragement through research challenges, your “*ya you can do that*” mentality, along with the thoughtful Christmas chocolates and cards on my desk, always made a difference. Beyond lab, your support in my personal life and during critical moments of my journey has been truly invaluable. I will never forget your kindness through all the ups and downs.

Prof. Tolmachev, and **Prof. Orlova**, thanks for our interesting discussions over science and life. Your dedication to science is inspiring. **Olga** thank you so much for taking care of me and most of my logistics in the lab. Without

your support, patience, knowledge, and kindness, it was not possible to perform in the lab. **Torbjörn Hartman**, it was pleasure to be your TA for couple of years. You taught me a lot about radiation detectors, teaching, and of course Swedish history and culture. **Andris**, thank you for your work on your last PhD project, which I had the opportunity to take over, and for introducing me to the immunohistochemistry. **Prof. Sten Nillson**, thank you for your immense knowledge in prostate cancer and for our fruitful collaboration on Ra-223 project. **Prof. Fredrik Frejd**, thank you for your positivity and magic smile, which always leave me feeling like a better person after our meetings. **Kristina Viktorsson**, thank you for your support, great advice, and encouragement. **Alexandru Dasu**, thank you for your kindness and help with proton irradiation at Scandion Klinik. **Prof. Siamak Haghdoost**, thank you for coordinating the amazing Pianoforte workshop in France, which I learned from and enjoyed a lot. **Javad**, thanks for your friendship and sharing your amazing science and life experience with me. **Mohamed Altai**, Thanks for your friendship and sharing your valuable experience. **Anzhelika**, thank you for our talks about science, food, sports, and life, and for all the happy Friday Fikas.

To my Rudbeck lab friends and colleagues

Tianqi you were my first office mate and lab friend. Thank you for your kindness, the countless Chinese souvenirs, your brilliant mind, and your invaluable friendship. You stood by my side during the most critical moments of my life, even when you were sick and exhausted. I'm also grateful for introducing me to **Yongsheng** a reliable colleague and supportive friend and the wonderful **Mia**, who have become part of our family. **Tabassom**, it was pleasure sharing office with you. Thanks for bringing joy to the office, always being helpful, and supportive even in challenging days, and for introducing **Sadra** to me which we had amazing late-night talks in the lab over economy, immigration, and sport. **Lefteris**, you joined our lab at the peak of Covid, during one of the most challenging times of my PhD. You brought a light into office. I learned so much from you and your big heart. You became the brother I turned to when all doors seemed closed. I cannot be grateful enough for having you in my life. **Nadja**, you are by far the most social human that I know. Your joy, will power, positivity, energy, leadership, and humility are truly unbelievable. Thank you for your friendship, board game nights, endless talks, nature walks, and unforgettable parties. You and **Lefteris** are our GrekoDutch family. **Alice**, you are one of the kindest and most caring friends one can have. Your critical thinking, intelligence, business mind, big heart, and sense of humor are absolutely unique. I'm so grateful to know **Michael** through you. **Michael**, I cherish the time spent talking to you. Thank you for your knowledge, friendship, support, and generosity. You taught me a lot about volleyball, and Swedish culture. You, **Alice**, and **Hank Stevens** hearts have always been welcoming to us. **Sara Lundsten**, your happiness is contagious. It is impossible to stay in a bad mood while meeting you. You are productivity example. **Sara Rinne**,

thank you for sharing your valuable experience and for your kindness and support. You are fantastic scientist and valuable friend. **Hanna Berglund**, thank you for being always supportive and helpful and introducing me to **Pontus Julia**, your joy and positivity are absolutely unique. Thank you for being my friend, co-author, and for introducing me to fantastic **Carlos** and your two wonderful kids. **Rima**, I really enjoyed working with you during your time in our lab. Thank you for all the joy, happy moments, and lab gossip we shared. **Sina**, thank you for all our interesting talks over science and life. You are awesome friend and valuable colleague. **Anna Bostrom**, your LiganTracer knowledge, willingness to help, positivity, patience, and social skills are absolutely fantastic. **Anja Mortensen**, my cheerleader for having a baby during my PhD. You're not just a fantastic scientist; you're an encyclopedia of parental leave. Thank you for sharing your amazing life and work experience with me. **Saloni**, thank you for all our conversations about science, life, and food, and, of course, for the many delicious Indian treats. **Amanda** I wish you a fantastic PhD journey. **Hanna Yushchyshyna**, you are a true inspiration. Your life journey can be a wonderful novel or even a movie. Your curiosity, sharp mind, and sense of humor, is absolutely remarkable. **Panous, Thanous, and Moeen**, it was pleasure to share the lab with you. Thanks for your kindness, our talks over barbeque, and always being friendly and helpful. **Katia**, thank you for your good energy and always being nice. **Ayman**, thank you for your friendship, sharing your amazing science and life experience with me and always being there to help. **Mahsa**, I am so happy to know you and to work with such an intelligent and hardworking scientist. I wish you all the best on your journey. **Justina**, thank you for hosting us, and for your kindness and care. You are a fantastic friend. **Ellah**, thank you for your kindness, friendship, excellent life advice, and always being there for me. **Teymur**, thank you for your friendship and our long talks about bioinformatics and life. You are a brilliant mind and a valuable friend. **Maryam**, thank you for many pleasant lab moments and talks, and being supportive friend through all these years. **Seddighe and Ahmad**, thank you for sharing your knowledge and experience with me, and for always being willing to help. **Anish**, thank you for your kindness, friendship and brilliant mind for giving me fantastic advice. You are a reliable friend. **Amol, Feria, Sergei (Siarhei), Yu-Fang, Berta, Natalia, and Marit**, it was absolute pleasure to share the lab with you. Thank you so much for always being kind and supportive through these years.

To my friends outside the lab

Prof. Mahmood Karami, thank you for your unwavering support and belief in me. You saw in me what I had yet to see in myself. You taught me how to think, how to learn, and how to grow. Your guidance shaped not only my approach to science but also my path in life. I am forever grateful. **Amir**, you are the Rumi (Shams Tabrizi) I had always sought. While magic unfolded when Molana found you, our distance is equally painful, my brother. We

started this journey together, and without your support, encouragement, and unwavering friendship, it would have been impossible. You opened doors I never knew existed. **Benyamin**, thank you for your unconditional kindness and care. You are my hope on the other side, and the person I can always reach out to. We've shared so much, and our conversations could go on forever. Thank you for introducing me to **Shaghayegh. Alireza Azimi**, thank you for helping me through my stressful times with your wisdom, patience, and honest advice. Without your guidance, my journey wouldn't have been possible. **Shadi Jafari**, your words have impacted me far more than you realize. Thank you for planting those thoughts in my mind. **Ehsan**, thank you for always being there to help and for your friendship and kindness. **Mitra**, thank you for your kindness, unwavering support, and willingness to help, even after all these years. **Nadia, and Mostafa** thank you for being fantastic and supportive friends through all these years. **Siamak and Mona**, my Persian family here. Your home is our guiding light and hope. Thank you for always welcoming us and allowing me to share beautiful Persian traditions and everything good about Persian home with my family. **Sandra and Markus**, how lucky we are to have you. Thank you for the amazing dinners, board games, nature walks, and our endless talks about food and family life. **Marieta and Salva**, my favorite Spanish couple. Thank you for always welcoming us with your warm southern sun. I feel at home with you. **Iris and Fredrik**, thank you for the amazing Swedish crayfish party, your friendship, and the fantastic times we shared together.

To my parents, my brother and sister

I feel unable to thank my family enough. Thank you for giving me the permission to follow my dream, even though I know how difficult this distance is for you. Thank you for raising me with joy, love, support, and principles. Dear **Mom and Dad**, if I can be even 10% of the person you are, my life will not have been wasted. My dear Mom, **Ashi**, my first teacher, my anchor, my savior, my angel. You are greater than life. You are the manifestation of love. You are my all reasons. My dear Dad, **Haji**, hearing your voice washes away the biggest worries of this world from my mind. You are my rock, my shelter, and my support. You are my last card, my last trick, and my last key that never fails to open the toughest locks in this world. **Ashi and Haji**, I searched a lot to find the right words of appreciation, but I couldn't find them. I just want you to know that I owe everything in my life to you. I love you so much.

To my dear bother **Mahdi dadash**, you are my role model, my rock, best friend, and the genius that I know. You hold my back no matter what I am facing. I remain your fan and cheerleader. Thank you for being the pioneer in our family in science and thought me a lot about science, and life. I look forward to tell you that **Mahdi**, make a tea, I am reaching home. Thank you for bringing **Zeinab** to our family and gifting beautiful **Zahra**, and **Maleka**, to us. **Shadi** my dear sister, you are the light of my life, your smile can bright

the darkest days. You are the angel. Your kindness and will power are unmatched. Thank you for saving me from most difficult days and always loving me. I love you from bottom of my heart little sister.

To my wife & daughter

Iciar, my love, my partner through ups and downs, the captain of my ship, my boss at home, my permanent audience in every presentation, my everyday hope, my biggest fan, my second brain, my comfort, my peace, my helping hand in everything, and the better version of me. Thank you for putting up with me through long hours of work. Without your magical patience, love, and support this achievement would not have been possible. To my little angel, **Alma**, who was born during my PhD, I feel truly blessed to have you in my life. Your smile is the most priceless gift I have ever received.

To my in-laws

My mother-in-law **Cristina** and my father-in-law **Alberto**, thank you for accepting me with open arms and hearts into your family, and for always being incredibly kind and supportive. You have given me so much love. I am so lucky to have you and cannot express my gratitude enough for your generosity and support. **Inigo** and **Analia**, thank you for all your support and kindness. **Cris**, thank you for always being there to help, and bringing joy to the family with your unique musical talent. **Paula**, thank you for your kindness and always being there to help. You guys have stood by us, no matter where we are in this world.

تقدیم به پدر، مادر، برادر، و خواهر عزیزم

من هرگز قادر نیستم به اندازه کافی از شما تشکر کنم. ممنونم که به من اجازه پرواز برای دنبال کردن روهایم رو دادید. با وجود اینکه میدونم که تحمل این دوری براتون چقدر سخته. ممنونم که منو با عشق، فداکاری و اصول انسانی و اخلاقی تربیت کردید. پدر و مادر عزیزم، اگر بتوانم حتی ۱۰٪ از آن چیزی باشم که شما هستید، زندگی‌ام بهبود خواهد بود.

مامان عزیزم، اشی جون، اولین معلم، تکیه گاهم، ناجی‌ام، فرشته‌ام. تو بزرگتر از زندگی هستی. تو تجسم عشقی. تو تمام دلایل منی.

بابای عزیزم، حاجی، شنیدن صدای تو، بزرگترین نگرانی‌های این دنیا را از ذهنم می‌شوره. تو پناه و حامی من هستی. تو آخرین برگ برنده من، آخرین ترفندم و آخرین کلیدی هستی که سخت‌ترین قفل‌های این دنیا را باز می‌کنه. تمام لحظاتم با تو زیباست.

اشی جون و حاجی، خیلی تلاش کردم تا کلمات مناسبی برای قدردانی از شما پیدا کنم، اما موفق نشدم. فقط می‌خوام بدانید که همه چیز زندگی‌ام را مدیون شما هستم. خیلی دوستتان دارم.

برادر عزیزم، مهدی داداش، چه طوفانهایی رو با هم پشت سر گذاشتیم. تو الگوی من، تکیه گاهم، بهترین دوستم و تنها نابغه‌ای هستی که می‌شناسم. در هر شرایطی هوای منو داری. همیشه طرفدار تم. ممنون که پیشگام خانواده ما در علم بودی. بی‌صبرانه منتظرم تا بگم: "داداش، جای بریز، دارم میرسم خونه".

ممنون که زینب عزیز را به خانواده‌مان آوردی که با حضور صمیمی و دلگرم کننده‌اش و با
مهربانی و حمایتش و با هدیه دادن زهرا و ملکا، خانواده ما رو زیباتر کرد، برای تمام محبت‌ها و
حمایتش در این مسیر سپاسگزارم.
شادی، خواهر عزیزم، تو نور زندگی من هستی. لبخندت می‌تونه تاریکترین روزها را روشن
کند. تو یک فرشته‌ای. مهربانی و اراده‌ات هر دو بی‌نظیره.
ممنون که پناهگاه من در سختترین روزها بودی و همیشه دوستم داشتی. از صمیم قلب دوستت
دارم، خواهر کوچولوی عزیزم.

7. References

1. Discovery of DNA Double Helix: Watson and Crick | Learn Science at Scitable [Internet]. [cited 2023 Feb 12]. Available from: <http://www.nature.com/scitable/topicpage/discovery-of-dna-structure-and-function-watson-397>
2. Serra-Cardona A, Zhang Z. Replication-coupled nucleosome assembly as a passage of epigenetic information and cell identity. *Trends Biochem Sci*. 2018 Feb;43(2):136–48.
3. Martire S, Banaszynski LA. The roles of histone variants in fine-tuning chromatin organization and function. *Nat Rev Mol Cell Biol*. 2020 Sep;21(9):522–41.
4. Fyodorov DV, Zhou BR, Skoultchi AI, Bai Y. Emerging roles of linker histones in regulating chromatin structure and function. *Nat Rev Mol Cell Biol*. 2018 Mar;19(3):192–206.
5. Cannan WJ, Pederson DS. Mechanisms and Consequences of Double-strand DNA Break Formation in Chromatin. *J Cell Physiol*. 2016 Jan;231(1):3–14.
6. Blackford AN, Jackson SP. ATM, ATR, and DNA-PK: The Trinity at the Heart of the DNA Damage Response. *Molecular Cell*. 2017 Jun;66(6):801–17.
7. Sage E, Shikazono N. Radiation-induced clustered DNA lesions: Repair and mutagenesis. *Free Radical Biology and Medicine*. 2017;107:125–35.
8. Lindahl T. Instability and decay of the primary structure of DNA. *Nature*. 1993 Apr;362(6422):709–15.
9. Gates KS. An Overview of Chemical Processes That Damage Cellular DNA: Spontaneous Hydrolysis, Alkylation, and Reactions with Radicals. :14.
10. Hegde ML, Hazra TK, Mitra S. Early steps in the DNA base excision/single-strand interruption repair pathway in mammalian cells. *Cell Res*. 2008 Jan;18(1):27–47.
11. Yang W. Structure and mechanism for DNA lesion recognition. *Cell Res*. 2008 Jan;18(1):184–97.
12. Caldecott KW. Single-strand break repair and genetic disease. *Nat Rev Genet*. 2008 Aug;9(8):619–31.
13. Cao H, Salazar-García L, Gao F, Wahlestedt T, Wu CL, Han X, et al. Novel approach reveals genomic landscapes of single-strand DNA breaks with nucleotide resolution in human cells. *Nat Commun*. 2019 Dec 20;10(1):5799.
14. Deckbar D, Jeggo PA, Löbrich M. Understanding the limitations of radiation-induced cell cycle checkpoints. *Critical Reviews in Biochemistry and Molecular Biology*. 2011 Aug;46(4):271–83.
15. Khanna KK, Jackson SP. DNA double-strand breaks: signaling, repair and the cancer connection. *Nature Genetics*. 2001 Mar;27(3):247–54.
16. Blaisdell JO, Harrison L, Wallace SS. Base excision repair processing of radiation-induced clustered DNA lesions. *Radiat Prot Dosimetry*. 2001;97(1):25–31.
17. Jiang M, Jia K, Wang L, Li W, Chen B, Liu Y, et al. Alterations of DNA damage response pathway: Biomarker and therapeutic strategy for cancer immunotherapy. *Acta Pharmaceutica Sinica B*. 2021 Oct;11(10):2983–94.

18. Abramenkova A, Hariri M, Spiegelberg D, Nilsson S, Stenerlöv B. Ra-223 induces clustered DNA damage and inhibits cell survival in several prostate cancer cell lines. *Translational Oncology*. 2022 Dec;26:101543.
19. Dedon PC, Salzberg AA, Xu J. Exclusive production of bistranded DNA damage by calicheamicin. *Biochemistry*. 1993 Apr 13;32(14):3617–22.
20. Wheatley DN, Mueller GC, Kajiwara K. Anti-mitotic Activity of Bleomycin: Time of Action in the Mammalian Cell Cycle. *Br J Cancer*. 1974 Feb;29(2):117–31.
21. Le TT, Wu M, Lee JH, Bhatt N, Inman JT, Berger JM, et al. Etoposide promotes DNA loop trapping and barrier formation by topoisomerase II. *Nat Chem Biol*. 2023 May;19(5):641–50.
22. Singh V, Johansson P, Ekedahl E, Lin YL, Hammarsten O, Westerlund F. Quantification of single-strand DNA lesions caused by the topoisomerase II poison etoposide using single DNA molecule imaging. *Biochemical and Biophysical Research Communications*. 2022 Feb;594:57–62.
23. Bromberg KD, Burgin AB, Osheroff N. Quinolone Action against Human Topoisomerase II α : Stimulation of Enzyme-Mediated Double-Stranded DNA Cleavage. *Biochemistry*. 2003 Apr 1;42(12):3393–8.
24. Eckerdt F, Plataniias LC. Emerging Role of Glioma Stem Cells in Mechanisms of Therapy Resistance. *Cancers*. 2023 Jul 1;15(13):3458.
25. Taverna P, Liu L, Hwang HS, Hanson AJ, Kinsella TJ, Gerson SL. Methoxyamine potentiates DNA single strand breaks and double strand breaks induced by temozolomide in colon cancer cells. *Mutation Research/DNA Repair*. 2001 May;485(4):269–81.
26. Russ E, Davis CM, Slaven JE, Bradfield DT, Selwyn RG, Day RM. Comparison of the Medical Uses and Cellular Effects of High and Low Linear Energy Transfer Radiation. *Toxics*. 2022 Oct 21;10(10):628.
27. Riquier H, Wera AC, Heuskin AC, Feron O, Lucas S, Michiels C. Comparison of X-ray and alpha particle effects on a human cancer and endothelial cells: Survival curves and gene expression profiles. *Radiotherapy and Oncology*. 2013 Mar;106(3):397–403.
28. Alizadeh E, Sanz AG, García G, Sanche L. Radiation Damage to DNA: The Indirect Effect of Low-Energy Electrons. *J Phys Chem Lett*. 2013 Mar 7;4(5):820–5.
29. Sage E, Harrison L. Clustered DNA lesion repair in eukaryotes: Relevance to mutagenesis and cell survival. *Mutation Research/Fundamental and Molecular Mechanisms of Mutagenesis*. 2011 Jun;711(1–2):123–33.
30. Schipler A, Iliakis G. DNA double-strand-break complexity levels and their possible contributions to the probability for error-prone processing and repair pathway choice. *Nucleic Acids Res*. 2013 Sep;41(16):7589–605.
31. Goodhead DT. Initial Events in the Cellular Effects of Ionizing Radiations: Clustered Damage in DNA. *International Journal of Radiation Biology*. 1994 Jan;65(1):7–17.
32. Lavelle C, Foray N. Chromatin structure and radiation-induced DNA damage: From structural biology to radiobiology. *The International Journal of Biochemistry & Cell Biology*. 2014 Apr;49:84–97.
33. Mognato M, Burdak-Rothkamm S, Rothkamm K. Interplay between DNA replication stress, chromatin dynamics and DNA-damage response for the maintenance of genome stability. *Mutation Research/Reviews in Mutation Research*. 2021 Jan;787:108346.

34. Gustafsson AS, Abramenkova A, Stenerlöv B. Suppression of DNA-dependent protein kinase sensitizes cells to radiation without affecting DSB repair. *Mutat Res*. 2014 Nov;769:1–10.
35. Chiolo I, Altmeyer M, Legube G, Mekhail K. Nuclear and genome dynamics underlying DNA double-strand break repair. *Nat Rev Mol Cell Biol* [Internet]. 2025 Mar 17 [cited 2025 Mar 18]; Available from: <https://www.nature.com/articles/s41580-025-00828-1>
36. Friedberg EC. A brief history of the DNA repair field. *Cell Research*. 2008 Jan;18(1):3–7.
37. Ciccia A, Elledge SJ. The DNA damage response: making it safe to play with knives. *Mol Cell*. 2010 Oct 22;40(2):179–204.
38. Tubbs A, Nussenzweig A. Endogenous DNA Damage as a Source of Genomic Instability in Cancer. *Cell*. 2017 Feb;168(4):644–56.
39. Huang R, Zhou PK. DNA damage repair: historical perspectives, mechanistic pathways and clinical translation for targeted cancer therapy. *Sig Transduct Target Ther*. 2021 Dec;6(1):254.
40. Dianov GL, Hübscher U. Mammalian Base Excision Repair: the Forgotten Archangel. *Nucleic Acids Research*. 2013 Apr;41(6):3483–90.
41. Marteijn JA, Lans H, Vermeulen W, Hoeijmakers JHJ. Understanding nucleotide excision repair and its roles in cancer and ageing. *Nat Rev Mol Cell Biol*. 2014 Jul;15(7):465–81.
42. Li GM. Mechanisms and functions of DNA mismatch repair. *Cell Research*. 2008;18(1).
43. Rothkamm K, Barnard S, Moquet J, Ellender M, Rana Z, Burdak-Rothkamm S. DNA damage foci: Meaning and significance. *Environmental and Molecular Mutagenesis*. 2015;56(6):491–504.
44. Jackson SP, Bartek J. The DNA-damage response in human biology and disease. *Nature*. 2009 Oct;461(7267):1071–8.
45. Mirza-Aghazadeh-Attari M, Mohammadzadeh A, Yousefi B, Mihanfar A, Karimian A, Majidinia M. 53BP1: A key player of DNA damage response with critical functions in cancer. *DNA Repair (Amst)*. 2019;73:110–9.
46. Iwabuchi K, Bartel PL, Li B, Marraccino R, Fields S. Two cellular proteins that bind to wild-type but not mutant p53. *Proc Natl Acad Sci U S A*. 1994 Jun 21;91(13):6098–102.
47. Tudor Domains as Methyl-Lysine and Methyl-Arginine Readers - ScienceDirect [Internet]. [cited 2023 Feb 20]. Available from: <https://www.sciencedirect.com/science/article/pii/B9780128023891000083>
48. Botuyan MV, Lee J, Ward IM, Kim JE, Thompson JR, Chen J, et al. Structural Basis for the Methylation State-Specific Recognition of Histone H4-K20 by 53BP1 and Crb2 in DNA Repair. *Cell*. 2006 Dec 29;127(7):1361–73.
49. Acs K, Luijsterburg MS, Ackermann L, Salomons FA, Hoppe T, Dantuma NP. The AAA-ATPase VCP/p97 promotes 53BP1 recruitment by removing L3MBTL1 from DNA double-strand breaks. *Nat Struct Mol Biol*. 2011 Dec;18(12):1345–50.
50. Feng L, Li N, Li Y, Wang J, Gao M, Wang W, et al. Cell cycle-dependent inhibition of 53BP1 signaling by BRCA1. *Cell Discov*. 2015 Aug 4;1(1):1–11.
51. Bouwman P, Aly A, Escandell JM, Pieterse M, Bartkova J, van der Gulden H, et al. 53BP1 loss rescues BRCA1 deficiency and is associated with triple-negative and BRCA-mutated breast cancers. *Nat Struct Mol Biol*. 2010 Jun;17(6):688–95.

52. Noubissi FK, McBride AA, Leppert HG, Millet LJ, Wang X, Davern SM. Detection and quantification of γ -H2AX using a dissociation enhanced lanthanide fluorescence immunoassay. *Sci Rep*. 2021 Apr 26;11(1):8945.
53. Bonner WM, Redon CE, Dickey JS, Nakamura AJ, Sedelnikova OA, Solier S, et al. γ H2AX and cancer. *Nat Rev Cancer*. 2008 Dec;8(12):957–67.
54. Rothkamm K, Horn S. gamma-H2AX as protein biomarker for radiation exposure. *Ann Ist Super Sanita*. 2009;45(3):265–71.
55. Xie A, Puget N, Shim I, Odate S, Jarzyna I, Bassing CH, et al. Control of sister chromatid recombination by histone H2AX. *Mol Cell*. 2004 Dec 22;16(6):1017–25.
56. Unal E, Arbel-Eden A, Sattler U, Shroff R, Lichten M, Haber JE, et al. DNA damage response pathway uses histone modification to assemble a double-strand break-specific cohesin domain. *Mol Cell*. 2004 Dec 22;16(6):991–1002.
57. Savic V, Yin B, Maas NL, Bredemeyer AL, Carpenter AC, Helmink BA, et al. Formation of dynamic gamma-H2AX domains along broken DNA strands is distinctly regulated by ATM and MDC1 and dependent upon H2AX densities in chromatin. *Mol Cell*. 2009 May 15;34(3):298–310.
58. Simonsson M, Qvarnström F, Nyman J, Johansson KA, Garmo H, Turesson I. Low-dose hypersensitive gammaH2AX response and infrequent apoptosis in epidermis from radiotherapy patients. *Radiother Oncol*. 2008 Sep;88(3):388–97.
59. Mah LJ, El-Osta A, Karagiannis TC. γ H2AX: a sensitive molecular marker of DNA damage and repair. *Leukemia*. 2010 Apr;24(4):679–86.
60. Karnitz LM, Zou L. Molecular Pathways: Targeting ATR in Cancer Therapy. *Clin Cancer Res*. 2015 Nov 1;21(21):4780–5.
61. Yazinski SA, Zou L. Functions, Regulation, and Therapeutic Implications of the ATR Checkpoint Pathway. *Annu Rev Genet*. 2016 Nov 23;50:155–73.
62. Shibata A, Jeggo PA. ATM's Role in the Repair of DNA Double-Strand Breaks. *Genes (Basel)*. 2021 Aug 31;12(9):1370.
63. Shibata A, Jeggo P, Löbrich M. The pendulum of the Ku-Ku clock. *DNA repair*. 2018;71:164–71.
64. Rothkamm K. Radiation-induced Genomic Rearrangements Formed by Non-homologous End-Joining of DNA Double-Strand Breaks.
65. Mjelle R, Hegre SA, Aas PA, Slupphaug G, Drabløs F, Saetrom P, et al. Cell cycle regulation of human DNA repair and chromatin remodeling genes. *DNA Repair (Amst)*. 2015 Jun;30:53–67.
66. Shibata A, Jeggo P. A historical reflection on our understanding of radiation-induced DNA double strand break repair in somatic mammalian cells; interfacing the past with the present. *Int J Radiat Biol*. 2019 Jul;95(7):945–56.
67. Yasuhara T, Kato R, Hagiwara Y, Shiotani B, Yamauchi M, Nakada S, et al. Human Rad52 Promotes XPG-Mediated R-loop Processing to Initiate Transcription-Associated Homologous Recombination Repair. *Cell*. 2018 Oct 4;175(2):558–570.e11.
68. Liu X, Shao Z, Jiang W, Lee BJ, Zha S. PAXX promotes KU accumulation at DNA breaks and is essential for end-joining in XLF-deficient mice. *Nat Commun*. 2017 Jan 4;8(1):13816.
69. Jette N, Lees-Miller SP. The DNA-dependent protein kinase: A multifunctional protein kinase with roles in DNA double strand break repair and mitosis. *Progress in Biophysics and Molecular Biology*. 2015 Mar 1;117(2):194–205.
70. Fell VL, Schild-Poulter C. The Ku heterodimer: function in DNA repair and beyond. *Mutat Res Rev Mutat Res*. 2015;763:15–29.

71. Li G, Nelsen C, Hendrickson EA. Ku86 is essential in human somatic cells. *Proc Natl Acad Sci USA*. 2002 Jan 22;99(2):832–7.
72. Dylgjeri E, Knudsen KE. DNA-PKcs: A Targetable Protumorigenic Protein Kinase. *Cancer Research*. 2022 Feb 15;82(4):523–33.
73. Singleton BK, Torres-Arzayus MI, Rottinghaus ST, Taccioli GE, Jeggo PA. The C Terminus of Ku80 Activates the DNA-Dependent Protein Kinase Catalytic Subunit. *Mol Cell Biol*. 1999 May;19(5):3267–77.
74. Burger K, Ketley RF, Gullerova M. Beyond the Trinity of ATM, ATR, and DNA-PK: Multiple Kinases Shape the DNA Damage Response in Concert With RNA Metabolism. *Front Mol Biosci* [Internet]. 2019 [cited 2019 Aug 22];6. Available from: <https://www.frontiersin.org/articles/10.3389/fmolb.2019.00061/full>
75. Goodwin JF, Knudsen KE. Beyond DNA repair: DNA-PK function in cancer. *Cancer Discov*. 2014 Oct;4(10):1126–39.
76. Kaniecki K, De Tullio L, Greene EC. A change of view: homologous recombination at single-molecule resolution. *Nat Rev Genet*. 2018 Apr;19(4):191–207.
77. Frit P, Barboule N, Yuan Y, Gomez D, Calsou P. Alternative end-joining pathway(s): Bricolage at DNA breaks. *DNA Repair*. 2014 May;17:81–97.
78. Howard SM, Yanez DA, Stark JM. DNA Damage Response Factors from Diverse Pathways, Including DNA Crosslink Repair, Mediate Alternative End Joining. Maizels N, editor. *PLoS Genet*. 2015 Jan 28;11(1):e1004943.
79. Chang HHY, Pannunzio NR, Adachi N, Lieber MR. Non-homologous DNA end joining and alternative pathways to double-strand break repair. *Nature Reviews Molecular Cell Biology*. 2017 Aug;18(8):495–506.
80. Scully R, Panday A, Elango R, Willis NA. DNA double-strand break repair-pathway choice in somatic mammalian cells. *Nature Reviews Molecular Cell Biology*. 2019 Nov;20(11):698–714.
81. Ceccaldi R, Rondinelli B, D’Andrea AD. Repair Pathway Choices and Consequences at the Double-Strand Break. *Trends in Cell Biology*. 2016 Jan;26(1):52–64.
82. Van De Kooij B, Kruswick A, Van Attikum H, Yaffe MB. Multi-pathway DNA-repair reporters reveal competition between end-joining, single-strand annealing and homologous recombination at Cas9-induced DNA double-strand breaks. *Nat Commun*. 2022 Sep 8;13(1):5295.
83. Symington LS. Mechanism and regulation of DNA end resection in eukaryotes. *Critical Reviews in Biochemistry and Molecular Biology*. 2016 May 3;51(3):195–212.
84. Beucher A, Birraux J, Tchouandong L, Barton O, Shibata A, Conrad S, et al. ATM and Artemis promote homologous recombination of radiation-induced DNA double-strand breaks in G2. *EMBO J*. 2009 Nov 4;28(21):3413–27.
85. Shibata A, Jeggo PA. Roles for the DNA-PK complex and 53BP1 in protecting ends from resection during DNA double-strand break repair. *Journal of Radiation Research*. 2020 Sep 8;61(5):718–26.
86. Pennycook BR, Barr AR. Restriction point regulation at the crossroads between quiescence and cell proliferation. *FEBS Letters*. 2020;594(13):2046–60.
87. Rubin SM, Sage J, Skotheim JM. Integrating Old and New Paradigms of G1/S Control. *Molecular Cell*. 2020 Oct;80(2):183–92.
88. Löbrich M, Jeggo PA. The impact of a negligent G2/M checkpoint on genomic instability and cancer induction. *Nature Reviews Cancer*. 2007 Nov;7(11):861–9.
89. Matthews HK, Bertoli C, de Bruin RAM. Cell cycle control in cancer. *Nat Rev Mol Cell Biol*. 2022 Jan;23(1):74–88.

90. Panagopoulos A, Altmeyer M. The Hammer and the Dance of Cell Cycle Control. *Trends in Biochemical Sciences*. 2021 Apr;46(4):301–14.
91. Toledo L, Neelsen KJ, Lukas J. Replication Catastrophe: When a Checkpoint Fails because of Exhaustion. *Molecular Cell*. 2017 Jun 15;66(6):735–49.
92. Yam CQX, Lim HH, Surana U. DNA damage checkpoint execution and the rules of its disengagement. *Front Cell Dev Biol* [Internet]. 2022 Oct 6 [cited 2025 Mar 21];10. Available from: <https://www.frontiersin.org/journals/cell-and-developmental-biology/articles/10.3389/fcell.2022.1020643/full>
93. Audrey A, de Haan L, van Vugt MATM, de Boer HR. Processing DNA lesions during mitosis to prevent genomic instability. *Biochemical Society Transactions*. 2022 Aug 30;50(4):1105–18.
94. Shibata A. Regulation of repair pathway choice at two-ended DNA double-strand breaks. *Mutation Research/Fundamental and Molecular Mechanisms of Mutagenesis*. 2017 Oct;803–805:51–5.
95. Rothkamm K, Krüger I, Thompson LH, Löbrich M. Pathways of DNA Double-Strand Break Repair during the Mammalian Cell Cycle. *MCB*. 2003 Aug 15;23(16):5706–15.
96. Roos WP, Kaina B. DNA damage-induced cell death by apoptosis. *Trends in Molecular Medicine*. 2006 Sep 1;12(9):440–50.
97. Roos WP, Thomas AD, Kaina B. DNA damage and the balance between survival and death in cancer biology. *Nat Rev Cancer*. 2016 Jan;16(1):20–33.
98. Roos WP, Kaina B. DNA damage-induced cell death: From specific DNA lesions to the DNA damage response and apoptosis. *Cancer Letters*. 2013 May;332(2):237–48.
99. Galluzzi L, Kroemer G. Necroptosis: A Specialized Pathway of Programmed Necrosis. *Cell*. 2008 Dec 26;135(7):1161–3.
100. Hitomi J, Christofferson DE, Ng A, Yao J, Degtarev A, Xavier RJ, et al. Identification of a Molecular Signaling Network that Regulates a Cellular Necrotic Cell Death Pathway. *Cell*. 2008 Dec 26;135(7):1311–23.
101. Murata MM, Kong X, Moncada E, Chen Y, Imamura H, Wang P, et al. NAD⁺ consumption by PARP1 in response to DNA damage triggers metabolic shift critical for damaged cell survival. *Mol Biol Cell*. 2019 Sep 15;30(20):2584–97.
102. Necroptosis in development, inflammation and disease | *Nature Reviews Molecular Cell Biology* [Internet]. [cited 2025 Mar 21]. Available from: <https://www.nature.com/articles/nrm.2016.149>
103. Vandenabeele P, Galluzzi L, Vanden Berghe T, Kroemer G. Molecular mechanisms of necroptosis: an ordered cellular explosion. *Nat Rev Mol Cell Biol*. 2010 Oct;11(10):700–14.
104. Fulda S. Therapeutic exploitation of necroptosis for cancer therapy. *Semin Cell Dev Biol*. 2014 Nov;35:51–6.
105. Malik SS, Iqra. DNA Damage Response Pathways in Cancer Predisposition and Metastasis. In: Masood N, Shakil Malik S, editors. *Essentials of Cancer Genomic, Computational Approaches and Precision Medicine* [Internet]. Singapore: Springer; 2020 [cited 2025 Mar 21]. p. 155–70. Available from: https://doi.org/10.1007/978-981-15-1067-0_7
106. Hanahan D. Hallmarks of Cancer: New Dimensions. *Cancer Discov*. 2022 Jan;12(1):31–46.
107. Kwok M, Agathangelou A, Stankovic T. DNA damage response defects in hematologic malignancies: mechanistic insights and therapeutic strategies. *Blood*. 2024 May 23;143(21):2123–44.

108. Wang SW, Zheng QY, Hong WF, Tang BF, Hsu SJ, Zhang Y, et al. Mechanism of immune activation mediated by genomic instability and its implication in radiotherapy combined with immune checkpoint inhibitors. *Radiotherapy and Oncology*. 2024 Oct 1;199:110424.
109. Jiang M, Jia K, Wang L, Li W, Chen B, Liu Y, et al. Alterations of DNA damage repair in cancer: from mechanisms to applications. *Annals of Translational Medicine*. 2020 Dec;8(24):1685–1685.
110. Qian J, Liao G, Chen M, Peng RW, Yan X, Du J, et al. Advancing cancer therapy: new frontiers in targeting DNA damage response. *Front Pharmacol* [Internet]. 2024 Sep 20 [cited 2025 Mar 21];15. Available from: <https://www.frontiersin.org/journals/pharmacology/articles/10.3389/fphar.2024.1474337/full>
111. de las Alas MM, Aebi S, Fink D, Howell SB, Los G. Loss of DNA mismatch repair: effects on the rate of mutation to drug resistance. *J Natl Cancer Inst*. 1997 Oct 15;89(20):1537–41.
112. Hsu FM, Zhang S, Chen BPC. Role of DNA-dependent protein kinase catalytic subunit in cancer development and treatment. *Transl Cancer Res*. 2012 Jun 1;1(1):22–34.
113. Parikh RA, Appleman LJ, Bauman JE, Sankunni M, Lewis DW, Vlad A, et al. Upregulation of the ATR-CHEK1 pathway in oral squamous cell carcinomas. *Genes Chromosomes Cancer*. 2014 Jan;53(1):25–37.
114. Smith HL, Southgate H, Tweddle DA, Curtin NJ. DNA damage checkpoint kinases in cancer. *Expert Reviews in Molecular Medicine*. 2020 Jan;22:e2.
115. Akhoundova D, Francica P, Rottenberg S, Rubin MA. DNA Damage Response and Mismatch Repair Gene Defects in Advanced and Metastatic Prostate Cancer. *Advances in Anatomic Pathology*. 2024 Mar;31(2):61.
116. Ovejero-Sánchez M, González-Sarmiento R, Herrero AB. DNA Damage Response Alterations in Ovarian Cancer: From Molecular Mechanisms to Therapeutic Opportunities. *Cancers (Basel)*. 2023 Jan 10;15(2):448.
117. Li J, Jia Z, Dong L, Cao H, Huang Y, Xu H, et al. DNA damage response in breast cancer and its significant role in guiding novel precise therapies. *Biomarker Research*. 2024 Sep 27;12(1):111.
118. Qian J, Liao G, Chen M, Peng RW, Yan X, Du J, et al. Advancing cancer therapy: new frontiers in targeting DNA damage response. *Front Pharmacol* [Internet]. 2024 Sep 20 [cited 2025 Mar 21];15. Available from: <https://www.frontiersin.org/journals/pharmacology/articles/10.3389/fphar.2024.1474337/full>
119. Ovejero-Sánchez M, González-Sarmiento R, Herrero AB. DNA Damage Response Alterations in Ovarian Cancer: From Molecular Mechanisms to Therapeutic Opportunities. *Cancers*. 2023 Jan;15(2):448.
120. Huang JL, Chang YT, Hong ZY, Lin CS. Targeting DNA Damage Response and Immune Checkpoint for Anticancer Therapy. *International Journal of Molecular Sciences*. 2022 Jan;23(6):3238.
121. Wang Y, Zheng K, Xiong H, Huang Y, Chen X, Zhou Y, et al. PARP Inhibitor Upregulates PD-L1 Expression and Provides a New Combination Therapy in Pancreatic Cancer. *Front Immunol* [Internet]. 2021 Dec 17 [cited 2025 Mar 21];12. Available from: <https://www.frontiersin.org/journals/immunology/articles/10.3389/fimmu.2021.762989/full>
122. Halazonetis TD, Gorgoulis VG, Bartek J. An Oncogene-Induced DNA Damage Model for Cancer Development. *Science*. 2008 Mar 7;319(5868):1352–5.

123. Bukhari AB, Lewis CW, Pearce JJ, Luong D, Chan GK, Gamper AM. Inhibiting Wee1 and ATR kinases produces tumor-selective synthetic lethality and suppresses metastasis. *J Clin Invest*. 2019 Mar 1;129(3):1329–44.
124. Mortensen ACL, Mohajershojai T, Hariri M, Pettersson M, Spiegelberg D. Overcoming Limitations of Cisplatin Therapy by Additional Treatment With the HSP90 Inhibitor Onalespib. *Front Oncol*. 2020 Sep 30;10:532285.
125. D'Andrea AD. Mechanisms of PARP inhibitor sensitivity and resistance. *DNA Repair*. 2018 Nov 1;71:172–6.
126. Ma Q, Wang J, Qi J, Peng D, Guan B, Zhang J, et al. Increased chromosomal instability characterizes metastatic renal cell carcinoma. *Transl Oncol*. 2021 Jan;14(1):100929.
127. Lasolle H, Elsensohn MH, Wierinckx A, Alix E, Bonnefille C, Vasiljevic A, et al. Chromosomal instability in the prediction of pituitary neuroendocrine tumors prognosis. *Acta Neuropathol Commun*. 2020 Nov 10;8(1):190.
128. Huang R, Liu X, Li H, Zhou Y, Zhou PK. Integrated analysis of transcriptomic and metabolomic profiling reveal the p53 associated pathways underlying the response to ionizing radiation in HBE cells. *Cell & Bioscience*. 2020 Apr 15;10(1):56.
129. Dasari S, Bernard Tchounwou P. Cisplatin in cancer therapy: Molecular mechanisms of action. *European Journal of Pharmacology*. 2014 Oct;740:364–78.
130. Fuertes MA, Castilla J, Alonso C, Pérez JM. Cisplatin biochemical mechanism of action: from cytotoxicity to induction of cell death through interconnections between apoptotic and necrotic pathways. *Curr Med Chem*. 2003 Feb;10(3):257–66.
131. Oun R, Moussa YE, Wheate NJ. The side effects of platinum-based chemotherapy drugs: a review for chemists. *Dalton Trans*. 2018 May 15;47(19):6645–53.
132. Holmes D. Ovarian cancer: beyond resistance. *Nature*. 2015 Nov;527(7579):S217–S217.
133. Galluzzi L, Senovilla L, Vitale I, Michels J, Martins I, Kepp O, et al. Molecular mechanisms of cisplatin resistance. *Oncogene*. 2012 Apr 12;31(15):1869–83.
134. Holzer AK, Manorek GH, Howell SB. Contribution of the major copper influx transporter CTR1 to the cellular accumulation of cisplatin, carboplatin, and oxaliplatin. *Mol Pharmacol*. 2006 Oct;70(4):1390–4.
135. Holzer AK, Howell SB. The Internalization and Degradation of Human Copper Transporter 1 following Cisplatin Exposure. *Cancer Research*. 2006 Nov 15;66(22):10944–52.
136. Kuo MT, Chen HHW, Song IS, Savaraj N, Ishikawa T. The roles of copper transporters in cisplatin resistance. *Cancer Metastasis Rev*. 2007 Mar;26(1):71–83.
137. Li Q, Yu JJ, Mu C, Yunbam MK, Slavsky D, Cross CL, et al. Association between the level of ERCC-1 expression and the repair of cisplatin-induced DNA damage in human ovarian cancer cells. *Anticancer Res*. 2000 Apr;20(2A):645–52.
138. Taipale M, Jarosz DF, Lindquist S. HSP90 at the hub of protein homeostasis: emerging mechanistic insights. *Nat Rev Mol Cell Biol*. 2010 Jul;11(7):515–28.
139. Spiegelberg D, Dascalu A, Mortensen AC, Abramenkova A, Kuku G, Nestor M, et al. The novel HSP90 inhibitor AT13387 potentiates radiation effects in squamous cell carcinoma and adenocarcinoma cells. *Oncotarget*. 2015 Nov 3;6(34):35652–66.

140. Spiegelberg D, Mortensen AC, Selvaraju RK, Eriksson O, Stenerlöv B, Nestor M. Molecular imaging of EGFR and CD44v6 for prediction and response monitoring of HSP90 inhibition in an in vivo squamous cell carcinoma model. *Eur J Nucl Med Mol Imaging*. 2016 May 1;43(5):974–82.
141. Yuno A, Lee MJ, Lee S, Tomita Y, Rekhman D, Moore B, et al. Clinical Evaluation and Biomarker Profiling of Hsp90 Inhibitors. *Methods Mol Biol*. 2018 Jan 1;1709:423–41.
142. Zhang Z, Xie Z, Sun G, Yang P, Li J, Yang H, et al. Reversing drug resistance of cisplatin by hsp90 inhibitors in human ovarian cancer cells. *Int J Clin Exp Med*. 2015;8(5):6687–701.
143. Bagatell R, Beliakoff J, David CL, Marron MT, Whitesell L. Hsp90 inhibitors deplete key anti-apoptotic proteins in pediatric solid tumor cells and demonstrate synergistic anticancer activity with cisplatin. *Int J Cancer*. 2005 Jan 10;113(2):179–88.
144. Hanif F, Muzaffar K, Perveen kakhkashan, Malhi S, Simjee S. Glioblastoma Multiforme: A Review of its Epidemiology and Pathogenesis through Clinical Presentation and Treatment. *APJCP* [Internet]. 2017 Jan [cited 2025 Jan 8];18(1). Available from: <https://doi.org/10.22034/APJCP.2017.18.1.3>
145. Singla AK, Madan R, Gupta K, Goyal S, Kumar N, Sahoo SK, et al. Clinical behaviour and outcome in pediatric glioblastoma: current scenario. *Radiat Oncol J*. 2021 Mar 30;39(1):72–7.
146. Birbo B, Madu EE, Madu CO, Jain A, Lu Y. Role of HSP90 in Cancer. *IJMS*. 2021 Sep 25;22(19):10317.
147. Chen H, Gong Y, Ma Y, Thompson RC, Wang J, Cheng Z, et al. A Brain-Penetrating Hsp90 Inhibitor NXD30001 Inhibits Glioblastoma as a Monotherapy or in Combination With Radiation. *Front Pharmacol* [Internet]. 2020 Jun 30 [cited 2025 Jan 8];11. Available from: <https://www.frontiersin.org/journals/pharmacology/articles/10.3389/fphar.2020.00974/full>
148. Orth M, Albrecht V, Seidl K, Kinzel L, Unger K, Hess J, et al. Inhibition of HSP90 as a Strategy to Radiosensitize Glioblastoma: Targeting the DNA Damage Response and Beyond. *Front Oncol* [Internet]. 2021 Mar 17 [cited 2025 Jan 8];11. Available from: <https://www.frontiersin.org/journals/oncology/articles/10.3389/fonc.2021.612354/full>
149. Spiegelberg D, Abramenkova A, Mortensen ACL, Lundsten S, Nestor M, Stenerlöv B. The HSP90 inhibitor Onalespib exerts synergistic anti-cancer effects when combined with radiotherapy: an in vitro and in vivo approach. *Scientific Reports*. 2020 Apr 3;10(1):1–11.
150. Lundsten S, Spiegelberg D, Raval NR, Nestor M. The radiosensitizer Onalespib increases complete remission in 177Lu-DOTATATE-treated mice bearing neuroendocrine tumor xenografts. *Eur J Nucl Med Mol Imaging*. 2020 Apr 1;47(4):980–90.
151. Xu J, Wu PJ, Lai TH, Sharma P, Canella A, Welker AM, et al. Disruption of DNA Repair and Survival Pathways through Heat Shock Protein Inhibition by Onalespib to Sensitize Malignant Gliomas to Chemoradiation Therapy. *Clinical Cancer Research*. 2022 May 2;28(9):1979–90.
152. Lundsten S, Spiegelberg D, Stenerlöv B, Nestor M. The HSP90 inhibitor onalespib potentiates 177Lu-DOTATATE therapy in neuroendocrine tumor cells. *Int J Oncol*. 2019 Dec;55(6):1287–95.
153. Kamal A, Thao L, Sensintaffar J, Zhang L, Boehm MF, Fritz LC, et al. A high-affinity conformation of Hsp90 confers tumour selectivity on Hsp90 inhibitors. *Nature*. 2003 Sep 25;425(6956):407–10.

154. Do K, Speranza G, Chang LC, Polley EC, Bishop R, Zhu W, et al. Phase I study of the heat shock protein 90 (Hsp90) inhibitor onalespib (AT13387) administered on a daily for 2 consecutive days per week dosing schedule in patients with advanced solid tumors. *Invest New Drugs*. 2015 Aug;33(4):921–30.
155. Canella A, Welker AM, Yoo JY, Xu J, Abas FS, Kesanakurti D, et al. Efficacy of Onalespib, a Long-Acting Second-Generation HSP90 Inhibitor, as a Single Agent and in Combination with Temozolomide against Malignant Gliomas. *Clin Cancer Res*. 2017 Oct 15;23(20):6215–26.
156. Williams NO, Quiroga D, Johnson C, Brufsky A, Chambers M, Bhattacharya S, et al. Phase Ib study of HSP90 inhibitor, onalespib (AT13387), in combination with paclitaxel in patients with advanced triple-negative breast cancer. *Ther Adv Med Oncol*. 2023;15:17588359231217976.
157. Xie Y, Bergström T, Jiang Y, Johansson P, Marinescu VD, Lindberg N, et al. The Human Glioblastoma Cell Culture Resource: Validated Cell Models Representing All Molecular Subtypes. *EBioMedicine*. 2015 Oct;2(10):1351–63.
158. Liew HY, Tan XY, Chan HH, Khaw KY, Ong YS. Natural HSP90 inhibitors as a potential therapeutic intervention in treating cancers: A comprehensive review. *Pharmacol Res*. 2022 Jul;181:106260.
159. Slovin S, Hussain S, Saad F, Garcia J, Picus J, Ferraldeschi R, et al. Pharmacodynamic and Clinical Results from a Phase I/II Study of the HSP90 Inhibitor Onalespib in Combination with Abiraterone Acetate in Prostate Cancer. *Clin Cancer Res*. 2019 Aug 1;25(15):4624–33.
160. Shapiro GI, Kwak E, Dezube BJ, Yule M, Ayrton J, Lyons J, et al. First-in-human phase I dose escalation study of a second-generation non-ansamycin HSP90 inhibitor, AT13387, in patients with advanced solid tumors. *Clin Cancer Res*. 2015 Jan 1;21(1):87–97.
161. Tani T, Tojo N, Ohnishi K. Preferential radiosensitization to glioblastoma cancer stem cell-like cells by a Hsp90 inhibitor, N-vinylpyrrolidone-AUY922. *Oncol Lett*. 2022 Mar;23(3):102.
162. Zhu H, Woolfenden S, Bronson RT, Jaffer ZM, Barluenga S, Winssinger N, et al. The novel Hsp90 inhibitor NXD30001 induces tumor regression in a genetically engineered mouse model of glioblastoma multiforme. *Mol Cancer Ther*. 2010 Sep;9(9):2618–26.
163. Annamalai B, Liu X, Gopal U, Isaacs JS. Hsp90 is an essential regulator of EphA2 receptor stability and signaling: implications for cancer cell migration and metastasis. *Mol Cancer Res*. 2009 Jul;7(7):1021–32.
164. Gopal U, Bohonowych JE, Lema-Tome C, Liu A, Garrett-Mayer E, Wang B, et al. A novel extracellular Hsp90 mediated co-receptor function for LRP1 regulates EphA2 dependent glioblastoma cell invasion. *PLoS One*. 2011 Mar 8;6(3):e17649.
165. Manousakis E, Miralles CM, Esquerda MG, Wright RHG. CDKN1A/p21 in Breast Cancer: Part of the Problem, or Part of the Solution? *Int J Mol Sci*. 2023 Dec 14;24(24):17488.
166. Romanov VS, Pospelov VA, Pospelova TV. Cyclin-dependent kinase inhibitor p21(Waf1): contemporary view on its role in senescence and oncogenesis. *Biochemistry (Mosc)*. 2012 Jun;77(6):575–84.
167. England K. Cell cycle regulation: p53-p21-RB signaling. *Cell Death Differ*. 2022 May;29(5):946–60.
168. Jakob B, Scholz M, Taucher-Scholz G. Immediate localized CDKN1A (p21) radiation response after damage produced by heavy-ion tracks. *Radiat Res*. 2000 Oct;154(4):398–405.

169. Montinaro A, Walczak H. Harnessing TRAIL-induced cell death for cancer therapy: a long walk with thrilling discoveries. *Cell Death Differ.* 2023 Feb;30(2):237–49.
170. Hu L, Wang Y, Chen Z, Fu L, Wang S, Zhang X, et al. Hsp90 Inhibitor SNX-2112 Enhances TRAIL-Induced Apoptosis of Human Cervical Cancer Cells via the ROS-Mediated JNK-p53-Autophagy-DR5 Pathway. *Oxid Med Cell Longev.* 2019;2019:9675450.
171. Thang M, Mellows C, Mercer-Smith A, Nguyen P, Hingtgen S. Current approaches in enhancing TRAIL therapies in glioblastoma. *Neurooncol Adv.* 2023;5(1):vdad047.
172. Allen M, Bjerke M, Edlund H, Nelander S, Westermark B. Origin of the U87MG glioma cell line: Good news and bad news. *Sci Transl Med.* 2016 Aug 31;8(354):354re3.
173. Poeppel TD, Handkiewicz-Junak D, Andreeff M, Becherer A, Bockisch A, Fricke E, et al. EANM guideline for radionuclide therapy with radium-223 of metastatic castration-resistant prostate cancer. *Eur J Nucl Med Mol Imaging.* 2018 May 1;45(5):824–45.
174. Schumann S, Eberlein U, Muhtadi R, Lassmann M, Scherthan H. DNA damage in leukocytes after internal ex-vivo irradiation of blood with the α -emitter Ra-223. *Sci Rep.* 2018 Feb 2;8(1):2286.
175. Hoglund, E. Blomquist, J. Carlsson, E. DNA damage induced by radiation of different linear energy transfer: initial fragmentation. *International Journal of Radiation Biology.* 2000 Jan;76(4):539–47.
176. Claesson AK, Stenerlöv B, Jacobsson L, Elmroth K. Relative biological effectiveness of the α -particle emitter ²¹¹At for double-strand break induction in human fibroblasts. *Radiation Research.* 2007;167(3):312–8.
177. Costes SV, Boissière A, Ravani S, Romano R, Parvin B, Barcellos-Hoff MH. Imaging features that discriminate between foci induced by high- and low-LET radiation in human fibroblasts. *Radiat Res.* 2006 May;165(5):505–15.
178. Radulescu I, Elmroth K, Stenerlöv B. Chromatin Organization Contributes to Non-randomly Distributed Double-Strand Breaks after Exposure to High-LET Radiation. *Radiation Research.* 2004 Jan;161(1):1–8.
179. Abramenkova A, Stenerlöv B. Measurement of DNA-Dependent Protein Kinase Phosphorylation Using Flow Cytometry Provides a Reliable Estimate of DNA Repair Capacity. *rare.* 2017 Sep;188(6):677–84.
180. Gustafsson AS, Hartman T, Stenerlöv B. Formation and repair of clustered damaged DNA sites in high LET irradiated cells. *International Journal of Radiation Biology.* 2015 Oct 3;91(10):820–6.
181. Abou DS, Ulmert D, Doucet M, Hobbs RF, Riddle RC, Thorek DLJ. Whole-Body and Microenvironmental Localization of Radium-223 in Naïve and Mouse Models of Prostate Cancer Metastasis. *JNCIJ.* 2016 May;108(5):djv380.
182. K Y, T K, S T, M S, T K, A H, et al. Pharmacokinetics of single dose radium-223 dichloride (BAY 88-8223) in Japanese patients with castration-resistant prostate cancer and bone metastases. *Annals of nuclear medicine [Internet].* 2016 Aug [cited 2023 Feb 22];30(7). Available from: <https://pubmed.ncbi.nlm.nih.gov/27272279/>
183. Sj C, C H, Cc P, Vj L, Be P, B J, et al. A Phase 1, Open-Label Study of the Biodistribution, Pharmacokinetics, and Dosimetry of ²²³Ra-Dichloride in Patients with Hormone-Refractory Prostate Cancer and Skeletal Metastases. *Journal of nuclear medicine : official publication, Society of Nuclear Medicine*

- [Internet]. 2015 Sep [cited 2023 Feb 22];56(9). Available from: <https://pubmed.ncbi.nlm.nih.gov/26182965/>
184. Ae M, Ar J, T H, B S, Lm P, N T, et al. Dose and time dependent apoptotic response in a human melanoma cell line exposed to accelerated boron ions at four different LET. *International journal of radiation biology* [Internet]. 2005 Apr [cited 2023 Feb 22];81(4). Available from: <https://pubmed.ncbi.nlm.nih.gov/16019936/>
 185. Böttger F, Vallés-Martí A, Cahn L, Jimenez CR. High-dose intravenous vitamin C, a promising multi-targeting agent in the treatment of cancer. *J Exp Clin Cancer Res*. 2021 Dec;40(1):343.
 186. Furqan M, Abu-Hejleh T, Stephens LM, Hartwig SM, Mott SL, Pulliam CF, et al. Pharmacological ascorbate improves the response to platinum-based chemotherapy in advanced stage non-small cell lung cancer. *Redox Biology*. 2022 Jul 1;53:102318.
 187. Ma Y, Chapman J, Levine M, Polireddy K, Drisko J, Chen Q. High-dose parenteral ascorbate enhanced chemosensitivity of ovarian cancer and reduced toxicity of chemotherapy. *Sci Transl Med*. 2014 Feb 5;6(222):222ra18.
 188. Buranasudja V, Doskey CM, Gibson AR, Wagner BA, Du J, Gordon DJ, et al. Pharmacologic Ascorbate Primes Pancreatic Cancer Cells for Death by Rewiring Cellular Energetics and Inducing DNA Damage. *Molecular Cancer Research*. 2019 Oct 1;17(10):2102–14.
 189. Ma Y, Chapman J, Levine M, Polireddy K, Drisko J, Chen Q. High-dose parenteral ascorbate enhanced chemosensitivity of ovarian cancer and reduced toxicity of chemotherapy. *Sci Transl Med*. 2014 Feb 5;6(222):222ra18.
 190. Ding D, Zhang Y, Wang J, Zhang X, Gao Y, Yin L, et al. Induction and inhibition of the pan-nuclear gamma-H2AX response in resting human peripheral blood lymphocytes after X-ray irradiation. *Cell Death Discovery*. 2016 Dec;2(1):16011.
 191. Basak D, Uddin MN, Hancock J. The Role of Oxidative Stress and Its Counteractive Utility in Colorectal Cancer (CRC). *Cancers (Basel)*. 2020 Nov 11;12(11):3336.
 192. Ferrada L, Magdalena R, Barahona MJ, Ramírez E, Sanzana C, Gutiérrez J, et al. Two Distinct Faces of Vitamin C: AA vs. DHA. *Antioxidants*. 2021 Feb 1;10(2):215.
 193. Bijur GN, Briggs B, Hitchcock CL, Williams MV. Ascorbic acid-dehydroascorbate induces cell cycle arrest at G2/M DNA damage checkpoint during oxidative stress. *Environmental and Molecular Mutagenesis*. 1999;33(2):144–52.
 194. Antiproliferative and Proapoptotic Effect of Ascorbyl Stearate in Human Pancreatic Cancer Cells: Association with Decreased Expression of Insulin-Like Growth Factor 1 Receptor. *Digestive Diseases and Sciences*. 2002;48(1).
 195. Brandt KE, Falls KC, Schoenfeld JD, Rodman SN, Gu Z, Zhan F, et al. Augmentation of intracellular iron using iron sucrose enhances the toxicity of pharmacological ascorbate in colon cancer cells. *Redox Biology*. 2018 Apr 1;14:82–7.
 196. O’Leary BR, Alexander MS, Du J, Moose DL, Henry MD, Cullen JJ. Pharmacological ascorbate inhibits pancreatic cancer metastases via a peroxide-mediated mechanism. *Sci Rep*. 2020 Oct 19;10(1):17649.
 197. Yun J, Mullarky E, Lu C, Bosch KN, Kavalier A, Rivera K, et al. Vitamin C selectively kills KRAS and BRAF mutant colorectal cancer cells by targeting GAPDH. *Science*. 2015 Dec 11;350(6266):1391–6.

198. Barnard S, Bouffler S, Rothkamm K. The shape of the radiation dose response for DNA double-strand break induction and repair. *Genome Integrity* [Internet]. 2013 [cited 2025 Mar 22];4. Available from: <https://scienceopen.com/hosted-document?doi=10.1186/2041-9414-4-1>
199. Stinson BM, Loparo JJ. Repair of DNA Double-Strand Breaks by the Nonhomologous End Joining Pathway. *Annu Rev Biochem*. 2021 Jun 20;90:137–64.
200. Bannik K, Madas B, Jarzombek M, Sutter A, Siemeister G, Mumberg D, et al. Radiobiological effects of the alpha emitter Ra-223 on tumor cells. *Scientific Reports*. 2019 Dec 6;9(1):1–11.
201. Povirk LF. Processing of Damaged DNA Ends for Double-Strand Break Repair in Mammalian Cells. *ISRN Molecular Biology*. 2012 Dec 4;2012:1–16.
202. Pastwa E, Neumann RD, Mezhevaya K, Winters TA. Repair of Radiation-Induced DNA Double-Strand Breaks is Dependent upon Radiation Quality and the Structural Complexity of Double-Strand Breaks. *Radiation Research*. 2003 Feb;159(2):251–61.
203. Schipler A, Iliakis G. DNA double-strand-break complexity levels and their possible contributions to the probability for error-prone processing and repair pathway choice. *Nucleic Acids Research*. 2013 Sep 1;41(16):7589–605.
204. Zhao F, Kim W, Kloeber JA, Lou Z. DNA end resection and its role in DNA replication and DSB repair choice in mammalian cells. *Exp Mol Med*. 2020 Oct;52(10):1705–14.
205. Gupta A, Hunt CR, Chakraborty S, Pandita RK, Yordy J, Ramnarain DB, et al. Role of 53BP1 in the Regulation of DNA Double-Strand Break Repair Pathway Choice. *Radiat Res*. 2014 Jan;181(1):1–8.
206. Okayasu R, Okada M, Okabe A, Noguchi M, Takakura K, Takahashi S. Repair of DNA Damage Induced by Accelerated Heavy Ions in Mammalian Cells Proficient and Deficient in the Non-homologous End-Joining Pathway. *Radiation Research*. 2006 Jan;165(1):59–67.
207. Abramenkova A, Stenerlöv B. Removal of heat-sensitive clustered damaged DNA sites is independent of double-strand break repair. *PLoS One*. 2018;13(12):e0209594.
208. Povirk LF, Han YH, Steighner RJ. Structure of bleomycin-induced DNA double-strand breaks: predominance of blunt ends and single-base 5' extensions. *Biochemistry*. 1989 Jul 11;28(14):5808–14.
209. Sleight MJ. The mechanism of DNA breakage by phleomycin in vitro. *Nucleic Acids Research*. 1976 Apr 1;3(4):891–902.
210. McGall GH, Rabow LE, Ashley GW, Wu SH, Kozarich JW, Stubbe J. New insight into the mechanism of base propenal formation during bleomycin-mediated DNA degradation. *J Am Chem Soc*. 1992 Jun;114(13):4958–67.
211. Povirk LF. DNA damage and mutagenesis by radiomimetic DNA-cleaving agents: bleomycin, neocarzinostatin and other enediynes. *Mutat Res*. 1996 Aug 17;355(1–2):71–89.
212. Mladenov E, Magin S, Soni A, Iliakis G. DNA double-strand-break repair in higher eukaryotes and its role in genomic instability and cancer: Cell cycle and proliferation-dependent regulation. *Semin Cancer Biol*. 2016 Jun;37–38:51–64.
213. Frei E, Holland JF, Schneiderman MA, Pinkel D, Selkirk G, Freireich EJ, et al. A Comparative Study of Two Regimens of Combination Chemotherapy in Acute Leukemia. *Blood*. 1958 Dec 1;13(12):1126–48.
214. Jin H, Wang L, Bernards R. Rational combinations of targeted cancer therapies: background, advances and challenges. *Nat Rev Drug Discov*. 2023 Mar;22(3):213–34.

215. Beijersbergen RL, Wessels LFA, Bernards R. Synthetic Lethality in Cancer Therapeutics. *Annu Rev Cancer Biol.* 2017 Mar 6;1(1):141–61.
216. Tatarova Z, Blumberg DC, Korkola JE, Heiser LM, Muschler JL, Schedin PJ, et al. A multiplex implantable microdevice assay identifies synergistic combinations of cancer immunotherapies and conventional drugs. *Nat Biotechnol.* 2022 Dec;40(12):1823–33.

Acta Universitatis Upsaliensis

Digital Comprehensive Summaries of Uppsala Dissertations from the Faculty of Medicine 2141

Editor: The Dean of the Faculty of Medicine

A doctoral dissertation from the Faculty of Medicine, Uppsala University, is usually a summary of a number of papers. A few copies of the complete dissertation are kept at major Swedish research libraries, while the summary alone is distributed internationally through the series Digital Comprehensive Summaries of Uppsala Dissertations from the Faculty of Medicine. (Prior to January, 2005, the series was published under the title “Comprehensive Summaries of Uppsala Dissertations from the Faculty of Medicine”.)

Distribution: publications.uu.se
urn:nbn:se:uu:diva-553099



ACTA UNIVERSITATIS
UPSALIENSIS
2025